LBL-6325 3/3
c.1

Energy and Environment Division

Telluric And D.C. Resistivity Techniques Applied To The Geophysical Investigation Of Basin And Range Geothermal Systems, Part III: The Analysis Of Data From Grass Valley, Nevada

J.H. Beyer
(Ph.D. thesis)

June 1977

Lawrence Berkeley Laboratory University of California/Berkeley

Prepared for the U.S. Energy Research and Development Administration under Contract No. W-7405-ENG-48

LBL-6325 3/3
c.1

TELLURIC AND D.C. RESISTIVITY TECHNIQUES APPLIED TO THE GEOPHYSICAL INVESTIGATION OF BASIN AND RANGE GEOTHERMAL SYSTEMS

PART III

THE ANALYSIS OF DATA FROM GRASS VALLEY, NEVADA

J. H. Beyer

ABSTRACT

This paper contains a detailed interpretation of E-field ratio telluric, bipole-dipole resistivity mapping, and dipole-dipole resistivity data obtained in the course of geophysical exploration of the Leach Hot Springs area of Grass Valley, Nevada. Several areas are singled out as being worthy of further investigation of their geothermal potential. Comparison of the three electrical exploration techniques indicates that: the bipole-dipole resistivity mapping method is the least useful; the dipole-dipole resistivity method can be very useful, but is, for practical purposes, exceptionally expensive and difficult to interpret; the E-field ratio telluric method can be a highly successful reconnaissance technique for delineating structures and relating the resistivities of different regions within the survey area.

B.WUOTKE

PREFACE

Starting in the Summer of 1973, the Lawrence Berkeley Laboratory of the University of California has been involved in a geothermal assessment program with three main goals:

1) To evaluate, on the basis of detailed geological, geochemical and geophysical data, some geothermal systems in the mid Basin and Range geologic province.

2) To compare and evaluate geophysical techniques used in the exploration and delineation of geothermal reservoirs.

3) To develop new exploration techniques, and the instrumentation required, specifically for the deep penetration desired in geothermal investigations.

This report addresses various aspects of each of these points.

It is well documented that hot water geothermal reservoirs tend to have lower electrical resistivity than surrounding cold and/or dry rock by virtue of: (1) increased ion mobility, (2) more dissolved solids, and (3) increased permeability and porosity of the reservoir rocks as a result of convection of the geothermal fluids. Vapor dominated geothermal systems are resistive in the steam zone, but display anomalously conductive halos in intermediate temperature regions where there is condensation. Thus, one distinctive feature of geothermal reservoirs is that they may be electrically conductive targets which, to be of economic importance, may be a few cubic kilometers in size, but with a depth of burial of one or more kilometers.

When confronted with the problem of initial exploration of a several hundred square kilometer region in the vicinity of a hot spring, a rapid reconnaissance electrical method is important to locate areas of low resistivity for more intensive investigation. The E-field ratio telluric method described in Part I of this report appears to satisfy this need quite adequately.

Subsequent to the location of conductive anomalies by reconnaissance techniques an electrical method providing higher resolution and affording more quantitative interpretation capability is needed. For this purpose, and for correlation with and evaluation of other electrical exploration techniques, d.c. resistivity measurements using the polar dipole-dipole array were performed as a part of the LBL geothermal exploration program. A second resistivity electrode configuration, the Schlumberger method, has been widely used by other investigators. Part II of this report is a numerical model study and comparison of these two resistivity techniques.

An extensive program of geophysical exploration was undertaken by LBL in the vicinity of Leach Hot Springs in Grass Valley, Nevada. The detailed interpretation of E-field ratio telluric, dipole-dipole resistivity, and bipole-dipole resistivity mapping data is treated in Part III of this report, along with a description of the implementation of high-power d.c. resistivity exploration techniques. Several areas in Grass Valley emerge as being worthy of further investigation for their geothermal potential, and the interpretation process has provided a means of evaluating and comparing the exploration techniques.

ACKNOWLEDGEMENTS

The major portion of this work has been supported by the U.S. Energy Research and Development Administration through the University of California - Lawrence Berkeley Laboratory. Some support at the initial stage of the field exploration program was provided by the National Science Foundation (Grant #GI-37905).

Special thanks are due Professor H.F. Morrison for numerous profitable ideas and discussions throughout the course of this work, and Abhijit Dey for his helpfullness in the use of his computer code for modeling the resistivity data.

The extensive field geophysical exploration program in which the author participated required the support of numerous helpful and capable employees of Lawrence Berkeley Laboratory. Notable among them are Harold Wollenberg, with whom the author had many discussions regarding the geology and exploration of Nevada geothermal systems, and Eugene Binnall, John Saarloos, and Harold Vogel, who developed reliable instrumentation to meet the demands of field exploration. Particular gratitude is expressed to Halvard Andersson, Milt Moebus, Ray Solbau, and the men who worked with them in the field for their conscientious effort at obtaining excellent field data.

TABLE OF CONTENTS

Part III: The Analysis of Data from Grass Valley, Nevada

INTRODUCTION

In the University of California-Lawrence Berkeley Laboratory program for geophysical investigation of the geothermal potential of Grass Valley, Nevada, considerable emphasis has been placed upon the development, interpretation, and evaluation of various electrical exploration techniques. This report deals with the analysis of data obtained using two reconnaissance techniques, the E-field ratio telluric and the bipole-dipole resistivity mapping methods, and the dipole-dipole resistivity method which, as a result of numerical modeling capability, offers the possibility of more detailed structural delineation. The first method makes use of natural electric fields as a source, while the latter two methods require a high-power controlled source.

The geophysical data which have been obtained in Grass Valley include gravity, magnetics, self-potential, E-field ratio tellurics, magnetotellurics, bipole-dipole resistivity, dipole-dipole resistivity, P-wave delay, microearthquake, seismic ground noise, and active seismic refraction/reflection. Only the data which are most pertinent to the interpretation of the E-field ratio telluric and d.c. resistivity data are presented in this report. Subsequent reports by other authors will present detailed analyses of other techniques. Regrettably, the magnetotelluric data has not been fully analyzed at the time of this writing, and will not be included in the discussion. A final interpretation of Grass Valley, giving equal weight to all methods of investigation is forthcoming (Morrison, et al., 1977).

THE ELECTRICAL EXPLORATION METHODS

The E-Field Ratio Telluric Method

The electric (E) field ratio telluric method is designed for reconnaissance electrical exploration of survey areas of several hundred square kilometers. A detailed description of the method, including a numerical model study of the response to various two-dimensional structures, is the topic of Part I of this report (Beyer, 1977a).

The E-field ratio telluric method is an abbreviated version of the conventional telluric current method in which the natural electric field of the earth is measured. Rather than using orthogonal electrode arrays to measure the electric field at a roving station with respect to that at a base station, a collinear, three-electrode array is used to measure the relative electric field strength between two consecutive dipoles. The array is leap-frogged along a survey line to obtain a set of ratios of the component of the electric field in the profile line direction. The ratios are successively multiplied together so that the value at each dipole location will be referred to that at the first location.

Instrumentation is simple and data reduction is easily accomplished in the field. Dipole lengths of 250 or 500 meters are used. The signals from the two consecutive dipoles, using the central electrode as common, are narrow bandpass filtered and used as inputs to the x and y channels of a battery powered x-y plotter. The phase shift between the two signals is generally negligible so that the plotter will trace a straight line, the slope of which equals the ratio of the two observed electric field strengths. In the field a protractor is used to measure the angle ϕ between this line and the horizontal axis of

the plotter, and a pocket calculator is used to find the slope, tan ϕ. Figure III-1 illustrates three successive E-field ratio telluric stations and the method of data presentation.

As the penetration depth of an electromagnetic field into conductive material is inversely proportional to the square root of the frequency, two frequencies have been used as a means of rudimentary depth discrimination. For the Basin and Range valleys of Nevada, 0.05 and 8 Hz, frequencies at which there is high amplitude in the natural electromagnetic spectrum, were found to be appropriate.

Only one component of the electric field is measured, and the associated magnetic field is not measured at all, so calculations of apparent resistivity cannot be made. The data are interpreted in terms of relative electric field strength. For example, at a semi-infinite vertical contact the current density normal to the contact must be continuous, so the ratio of the normal components of the electric field at the contact must be proportional to the resistivity ratio, whereas, away from the contact over a homogeneous half-space the electric field is proportional to the square root of the resistivity. Such qualitative interpretation, based upon some numerical modeling results, is quite adequate for a reconnaissance technique.

In the basin and range valleys of Nevada the LBL Field crew could generally drive along a straight line from one station to the next. The wire that was used for telluric surveys was approximately 20 gauge, containing a few steel strands in addition to several copper strands, making the wire exceptionally strong. It was found that a 500 meter length of wire could successfully be tied to the bumper of a jeep and dragged without stretching, along a straight line so that reeling and

unreeling of wire was generally unnecessary. Abrasion of the insulation was not severe because the dragged wire would often be suspended by sage brush or would slide easily over soft playa deposits. This enabled the field crew to limit each data gathering team to two people and two four-wheel drive vehicles. Under these conditions two people could obtain high and low frequency data at approximately eight stations per day along a previously surveyed line. Without steel stranded wire or over terrain where insulation abrasion would be severe from dragging, the wire has to be reeled up and laid out again along the survey line. This requires two people with a vehicle handling wire, and they will have difficulty keeping ahead of a third person recording data.

The Bipole-Dipole Resistivity Mapping Method

The bipole-dipole resistivity method is an electrical reconnaissance technique which employs a controlled-source, long-period transmitter. A thorough treatment of the method is given by Keller, et al., (1975).

Using a high power motor-generator set, up to 100 amperes of current is injected into the earth between two shallow grounded electrodes separated 1.5 to 2.5 kilometers. Numerous receiver stations are established at various locations. The potential field gradient resulting from the transmitted current is measured with an orthogonal array of two grounded dipoles, commonly 100 meters in length. The bipole-dipole electrode configuration is depicted in Figure III-2. A detailed description of the equipment used is given in the next section.

For each receiver station an apparent resistivity, ρ_a, is calculated as the homogeneous half-space resistivity necessary to produce the observed total electric field amplitude (regardless of

direction) at the centroid of the receiver array as a result of the transmitter bipole moment. Similarly, the apparent conductance, S_a, can be calculated as the conductance (conductivity-thickness product) of a layer over an infinitely resistive half-space required to produce the observed total electric field amplitude at the receiver array. These quantities are calculated from the equations

$$\rho_a = 2\pi \frac{E_T}{I} \left[\frac{R_1 R_2}{\left(R_1^4 + R_2^4 + R_1 R_2 \left[T_x^2 - R_1^2 - R_2^2 \right] \right)^{1/2}} \right]$$

and

$$S_a = \frac{I\, T_x}{2\pi R_1 R_2 E_T}$$

where, as illustrated in Figure III-2,

$E_T = (E_{\parallel}^2 + E_{\perp}^2)^{1/2}$ = the total electric field amplitude at the receiver array,

I = the transmitted current,

T_x = the transmitter length,

R_1 and R_2 = the distances from the transmitter electrodes to the centroid of the receiver array.

Bipole-dipole data are generally presented in the form of a contour map of apparent resistivity or apparent conductance, with the values plotted at the receiver station location. The purpose of both conductance and resistivity maps is the discrimination of layered models having a resistive basement from more nearly uniform models.

Interpretation is qualitative, based upon the patterns observed for simple resistivity structures which have been modeled numerically. Model results for horizontal layers and vertical contacts are

presented by Keller, et al. (1975), and for various two-dimensional structures by Dey and Morrison (1977). The dipole-dipole apparent resistivity pseudo-sections in Part II of this report (Beyer, 1977b) have some applicability to the interpretation of bipole-dipole resistivity data.

The LBL field crew of four people generally devoted about three days to setting up the bipole transmitter, which included burying several aluminum plates at each end of the bipole to obtain low contact resistance. Once this was accomplished, a team of two people could occupy six to twelve receiver locations per day, depending upon the terrain which had to be traversed, and the difficulty in determining the location of the receiver station. Later in the field program two motor-generator sets were used so that receiver stations would not have to be reoccupied for a second transmitter location. Furthermore, at one transmitter position, two orthogonal and a diagonal bipole were laid out. A two-person receiver crew could then record data for each transmitter bipole at about four receiver stations per day.

The Dipole-Dipole Resistivity Method

The dipole-dipole resistivity method employs a long-period, controlled-source transmitter, and is intended to yield the resistivity structure beneath a straight survey line. As is shown in Figure III-3 the dipole-dipole method employs constant transmitter and receiver dipole lengths, a, with increased depth of penetration being achieved by increasing the separation between the transmitter and receiver dipoles by integer (N) multiples of a. The upper limit on N is determined by the maximum depth of interest or the separation at

which the signal at the receiver is lost in the telluric or instrumental noise. Using the current, I, injected into the ground at the transmitter dipole, and the resulting potential difference, ΔV, observed at the receiver dipole, an apparent resistivity, ρ_a, is calculated:

$$\rho_a = \pi a N (N+1)(N+2) \frac{\Delta V}{I} \quad . \qquad \text{(III-1)}$$

The apparent resistivity is defined as the resistivity of a homogeneous half-space required to produce the observed potential difference at the receiver electrodes for the known current injected at the transmitter electrodes and for the geometric configuration of the four electrodes. The calculated values of ρ_a are conventionally plotted at the intersection of lines angling down at 45^o from the centers of transmitting and receiving dipoles to produce an apparent resistivity pseudo-section (Hallof, 1957; Marshal and Madden, 1959). The locations of point current sources and the positions at which the potential is calculated are the coordinates on the x-axis.

As has been demonstrated in Part II of this report (Beyer, 1977b), the interpretation of dipole-dipole apparent resistivity pseudo-section data obtained over laterally inhomogeneous structures requires, at very least, a knowledge of modeling results. Dey and Morrison (1976) and Dey (1976) have described a computer code for calculating the apparent resistivities over arbitrarily shaped two-dimensional structures. Such structures are of infinite extent in one lateral direction, which by definition is the geologic strike direction. The numerical formulation is a finite difference technique which calculates the potential

distribution at grid nodal points due to point current sources at desired locations in a half-space consisting of a resistivity model.

This computer program has been used extensively in a rather successful effort to invert (by trial and error) the dipole-dipole resistivity data obtained in Grass Valley, Nevada.

Resistivity methods involve forcing d.c. electrical current into the ground between electrodes at two points and measuring the resulting potential difference at two other electrodes. While the measurements are made under d.c. conditions, the transmitting current is a long-period square wave to separate signal from noise. The amplitude of the receiver voltage is measured only after transient effects due to electromagnetic coupling or induced polarization die out.

The dipole-dipole resistivity method has traditionally been used by the mining industry for mineral exploration. The dipole length commonly used is 400 feet (122 meters) and occasionally 800 feet (244 meters), with a maximum separation distance of 4 or 5 times the dipole length. As applied to geothermal exploration, to explore to the depths of interest in the conductive sediments of Basin and Range valleys, the Lawrence Berkeley Laboratory field crews commonly used dipole lengths of 1 kilometer with separations of N = 10 or greater. The resistivity of the sedimentary basin fill can easily be as low as 5 ohm-meters. Equation (III-1) can be used to estimate the amplitude of the observed potential difference as a function of the injected current; for these specifications ΔV will be 1.2 μ volt per ampere at N = 10. Hence, the injected current must be substantial, or the signal detection system must be sophisticated.

As a means of most quickly getting into the field the brute force

method was used quite successfully. A 60 kilowatt motor-generator set with rectifying and switching circuitry was designed, built, and mounted on a one ton, four-wheel drive truck.

The 60 kw aircraft type generator which was used yields 3-phase power at 400 Hz with an output voltage which can be continuously varied from 30 to a maximum of 203 volts. It operates at 6000 rpm, has self-contained blowers for cooling, and is small and light weight (60 kg). The generator is powered through a step-up V-belt drive train by a Hercules 120-horsepower industrial engine equipped with a governor for maintaining constant speed under varying load conditions.

The bulk of the resistance in the circuit through the ground is at the current electrodes, which are metal plates or sheets of window screen buried at shallow depths. This contact resistance, depending upon the number of plates emplaced and the type and moisture content of the soil, may range from 5 to over 100 ohms. To get significant current into the ground the output of the generator goes into a 3-phase step-up transformer which, when the secondary windings are connected in a Y-configuration, boosts the voltage to 707 volts rms, with full power (60 kw) taps at 565 volts. The transformer secondary can also be connected in a Δ-configuration to give output voltages of 408 and 327 volts rms. With these voltage options available the transmitter can be approximately impedance matched to the ground.

After the transformer, the high voltage 3-phase 400 Hz signal goes into a power supply consisting of two full-wave SCR rectifying bridges, wired with opposite polarity. Control circuitry, which is electrically isolated from the high voltage system with light emitting diodes, alternately switches on one and then the other bridge to produce the output current square wave. The switching rate can be varied between

1 and 99 seconds. The full-wave rectified signal has, depending upon the transformer configuration used, maximum D.C. levels of approximately ± 1000, ± 800, ± 577, or ± 462 volts, with a ripple of less than 10%. The maximum current capability is 100 amperes.

The transmitter system is controlled and the current amplitude monitored at a remote control box connected by a 100-foot long umbilical cord. This enables the operator to be removed from the noise made by the motor-generator set.

Additional information, including circuit diagrams, regarding the details of the high power resistivity system (motor-generator set, remote operator controls and monitoring, safety interlocks) can be obtained from the Manager, Special Projects Group, Lawrence Berkeley Laboratory, Berkeley, California 94720.

Number 4 AWG welding cable was used as transmitter wire to handle the 100 ampere current.

To measure the signals at the receiver dipoles battery-powered strip a chart recorders were used: The Esterline Angus T171B and the Simpson Model No. 2745 x-y, y-t Recorder. Non-polarizing copper-copper sulfate porous pot electrodes were used to ground the receiver dipoles. Signal amplitudes down to 20 microvolts were measured with these instruments.

Later in the program a smaller transmitter unit was built. The motor-generator set is a 25 kw, 4000 rpm, 3-phase aircraft type generator powered by a Volkswagen engine, which is manufactured as a unit by Geotronics, Inc., Austin, Texas. To this was added rectifying and switching circuitry similar to that discussed above, with the exception that mechanical relays rather than LED's were used to isolate

the high power components.

This lower power system was used in conjunction with clock-synchronized signal averagers which were designed and built for the project (Morrison, 1975). Polarity reversals of the transmitter at a period of 10 seconds are controlled by a crystal clock oscillator. At the receiver, a signal averager, whose clock is synchronized with that at the transmitter, digitally samples and averages voltage variations which are synchronous with the transmitter polarity reversals. A delay time of two seconds is introduced before sampling begins to eliminate the effects of electromagnetic coupling and induced polarization. The averaged receiver voltage is displayed digitally every 100 seconds (10 cycles).

The signal averagers were found to increase the data accuracy significantly such that larger transmitter-receiver separations were possible while reducing the power requirements of the transmitter. The source current could generally be kept below $\pm$ 30 amperes, which allowed the use of no. 10 gauge wire, and meant that less effort had to go into the reduction of contact resistance at the current electrodes. Also, data reduction was simplified and could accurately be performed in the field during the course of the survey. In addition to the synchronous detectors the strip chart recorders were still used to insure that a reasonable signal was being received and to produce a permanent record.

To perform a dipole-dipole survey at the scale discussed above--1 km length dipoles and separations of 10 km or greater--the logistics becomes a significant problem. The LBL field crew generally consisted of four people. Once the dipole-length distances along a profile line

were surveyed, the crew would devote two or three days to setting up a site for the motor-generator set from which several successive transmitter dipoles could be energized. Several current electrodes were emplaced which would involve burying the sheets of metal or screen in shallow pits with sprinklings of rock salt and detergent, and then flooding the filled pits with water. Wire capable of carrying the transmitter current was attached to each electrode and run to the generator location. With this accomplished a single operator at the transmitter could connect the appropriate wires to inject current at several dipole locations.

To receive the signal efficiently, two people, each with a chart recorder and a signal averager, occupy stations with receiver dipoles extending in both directions. With a particular transmitter dipole being energized each of them can alternately hook up one and then the second receiver dipole to the measuring equipment. This process is repeated as the transmitter operator successively energizes a series of dipoles. The set-up is illustrated in Figure III-4. During these measurements the fourth crewperson can be reeling out wire for new receiver locations.

As a result of the high data density, and the fact that current electrodes must be emplaced at every interval along the survey line if a complete pseudo-section is to be obtained, the dipole-dipole method is very slow. For 1 km length dipoles, and data obtained to a separation of ten dipole lengths, about five data points were obtained per day. This average includes the time required for the four-person field crew to set up the transmitter for several dipole source locations. When 500-meter length dipoles were used the average number of resistivity

values obtained per day increased to about ten.

As a note of warning to those interested in performing large scale electrical resistivity surveys, a peculiar problem was encountered as a result of having many long lengths of wire lying parallel to one another on the ground. On a particular occasion the amplitude of the long-period voltage square wave at the receiver dipole was found not to behave linearly with the amplitude of the transmitter current. Ultimately the problem was traced back to the high power circuitry at the transmitter. The 400 Hz 3-phase generator output is full-wave rectified with silicon controlled rectifier bridges. Each time an SCR switches on it produces a transient oscillation at several k Hz. The amplitude of this transient decreases as the voltage across the SCR is increased. This high frequency signal was found to be transmitted along any wire lying in the vicinity of the transmitter, whether or not it was grounded or actually connected to the generator. Furthermore, this high frequency noise would couple into any wire lying near and parallel to one emanating from the vicinity of the transmitter. By this means the noise could couple into a receiver dipole wire, producing erratic and non-linear behavior of the observed potential difference. The explanation of this appears to lie in the fact that at several k Hz the capacitance of a 1 km length of wire will allow for high current flow. The current polarizes the copper-copper sulfate electrode at the end of the dipole distant from the recording instrument, resulting in the erratic behavior.

The solution, of course, is simple. Successive lengths of wire cannot be allowed to lie parallel to both transmitter and receiver dipoles which are in use. If a piece of wire which overlaps with

both is cut at any point between the two, the high frequency noise will not be coupled through the system.

As is recorded in Figure III-5, other practical problems have been found with the use of long wires stretched across Basin and Range valleys.

THE INTERPRETATION OF TELLURIC AND D.C. RESISTIVITY DATA FROM GRASS VALLEY, NEVADA

Grass Valley is located in the Basin and Range physiographic province in north central Nevada. It lies within an area of higher than normal heat flow, the Battle Mountain heat flow high (Sass, et al., 1971). At the edge of Grass Valley, about 80 kilometers south of the city of Winnemucca, is Leach Hot Springs, which has a surface flow of about 130 liters per minute (Olmsted, et al., 1975), and surface temperatures which reach 94°, boiling at their 1430 meter altitude.

Grass Valley is bounded to the west by the East Range, and to the east by the Sonoma and Tobin Ranges. South of the hot springs area the valley is constricted by the Goldbanks Hills. The distribution of major lithographic units is illustrated in Figure III-6, and on a separate map, Figure III-7, is shown the intricate fault and lineament pattern, based heavily upon aerial photography interpretation (Noble, 1975). As is commonly true of Basin and Range hydrothermal springs, Leach Hot Springs is located at the intersection of two fault systems. The hot spring area (denoted by a small circle near the center of Figure III-7) lies on a northeast-southwest trending fault (Hot Springs Fault) at its intersection with the NNW-SSE trending range-front fault system. Opalized sinter deposits are found in the vicinity of the hot springs.

Most of the geophysical data were obtained along the survey lines, shown with 1 kilometer intervals in Figure III-8. Many of the lines are oriented northwest-southeast, roughly the principal axis direction of the telluric field ellipse. Other lines were used as tie lines or to

investigate features of interest as the survey progressed. In Appendix III-A (Figures III-A1 through III-A17) much of the data obtained along these lines is presented.

As they will be particularly useful for the analysis of the telluric and resistivity data, the complete Bouguer anomaly gravity map and P-wave delay map are reproduced in Figures III-9 and III-10, respectively. The dominant gravity feature is a NNW-SSE trending low along the eastern side of Grass Valley, which, in conjunction with seismic data, defines the region of greatest sedimentary thickness. There is a gradual thinning of the sedimentary section to the west. At the eastern edge of the gravity trough the steep gradient reveals a high-angle range-front fault. In the vicinity of Leach Hot Springs is a westward bulge in the range-front fault gravity gradient. This anomaly correlates with a negative P-wave delay--an advance over bedrock travel times--and is interpreted as resulting from extensive silicification of the sedimentary and a portion of the Paleozoic bedrock section in the area of the hot springs. Shallow drilling through Hot Springs Fault near 1 km E on Line E-E' showed the fault to be highly silicified.

During the exploration of Grass Valley it was determined that the bipole-dipole mapping method was a much less cost-effective reconnaissance technique than the E-field ratio telluric method, and that the bipole-dipole data could in some situations be misleading. (The reasons will be discussed later.) As a result there is considerably more coverage using the ratio telluric method, and it was more heavily relied upon in developing the interpretation. For these reasons there are presented below a detailed analysis of the telluric and dipole-dipole

resistivity data, and a separate discussion of the bipole-dipole mapping data. It will be useful, however, when viewing the E-field ratio telluric data in the geophysical data profile composites in Appendix III-A, to note the correspondence between them and the profile line plot of the bipole-dipole resistivity data. (The notations TX1 through TX5 refer to five bipole transmitter locations, which are shown in Figures III-23 through III-32.)

The Analysis of Telluric and Dipole-Dipole Resistivity Data

Line E-E' extends across Grass Valley from southeast to northwest, passing about 1 km NW of Leach Hot Springs. The line is oriented approximately parallel to the principle axis of the observed telluric field ellipse, and at 45^{o} to the local basin and range structure. The general bedrock topography along the line can be inferred from both the profile gravity and P-wave delay data in Figure III-A5. In the vicinity of 3 km E, dense, high velocity, tertiary gravels and Paleozoic rocks are faulted to the surface. To the NW lies a 2.5 km wide area of relatively thin sediments. At 0.25 km E a major steeply-dipping fault markedly increases the sedimentary section thickness. To the NW of 4 km W the sediments gradually thin, with indication of a horst at 10 km W. Both gravity and P-wave delay data display a regional gradient increasing to the NW along the line.

Additionally, the gravity contour map in Figure III-9 suggests that in the vicinity of the major range-front faulting at 0.25 km E,

Line E-E' is perpendicular to the structure. It is at this location that a fault--the one which apparently controls Leach Hot Springs--splays off to the SW from the SSE trending range-front fault system (see Figure III-7). The gravity bulge at Leach Hot Springs coincides with a very high P-wave velocity and is interpreted as a region of extensive silification. The resistivity structure may well be similar to the density structure.

Figure III-11 presents dipole-dipole apparent resistivity data for 500-meter dipoles along the eastern end of Line E-E'. To the west of 2 km W, the section appears to be quite uniformly layered containing a massive conductive zone overlain by a resistive surface layer. Evidence of a resistive basement is seen at the largest N-spacings. The eastern half of the pseudo-section is quite complex, but some distinctive features can be resolved. (1) The fault at 3.0 km E is made evident by the high apparent resistivity gradient across the diagonal down-to-the-left from this location (note the location of the 15 Ω-m contour). (2) The major range-front fault at 0.25 km E produces the apparent resistivity gradients across lines extending diagonally down-to-the-left and down-to-the-right from this location. The pseudo-section is complicated by the interference of the patterns resulting from the two faults and from varying resistivity of the sedimentary layer overlying the resistive bedrock between the two faults. (3) At 2.0 to 2.5 km E this surface layer is particularly conductive as is demonstrated by the fact that apparent resistivities down-to-the-left and down-to-the-right from this location are lower than adjacent values. A dip in both 0.05 and 8 Hz telluric profiles (Figure III-A5) supports this interpretation. (4) The large conductive region enclosed by the 3 ohm-meter contour

extends up closer to the surface in the vicinity of 0.0 to 0.5 km E as is seen by the low apparent resistivities down-to-the-left from this location.

Figure III-12 shows a pseudo-section which has been calculated numerically for the two-dimensional resistivity structure at the bottom of the figure. The profile line is at 45° to strike, and the structure is a projection in this direction. The model contains the points mentioned above, and the pseudo-section is a good representation of the field data in Figure III-11.

If the cross-section of the model in the profile line direction is kept the same (to maintain the identical location of electrodes with respect to contacts), but the model is rotated to be perpendicular to the profile line, the pseudo-section will be modified to that shown in Figure III-13. The contour lines depict anomalies which are somewhat closer in form to those seen in the actual data, suggesting that the survey line may, in fact, be more nearly perpendicular than at 45° to the local structure. The lowest apparent resistivities in this modeled pseudo-section are somewhat lower than those seen in the actual data, but could be adjusted by a slight increase in the resistivities of the 1 and 4 ohm-meter regions in the model.

The dipole-dipole method is not particularly sensitive to the resistivity of basement rocks lying beneath a more conductive sedimentary section unless one or both dipoles is located on the bedrock, e.g., at the edge of the valley (Beyer, 1977b). This is illustrated by Figure III-14: a model identical to that shown in Figure III-12 is used, with the exception that the bedrock resistivity is reduced from 150 to 20 ohm-meters. Only the apparent resistivities down-to-the-left from

3.25 and 3.75 km E are significantly affected. The apparent thickness of the large conductive region enclosed by the 3 ohm-meter contour is virtually unchanged. On the other hand, a similar model with the conductive region extending to a depth of 1.25 km (not shown) rather than 1.5 km shifts the 3 ohm-meter contour up to N=7. Thus, the dipole-dipole method, while not being sensitive to the resistivity of a resistive basement, does show significant response to variations in the depth to the basement.

Dipole-dipole resistivity data along Line E-E' was also obtained using 1 km-length dipoles. The pseudo-section in Figure III-15 displays features which are nearly identical to those observed using 500 meter dipoles. Comparison should be made for apparent resistivity values having the same maximum electrode separation, i.e., N = 1, 2, 3, 4, 5 for 1 km dipoles correspond to N = 3, 5, 7, 9, 11 for 500 meter dipoles, respectively.

The 1 km dipole-dipole data at the eastern end of the pseudo-section display generally increasing apparent resistivities at very large N-spacings. The values greater than 10 ohm-meters are obtained for transmitter-receiver arrays straddling the massive conductive region such that dipoles lie over the thin alluvial layer to the east of 0 km and over a thin sedimentary section to the west of 7 km. Thinning sediments to the west of 5 km W are clearly indicated by the gravity and P-wave delay data (Figure II-A5). In light of this the apparent resistivities at large N-spacing in the western portion of the pseudo-section are exceptionally low. For an extreme case such as a 20 ohm-meter basement overlain by a 0.5 km thick, 4 ohm-meter alluvial layer, apparent resistivities exceed 10 ohm-meters for N greater than 2, when 1 km

dipoles are used. The indication, then, is that a massive portion of the bedrock must be highly conductive. Such an explanation would seem improbable were it not for the fact that 23 kilometers to the south at the edge of Buena Vista Valley, Lawrence Berkeley Laboratory geophysical investigations revealed a massive low resistivity anomaly (modeled at 1 ohm-meter) which is several kilometers in lateral extent. Shallow drilling encountered graphitic, pyritic Paleozoic Valmy formation and a graphitic Mesozoic limestone (Goldstein, et al., 1976). It is reported (Hohmann, personal communication) that Bear Creek Mining Company (Kennecott) has also encountered graphitic, pyritic limestones in Nevada which cause resistivity lows. Similar conductive rock may lie beneath the Grass Valley sediments at the western end of Line E-E'.

The tightly confined anomaly enclosed by the 5 ohm-meter contour at 9 km W and N = 7 is a feature which, based upon numerical model results for simple resistivity structures (Beyer, 1977b), should be caused by two near-surface conductive inhomogeneities at 4-5 km W and at 13-15 km W. However, the 8 Hz E-field ratio telluric data (Figure III-A5) reveal no such anomalous features in the near-surface material. The 0.05 Hz tellurics indicates that a deeper portion of the section is conductive at these locations. This is an unresolved dilemma: modeling attempts have failed to reproduce such a tightly confined anomaly at large N-spacing for features buried greater than about one-half dipole length, yet the dipole-dipole data give no indication of a conductive feature at 4-5 km W (see Figure III-11).

Figure III-16 depicts a model which is moderately successful at reproducing the actual 1 km dipole-dipole pseudo-section. The structure at the eastern end of the line is similar to that obtained for the

modeling of the 500 meter dipole data. The 12 ohm-meter block at 4-5 km W is an attempt at slightly reducing the apparent resistivities on diagonals down from this location without producing an 8 Hz telluric anomaly. The effect is trivial, however, and is far exceeded by that resulting from the 3 ohm-meter block at greater depth (beneath 4-6 km W). This anomalous feature, and the larger 3 ohm-meter region farther to the west, are deemed to be masses of graphitic, pyritic bedrock. The shapes and resistivity used are highly conjectural; the lack of the shallow apparent resistivities to the west of 9 km W makes more precise modeling impossible. However, features of this sort are required to obtain low apparent resistivities at large N-spacing beneath 8 km W (see Figure III-16) and to produce a 0.05 Hz telluric low at 10-14 km W.

As a result of E-field ratio telluric measurements employing only one component of the electric field and no magnetic field information, it is not appropriate to perform detailed modeling of this reconnaissance method. However, if the E-field ratio telluric response is calculated over the model used to match the 1 km dipole-dipole data, the curves in Figure III-17 are obtained. (A computer code employing the finite element approach to calculate the response of plane electromagnetic waves incident upon two-dimensional resistivity structures, written by Ryu (1971) with modifications by Lee (personal communication), has been used.) As the 0.05 Hz total field telluric ellipse was observed to be roughly parallel to Line E-E', with ellipticity less than 0.3, the transverse magnetic (TM) mode was used for the calculation. The primary discrepancy between the modeled 0.05 Hz curve and the observed data is that the former displays anomalous responses with about twice the amplitude as those seen in the actual data. This effect

could be eliminated by reducing the bedrock resistivity; as has been discussed above, the dipole-dipole method is very insensitive to this parameter. Additionally, the dipole-dipole model for a survey line perpendicular to strike (Figure III-13) would allow for some reduction in both the conductivity and thickness of the 1 ohm-meter region. Another major discrepancy indicates that resistive basement material must display less relief between 5 to 11 km W. However, the major components of the field data are illustrated: a significant increase in the telluric field at the edges as well as in the central portion of the valley; a sharp rise over the major fault at 0.25 km E; a dip over conductive sediments at 2.5 km E.

At 8 Hz telluric ratio data over the same model structure (Figure III-17) is very similar to the field data. The telluric field does not significantly penetrate the 0.5 km-thick surface layer at this frequency, and displays a conductive anomaly in the vicinity of the Hot Springs, probably resulting from saturation of a thin layer of alluvium.

For the purpose of detailing in the immediate vicinity of Leach Hot Springs, a 250 meter dipole-length dipole-dipole survey was run along a portion of Line A-A'. The southern portion of the resistivity survey line coincides with Line A-A' as shown in Figure III-8, commencing at 0 km and extending to the northwest. Where Line A-A' bends northward near Leach Hot Springs, the resistivity line continues straight ahead such that 5.0 km N falls on Line E-E' at 0.75 km W. Figure III-18 displays an excellent numerical model fit to the dipole-dipole field data. Significant aspects of the model are (1) the 30 ohm-meter block from 3.0 to 3.5 km N, which represents resistive spring deposits, (2) the possibility of more extensive silicification to the north and northwest

(120 ohm-meter region), and (3) an increase in both the thickness and conductivity of sediments to the northwest of the Hot Springs Fault at 3.5 km N. There is an apparent contradiction between the seismic and gravity data, and the model in Figure III-18, which indicates that the resistive spring deposits at 3.0 to 3.5 km N do not extend down to bedrock. A reasonable explanation for this discrepancy is that the actual resistive structure is roughly circular in plan, whereas, it has been modeled as a two-dimensional feature with infinite lateral extent. The model has been devised to provide a conductive path for current flow beneath the resistive zone, while actually the conductive path is around the sides of the spring deposits. An attempt at fitting the Line A-A' data with the identical model having a 100 ohm-meter, rather than 20 ohm-meter basement, was unsuccessful. As there are Quarternary-Tertiary gravels outcropping one kilometer to the east of Leach Hot Springs (Figure III-6), the resistivity data suggest a moderately conductive layer of these gravels overlying more resistive Paleozoic basement between 0.0 and 3.5 km N on Line A-A'.

The 8 Hz telluric data along Line S-S' (Figure III-A17) which runs east-west through the hot springs area is not totally consistent with the resistivity model from Line A-A' (Figure III-18) in that it suggests a conductive surface zone at the location of the 30 ohm-meter block representing spring deposits (at 3.0 to 3.5 km N). However, a thin conductive surface layer would not be incompatable with the modeled data. The 0.05 Hz telluric data on Line S-S' display high resistivity associated with the major range-front fault and spring deposits east of 0.5 km W.

Parallel to Line E-E' and about 2 km to the southwest lies Line B-B'.

The contoured gravity data in Figure III-9 demonstrate that east of 0 km, Line B-B' skirts the southwestern edge of the silicified region and traverses the range-front fault system at an oblique angle. The profile line geophysical data are displayed in Figure III-A2. Dipole-dipole resistivity data suggest a broad conductive feature with a shallow depth of burial, centered at 0 km, and a surficial resistive layer west of 2 km W. The telluric ratio data are consistent with such a model, and in addition, indicate abrupt near-surface resistivity lows east of 1.5 km E, and at 5.25 and 6.75 km W. Comparison of the 0.05 Hz and 8 Hz data indicates that the latter two resistivity discontinuities do not reach the surface (lest the anomaly amplitude be the same at both frequencies), yet lie within the surface layer at a depth penetrated by the 8 Hz signal. The broad low at the center of the E-field ratio profile is not centered over the dipole-dipole anomaly because the 0.05 Hz telluric field is more responsive than d.c. resistivity methods to the rising resistive basement and/or spring deposits east of 0 km.

An entirely satisfying two-dimensional model fit to the Line B-B' dipole-dipole data has proved to be elusive. One of the better of many attempts is depicted in Figure III-19. The arcuate shape described by the 4 ohm-meter contour in the field data is similar to the anomaly which would be produced by a three dipole-length wide, very thin, conductive inhomogeneity at a shallow depth in an otherwise homogeneous half-space (Beyer, 1977b). However, gravity and seismic (Beyer, et al., 1976) data dictate a sedimentary section over one kilometer thick at 0 km on Line B-B', and it is reasonable to assume that this might be conductive at depth as appears to be the case along Line E-E', two kilometers to the north. Additionally, the dipole-dipole data indicate

a thick conductive layer (∿3 ohm-meters) west of about 2 km W. This thick, laterally extensive conductive model tends to broaden the low apparent resistivity anomaly pattern and eliminate the limbs which are observed down-to-the-left and down-to-the-right from 0 km.

A plausable explanation for the mediocre fit of the model data is that Line B-B' runs past the edge of the densified region around the Hot Springs. The conductive anomaly seen at N = 2 in the pseudo-section may be caused by water-saturated sediments surrounding the silicified zone; these would constitute a thin, steeply-dipping conductive feature off to the side of the survey line. While two-dimensional modeling is inappropriate for such a situation, model studies (Beyer, 1977b) do suggest that the conductive feature is considerably thinner than that shown in Figure III-19.

A thick conductive section northwest of 2 km W is required by the dipole-dipole data. This appears to be in contradiction to the concept of a thinning sedimentary section as is indicated by the gravity data (after allowing for a regional gradient of about 0.5 milligal per kilometer, increasing to the northwest). This situation would be resolved by graphitic, pyritic rocks in the Palezoic basement as was proposed as a solution to similar observed data and model results along the western portion of Line E-E', 2.5 kilometers to the north.

Lines M-M' and N-N' have a point of mutual intersection with Line B-B' at 0 km (Figure III-8) near the center of the conductive anomaly. Dipole-dipole resistivity data for each of these lines are presented in Figures III-A12 and III-A13., respectively. (The letters across the tops of these figures indicate intersection points with other survey lines.) In all cases the anomaly is seen to be shallow, and found to have

lateral boundaries in all directions except to the north.

The limited depth extent is perplexing as the feature lies at the center of the gravity "trough" which runs the length of Grass Valley (Figure III-9). It also coincides with the southwestward extension of Hot Springs Fault (Figure III-7). Perhaps hydrothermal water is being injected into the sedimentary section at a relatively shallow depth along a ridge of silicified sediments overlying Hot Springs Fault across the deep basement of the valley.

To the north of 3 km S the Line M-M' dipole-dipole data display the thick conductive section and resistive overburden layer which, on the basis of the Line E-E' data have been modeled as a 1 km-thick, 1 ohm-meter feature overlain by a 0.5 km-thick, 14 ohm-meter layer (Figure III-12). At the intersection of Lines M-M' and E-E', the former displays lower apparent resistivities at greater N-spacings because the survey line is oriented parallel to strike along axis of the gravity low, the area of greatest sedimentary thickness.

At the northern end of the gravity trough along the eastern edge of Grass Valley the geologic section displays increased density (note the closure at the top of Figure III-9)--the sedimentary section either thins or becomes more dense. To the south of the gravity closure the Line M-M' data indicate increased sedimentary resistivity north of 9 km N. (The deflection of the 4 ohm-meter contours down-to-the-left from 2.5 and 3.5 km N result from low surface resistivity in this location.) While a shallower depth to basement is quite likely, it also appears that the sedimentary section may undergo a facies change or a reduction in the degree of saturation or permeability north of 4 km N on Line M-M'.

Modeling of the Line M-M' resistivity data is unnecessary because an interpretation consistent with other modeled results is quite straightforward for this simple pseudo-section. Furthermore, the numerical algorithm used is incapable of modeling data obtained parallel to strike.

Similarly, the dipole-dipole data along the northeastern half of Line N-N' cannot be modeled using two-dimensional methods. An interesting effect was observed for the receiver dipole at 3 to 4 km NE and transmitters located to the southwest. The received voltage was noisy and very low in amplitude, resulting in the anomalously low apparent resistivities down-to-the-left from 3.5 km NE. An explanation appears to be that the survey line lies adjacent to the resistive depositional feature around the hot springs, and then traverses the major range front fault at a very oblique angle. The dipole source field will be deformed out into the valley sediments resulting in minimal current flow in the resistive bed rock. The receiver dipole at 3.5 km NE lies in a pocket of conductive material isolated from the valley sediments, hence, the surrounding bedrock shields it from high current flow, and the low material resistivity makes for an exceptionally low observed voltage. This low resistivity pocket is also observed in the Line F-F' telluric data (Figure III-A6) at 3 km E, and in the gravity data as a small circular low. At this location there is an outcropp of Tertiary sedimentary rocks among Quarternary-Tertiary gravels (Figure III-6).

Telluric data further to the northwest along Line F-F' is consistent with that from other methods. The lowest E-field ratios are observed between 2 and 3 km W where the line traverses the thickest sedimentary section as seen in the gravity data, and where Line M-M'

(at 4 km N in Figure III-A12) indicates a significant conductive anomaly at depth, and, to a lesser extent, in the surface layer.

At the southern end of Grass Valley Line D-D' extends in a northeast-southwest direction, approximately perpendicular to the range fronts. The geophysical data obtained along this line are shown in Figure III-A4. The profile gravity, P-wave delay, and telluric data indicate a dense, resistive feature at 5.0 to 6.5 km W. On the gravity map (Figure III-9) this feature appears as a "nose" in the contours 4 kilometers north of the Goldbanks Hills. Dipole-dipole resistivity data appear not to reveal this anomaly. What is actually the case, however, is that while the apparent resistivities at N = 1 indicate that a resistive feature does not lie near the surface, the low apparent resistivity anomaly (enclosed by the ρ_a = 7 and 8 ohm-meter contours) is caused by conductive regions to the east and west of a resistive anomaly located at 5 to 6 km W. Such a structure is clearly suggested by the telluric data, and as seen in Figure III-20, is consistent with an excellent two-dimensional numerical model fit to the dipole-dipole data. The model depicts a resistive surface layer similar to that observed to the north, underlain by two regions of more conductive sedimentary material separated by a resistive high in the electrical basement. Modeling of the dipole-dipole data clearly indicates that the deep sediments along Line D-D' are at very least twice as resistive as those observed in the gravity trough farther to the north in the valley.

The E-field ratio telluric data on Line D-D' display an interesting effect due to the orientation of the line with respect to the polarization direction of the observed telluric field. At 2 to 5 km W the

major E-field axis was measured and found to remain steady ($\pm$ 10°) in a northwest-southeast direction, which is at 75° to line D-D'. Under such conditions, with the profile line nearly perpendicular to the principal electric field axis, small deviations in the telluric field direction can produce large changes in the E-field ratio measured at two successive stations along the profile line, resulting in an amplification of E-field ratio telluric anomalies (Beyer, 1977a). The anomaly over the resistive feature near the center of Line D-D' is approximately twice the amplitude that would be observed for the E-field parallel to the profile line, and is considerably larger than any telluric anomaly observed over the sedimentary section along the other telluric lines in Grass Valley. The others are oriented more nearly parallel to the principal telluric field axis.

The overshoot, and then drop, in the E-field ratio at both ends of Line D-D' can be explained by the behavior of the telluric field at a surface resistivity contrast such as the sediment-bedrock contact at the edge of the valley. Upon encountering resistive material the electric field axis rotates perpendicular to the contact, which in this case is parallel to the traverse line and produces an E-field ratio high. With greater distance from the contact the axis rotates back toward that of the incident field, which can then reduce the E-field ratio anomaly, depending upon the profile line direction with respect to the telluric ellipse. At the eastern end of the line, however, the bipole-dipole resistivity data indicate that a more conductive feature is encountered in the Quarternary-Tertiary gravels.

Two-dimensional numerical modeling of the amplified E-field ratio telluric anomalies has been attempted, using the structure derived on

the basis of dipole-dipole resistivity modeling. However, it is impossible to reproduce the observed telluric field--with a polarization direction of about 45° to strike, an ellipticity less than 0.3, and either direction of rotation--without putting unrealistic constraints on the incident field. If a two-dimensional model such as that illustrated in Figure III-20 is used, the observed electric field over the thicker conductive areas rotates to be essentially parallel to strike regardless of the polarization direction and ellipticity of the incident field (except, of course, for a nearly linearly polarized incident electric field perpendicular to strike). The problem lies in the fact that Grass Valley does not look two-dimensional to 0.05 Hz incident electromagnetic fields, so two-dimensional modeling is not appropriate to a quantitative analysis of the telluric response along a line such as D-D' which is not approximately parallel to the principle electric field direction. However, with knowledge of the polarization direction, a qualitative interpretation is consistent with other data and appears to be quite valid.

At its southeastern end Line G-G' commences on Paleozoic rock in the Sonoma Range and extends to the northwest across valley sediments. The 0.05 Hz E-field ratio telluric data (Figure III-A7) indicate high resistivity at this end of the line (5 to 6 km E), with a steady decrease to the northwest, reaching a low at 2 km W. At 1.4 km E the line intersects Line D-D' (at 3.5 km W) over the axis of the gravity low. However, the dipole-dipole modeling for line D-D' (Figure III-20) indicates a more resistive sedimentary section than is found farther to the north. Line G-G' continues northwestward over thick sediments with decreasing resistivity, reaching a low at the intersection with Line

N-N' (at 2.9 km SW), at the edge of the shallow thin conductive anomaly discussed previously. To the northwest of Line N-N' the gravity data indicate thinning sediments; the tellurics appropriately indicate increasing resistivity.

Line K-K' lies 1 to 3 kilometers south of Line G-G'. The 0.05 and 8 Hz telluric profiles (Figure III-A10) are very similar, which implies that the anomalous resistivity structure is not buried at great depth beneath conductive material. However, the somewhat greater relief in the 0.05 Hz data east of 5 km W suggests that the lateral resistivity contrasts are not entirely surficial. The tellurics east of 1.5 km E display a very conductive anomaly, coincident with rapidly thickening sediments south of Panther Canyon (see the gravity map, Figure III-9). The resistive high at 1 km E coincides with that observed at the intersection with Line A-A' tellurics (4 km S in Figure III-A1), and with north-south trending faulting observed in the sediments (Figure III-7). As was indicated by the tellurics on Line G-G', the sediments in the gravity trough (traversed by Line K-K' at 0 to 1.5 km W) are not exceptionally conductive. The resistive feature encountered along Line D-D' (at 5 to 6 km W) is clearly evidenced in the Line K-K' data at 3 to 4 km W. To the west of this the gravity map indicates somewhat thickening sediments, which the telluric data indicate are particularly conductive.

Line H-H' is oriented east-west through the Grass Valley saddle between the Goldbanks Hills and Panther Canyon. The line lies over thin, relatively resistive sediments north of the Goldbanks Hills, which result in an E-field ratio telluric high (Figure III-A8). The decreasing telluric field west of 4 km W, with an abrupt rise at 6.75 km W, is

similar to the telluric anomaly observed in model results for the electric field perpendicular to the strike of a semi-infinite, horizontal conductive slab extending, in this case, to the east of 6.5 km W (Beyer, 1977a). However, it is somewhat unlikely, given the orientation of Line H-H' with respect to the geologic structure, that the strictly transverse magnetic (TM) mode electric field is being observed along this line. Another interpretation is that the sediments are thicker at this location (as indicated by gravity data) and that they serve as a subterranean channel for groundwater flow out of the canyon separating the East Range and the Goldbanks Hills (Figure III-7).

At 0 km Line H-H' traverses the gravity saddle point between the northern and southern parts of Grass Valley, and indicates that the sedimentary section in this constricted portion of the gravity trough are very resistive. To the east of 1 km E, however, the conductive area south of Panther Canyon is encountered.

Telluric data on Line R-R' (Figure III-A16) adds confirmation to features already mentioned. Commencing with high electric field over the resistive Palezoic rocks of the Goldbanks Hills (2 to 3 km W), the line displays increased conductivity over valley sediments (0 to 1 km W), a resistive anomaly over the faulted area near the intersection with Line A-A' (0.5 to 1.5 km E), and a conductive anomaly southwest of Panther Canyon. East of 4 km E the conductive sedimentary section appears to thin markedly, and the E-field ratio displays anomalies which are probably a function of the alluvial thickness in Panther Canyon.

Lines P-P' and Q-Q' traverse the southern Grass Valley goose neck between the Goldbanks Hills and the Tobin Range. The E-field ratio

telluric data along both of these lines (Figures III-A14 and III-A15) indicate a highly conductive section. Correlation with the substantial gravity low in this area suggests that the conductive anomaly is caused by saturated sediments. The telluric high seen at 1.25 km W on Line Q-Q' occurs at a small topographic high along a north-south trending ridge at the eastern edge of the Goldbanks Hills. The feature is seen in the Line P-P' telluric data at 0.25 km W. These anomalies correlate with the north-south trending faults associated with the resistivity high observed on Line H-H' at 0.5 km E, R-R' at 0.75 km E, A-A' at 4.5 km S, K-K' at 1.25 km E, and G-G' at 5 km E.

To further investigate the highly conductive sedimentary valley south of Panther Canyon dipole-dipole resistivity surveys using 500-meter length dipoles were performed along the eastern half of Line H-H' and along Line T-T'. These lines are perpendicular to one another in a narrow portion of the valley, so two-dimensional modeling cannot be expected to yield an exceptionally accurate portrayal of the resistivity structure. Two-dimensional model results which fit the observed data should indicate a thinner conductive sedimentary section than actually exists because, at large N-spacings, the field data will display high apparent resistivities due to resistive bedrock along edges of the valley parallel to the survey line. However, modeling results should be reasonably accurate for small N-spacings and should yield an estimate as to the bulk resistivity structure at greater depth.

The dipole-dipole apparent resistivity pseudo-sections, along with modeling results, for Lines H-H' and T-T' are presented in Figures III-21 and III-22, respectively. The data indicate that near the intersection of the two lines (at approximately 2.5 km in both cases) lies

the center of a near-surface conductive anomaly. There is no surface expression of anomalous conditions such as springs, but shallow-drilling in the area has revealed an abnormally high heat flow (Sass, et al., 1976).

The Line H-H' pseudo-section clearly indicates the sediment-bedrock contact with the high apparent resistivity gradient down-to-the-left from 4.5 km E. The resistive feature seen in the telluric data (Figure III-A8) at 0 to 1 km E is not clearly defined in the pseudo-section, except for separations of N = 1 at 0.25 km W and 0.25 km E. The model which was derived (Figure III-21) indicates a thin, exceptionally resistive (100 ohm-meter) layer at the surface in this area, underlain by moderately conductive sediments with constant thickness. This model is not entirely consistent with the topographic indication that there is bedrock very near the surface in this area, unless the observed faulting has fractured it sufficiently to reduce the resistivity. A model with resistive material extending up near the surface at 0 km on Line H-H' yielded a very poor dipole-dipole fit to the field data. While the model in Figure III-21 probably indicates a thicker conductive section and a more resistive surface layer than actually exist at 0 km, the modeling does suggest that a section of moderately conductive (∿8 ohm-meter) material does lie beneath a more resistive surface sedimentary layer.

At its northern end Line T-T' transverses resistive Paleozoic rocks, overlain in places by a thin veneer of dry alluvium. The gently sloping 20-ohm-meter contour extending down-to-the-right from 0 km in the field data pseudo-section (Figure III-22) suggests a region of increasing conductivity and slowly increasing thickness to the south.

The near-surface conductive anomaly at the intersection with Line H-H' clearly extends to the south beneath a resistive surface layer south of 4 km S. Whether or not the conductive region modeled as 3 ohm-meters is truncated at about 7 km S is not fully determined by the dipole-dipole data. There is the suggestion of this in the slightly higher apparent resistivities down-to-the-left from 7.5 km S, but more data to the south is required for a definitive answer. Truncation of this conductive region does tend to increase the apparent resistivities deep in the pseudo-section for better agreement with the field data, however this is immaterial because, in fact, it is the truncation of the conductive anomaly at the edges of the valley parallel to the survey line which is responsible for the high apparent resistivities at depth.

The break in the 40 ohm-meter contour beneath 1 km S is purely an artifact of the pseudo-section, as is illustrated by the model results. The apparent resistivities down-to-the-right from 0 to 1.5 km N are reduced when the second dipole of the electrode array is located over the shallow conductive region.

Line A-A' runs NNW-SSE, roughly parallel to the range-front fault system along the eastern edge of Grass Valley. The 0.05 Hz telluric data plotted in Figure III-A1 display many of the features discussed above, and are well correlated with the gravity data (Figures III-A1 and III-9). The trace of the line can be found in Figure III-8. (1) At the northernmost end of the line is a telluric low reflecting a thick sedimentary section. (2) A slight high at 7 to 8 km N corresponds with somewhat thinner sediments as is also suggested by the gravity data. (3) At 3.5 km N the line traverses the hot springs area and displays the resistive sinter deposition at depth. (4) Between 2 km N and 3 km S

gravity data indicate a relatively uniform depth to basement, but the tellurics increases markedly to the south. This area has been interpreted to have an increasingly resistive sedimentary section to the south. (5) At 4 km S is the north-south trending resistive anomaly which separates the northern and southern portions of Grass Valley. (6) South of 4.5 km S the E-field ratio decreases sharply as the sedimentary section thickens and becomes highly conductive in the narrow portion of Grass Valley south of Panther Canyon.

The Analysis of the Bipole-Dipole Resistivity Mapping Data

Bipole-dipole data were obtained for five bipole transmitter locations in the vicinity of Leach Hot Springs, with a total of 333 receiver stations being occupied along several of the geophysical survey lines. Both apparent resistivity and apparent conductance have been calculated; these data are presented as contour maps in Figures III-23 through III-32. The bipole transmitters are indicated by a pair of X's connected by a double line. The apparent resistivities along a particular survey line are presented in the geophysical data profile composites (Appendix III-A). The designations TX1 through TX5 refer to the five transmitter locations.

The purpose of calculating both apparent resistivity and apparent conductance is to differentiate between very thick uniform sections and thin conductive sections overlying a resistive basement. For a uniform earth the apparent resistivity remains constant for all locations, while the apparent conductance increases as a function of distance from the transmitter. For the case of a conductive surface layer overlying

an infinitely resistive basement the apparent conductance is nearly constant at all locations, while the apparent resistivity increases with distance from the transmitter. Depending upon the geologic situation, one mode of calculation could prove more useful than the other in terms of providing more uniform background values against which to observe anomalies.

However, in comparing the apparent resistivity and apparent conductance maps for a particular transmitter (Figure III-23 versus III-24, Figure III-25 versus III-26, etc.) the anomaly patterns are nearly identical: high resistivity features have low conductance, and vise versa. There are only a couple of minor exceptions to this. For transmitter no. 4, the apparent resistivities along Line A-A' (the string of numbers extending SSE from near the center of this transmitter) are nearly constant, while the corresponding apparent conductance values display a steady increase to the south. This implies a thick, uniform section, however, gravity data indicate that only a thin conductive layer exists under, or a short distance to the east of, these station locations. Telluric data (Figure III-A1) suggest increasing resistivity to the south.

The data for transmitter no. 5 (Figures III-31 and III-32) display generally increasing apparent resistivity to the north, and relatively constant apparent conductance. This implies a layered situation with a resistive basement, and is in contradiction to the transmitter no. 4 data. Furthermore, the data display this character for many stations located over the thickest sedimentary section, so the interpretation seems unreasonable.

If the bipole-dipole apparent resistivity maps (Figures III-23,

III-25, etc.) are compared it will be seen that some anomalies occur at the same location for more than one transmitter: the resistive Paleozoic rocks of the Sonoma Range east of the hot springs; the north-south trending resistive feature 3 kilometers west of Panther Canyon; the resistive anomaly southeast of transmitter no. 1. The northeastern end of this last feature appears in the Line B-B' dipole-dipole and telluric data (Figure III-A2); it appears to be an highly resistive portion of the sedimentary surface layer. The location of conductive areas on the bipole-dipole maps is a function of the transmitter location and orientation. For a given distance from the transmitter, receivers located along the transmitter axis do not sense as deeply as those located equatorially (Keller, et al, 1975). This is demonstrated in the bipole resistivity maps for transmitter nos. 1 and 2. Transmitter no. 2, which is roughly perpendicular to the range-front fault system, yields low apparent resistivities over the thick sedimentary section to the east. The values are comparable to those obtained by the 1 kilometer dipole length dipole-dipole surveys in this area. (See Figure III-33). However, to the east of transmitter no. 1, which approximately parallels the range-front fault system, the apparent resistivities are considerably higher. Presumably, for this transmitter orientation resistive bedrock is being sensed.

An attempt has been made at two-dimensional numerical modeling of the bipole-dipole data for the resistivity structure east of transmitter nos. 1, 2, and 3. The results are displayed in Figures III-34, III-35, and III-36. The model shown in these figures is similar to that devised using the dipole-dipole data on Line E-E' (Figure III-12), and depicts a thick conductive section west (left) of the major range-front

fault at 0 km. The conductive (1 ohm-meter) material is overlain by a more resistive surface layer, and thins to the west. The apparent resistivity and apparent conductance maps for transmitter nos. 1 and 2 are quite similar to the respective field data maps except in areas where shallow anomalous features lie. The modeled data for transmitter no. 3 is not quite as successful in reproducing the field data, but the problem here may be due to sampling: many fewer receiver stations were occupied for transmitter no. 3 than for the other transmitters.

It is interesting that these model results yield some of the characteristics of the field data, yet they are of questionable value to the interpretation of the Grass Valley structure. In comparing Figure III-23 with III-34 it can be seen that the model results suggest that the low resistivity anomaly 1 kilometer southwest of Leach Hot Springs is simply an artifact of the transmitter orientation, rather than being caused by a localized anomalous feature. However, a similar anomaly is present in the field data for transmitter no. 4 (Figure III-29), so it is unclear whether or not the source of the anomaly is a departure from the two-dimensional model structure. It appears, then, that two-dimensional modeling is not particularly helpful in resolving the three-dimensional data.

In the geophysical data profile composites of Appendix III-A the bipole-dipole apparent resistivity data are plotted along Lines A-A' through H-H'. In general, there is a high degree of correlation with the E-field ratio telluric data. Resistive features are, for the most part, consistently observed regardless of the transmitter location. (An exception is the sinter deposition at Leach Hot Springs--at 4 to 5 km N on Line A-A' in Figure III-A1.) Conductive features, however, are

erratic in their bipole-dipole expression, depending upon transmitter location or orientation. For example, for the data along Line E-E' (Figure III-A5) west of 0 km, the data for two transmitters (nos. 1 and 4) indicate decreasing resistivity, while for the other three, increasing resistivity is suggested. As has previously been mentioned, this may to some extent be qualitatively resolved by considering the location and orientation of each transmitter.

It is clear from the bipole-dipole profile plots that absolute values of apparent resistivity are meaningless. At many station locations there is an order of magnitude range in apparent resistivity, depending upon the transmitter location. This can to some degree be attributed to differing structure in the vicinities of the various transmitters.

THE RESISTIVITY STRUCTURE OF GRASS VALLEY

Based upon the interpretation of the d.c. resistivity and telluric data, in conjunction with geologic, gravity, and P-wave delay data, there are various regions in Grass Valley which can be delineated. These areas are outlined in Figure III-37, and are numbered to correlate with the text below. Most of the boundaries are not rigidly defined--they are gradational, and in some cases overlapping.

Before discussing specific areas it should be noted that virtually all of the Grass Valley sedimentary section north of the Goldbanks Hills and west of the major range-front fault system includes a resistive surface layer with a thickness up to 0.5 km and a resistivity of 12 to 18 ohm-meters. East of the range-front fault system is a thinning layer of alluvium, and Quarternary and Tertiary sediments (Figure III-6) which have about the same maximum thickness, 0.5 km, and in some locations a lower resistivity than the sediments to the west.

The exposed bedrock in the surrounding mountain ranges has a resistivity at least an order of magnitude higher than the sediments. Beneath the sedimentary section, however, the bedrock resistivity is somewhat ill-defined by these data. In some areas, particularly east of the range-front fault in the vicinity of Leach Hot Springs, fracture permeability may result in low resistivity.

Region 1. As outlined in Figure III-37, this area is associated with silica deposition around Leach Hot Springs. It lies at the juncture of Hot Springs Fault and the range-front fault system, and displays high density, high P-wave velocity, and, beneath a thin conductive surface layer, high resistivity.

Region 2. To the northeast of the hot springs lies this tightly confined gravity and resistivity low anomaly at the juncture of the surface expression of the range-front fault system with a fault parallel to, and about 1.5 km north of, Hot Springs Fault (see Figure III-7). The area lies over outcropping Quarternary-Tertiary gravels and Tertiary sediments (see Figure III-6).

Region 3. To the southeast of Leach Hot Springs is an area of thin conductive (3-7 ohm-meter) sediments at the surface, possibly due to runoff from the springs.

Region 4. To the southwest of the hot springs in the gravity trough, lying beneath a resistive sedimentary surface layer (250-500 meters thick; 12-15 ohm-meters), is a layer of very conductive sediments (250-500 meters thick; 1-1.5 ohm-meters). It is unclear why this conductive material does not extend to greater depth. The source of the anomaly may be runoff from Leach Hot Springs into a perched water table. Alternatively, as the area lies along the southwestward extension of Hot Springs Fault, subsurface spring activity may, as a result of silicification of the fault zone, inject water into the valley sediments at a relatively shallow depth.

Region 5. To the north of region 4 is a massive, highly conductive zone in the gravity trough of the valley. The resistivity is 1-1.5 ohm-meters, and the thickness, beneath the resistive surface layer, is up to 1 km. To the north of the indicated boundary the region becomes somewhat more resistive, reflecting a decrease in porewater conductivity or a facies change. The region is of interest in that it lies in the direction of hydrologic flow in Grass Valley and could conceivably be a plume of hot water emanating from the hot

spring area. However, shallow heat flow drilling over this feature has revealed no thermal anomaly (Sass, et al., 1976).

Region 6. At the western side of Grass Valley gravity and P-wave delay data indicate thinning sediments, while electrical methods suggest a considerable conductive section. The basement rock in this area may be the Paleozoic Valmy formation, which can be graphitic and pyritic, and therefore highly conductive.

Region 7. In the two regions labled 7 the resistive sedimentary surface layer is somewhat thicker and/or more resistive than in other portions of the valley.

Region 8. Gravity data suggest that north of the canyon separating the Goldbanks Hills from the East Range lies a subsurface bedrock canyon which curves to the northeast and merges with the major gravity trough. At its southern end the sediments in this subterranean canyon have a resistivity of about 5 ohm-meters, and there is the suggestion that the conductivity increases to the northeast.

Region 9. This feature appears as a shallow resistive anomaly and a gravity "nose" extending north from the Goldbanks Hills. It would attract little attention were it not for the fact that shallow drilling has revealed a heat flow high (5.1 HFU; see Sass, et al., 1976).

Region 10. This narrow, north-south trending anomaly, most prominently displayed in telluric data, is associated with faulting, and links topographic highs located at its northern and southern ends. A more highly conductive section is observed to the east than to the west. Gravity and resistivity data suggest that at the center the anomalous response over this region results from highly resistive surface material rather than extensive bedrock protrusions into the sedimentary section.

Region 11. Gravity and resistivity lows in this region suggest a very conductive (3 ohm-meter) sedimentary section about 750 meters thick, with little or no resistive overburden layer. There is no surface expression of moisture, but in the northeastern portion of this region shallow drilling displays high heat flow (Sass, et al., 1976). In the Panther Canyon area along the northern edge of this region, numerous microearthquakes have been recorded.

Region 12. The conductive feature of region 11 continues to the south beneath a resistive sedimentary surface layer.

RECOMMENDATIONS

Several of the regions which are delineated in Figure III-37 warrant further exploration or deep drilling to assess their geothermal potential.

Region 1. Hot Springs Fault and the surface expression of range-front faulting intersect at the northeastern edge of this region. This intersection appears to be responsible for the hot spring activity. Drilling in the northwestern half of this area could intersect these faults at depth.

Region 2. This conductive, low-density anomaly is at the junction of range-front faulting with a fault parallel to Hot Springs Fault. A shallow heat flow drillhole would be warranted.

Region 5. With the potential of being a plume of hot water extending northwest from Leach Hot Springs, this anomaly is of interest. However, shallow heat flow drilling to data has been unimpressive (Sass, et al., 1976), so it appears that the anomaly must be attributed to a thick, highly conductive, but cold sedimentary section.

Region 9. This resistive, high-density feature was found to display high heat flow. This suggests a basement horst structure, or an area of hydrothermal deposition if there is hot spring activity. There is no evidence of surface moisture, however, region 8 to the northeast of its contact with region 9 demonstrates increasing conductivity, so there may be subsurface hot spring flow into the sediments in this region. Heat flow drilling in the vicinity of region 9 and the northeastern part of region 8 is recommended.

Region 11. High heat flow along the northeastern portion of this region, in conjunction with a thick, conductive sedimentary section

(which extends to the south in region 12), and microearthquake activity in the Panther Canyon area, make region 11 a candidate for additional hydrologic, geophysical, and shallow heat flow exploration.

EVALUATION OF THE EXPLORATION METHODS

Bipole-Dipole Resistivity Mapping

Based upon the bipole-dipole mapping data obtained in Grass Valley, the method appears to have few redeeming qualities.

The comparison of apparent conductance and apparent resistivity data should allow a discrimination of layered models with a resistive basement from more nearly uniform structures. However, almost without exception the Grass Valley resistivity and conductance maps for a particular transmitter yield nearly identical patterns.

For a given transmitter location the bipole-dipole resistivity mapping method inherently suffers from a lack of ability to discriminate between shallow and deep anomalies. This has been demonstrated for receiver locations along the transmitter axis in Part II of this report (Beyer, 1977b) and for arbitrary locations on the surface by Dey (1977a). The fundamental difficulty is the single transmitter location. In an effort to resolve the ambiguity, multiple transmitter locations are required, but then the method becomes time consuming and expensive, and can no longer be considered as a reconnaissance technique. Worse yet, the apparent resistivity (or conductance) maps for two transmitter locations can be quite different, even contradictory, without there being sufficient information to resolve the differences. An additional transmitter location is just as likely to add to the confusion as it is to resolve the ambiguity. In concept, of course, the more transmitter locations which are employed, the more tightly constrained the problem becomes. In practice, however, only two or three transmitter locations are used, and it appears that two-dimensional modeling may be inadequate

for a method such as this which maps over the surface.

The bipole-dipole data in some locations demonstrate good correlation with E-field ratio telluric and dipole-dipole data, but in a number of locations do not. These differences, once again, must be resolved in terms of transmitter location, or more specifically, the resistivity structure in the vicinity of the transmitter.

E-Field Ratio Tellurics

The E-field ratio telluric data from the many survey lines in Grass Valley are very consistent with one another: anomalies tend to correlate from one line to the next, and similar response is found at the intersections of lines. For example, resistive bedrock and/or sinter deposits are expressed in the data from Lines A-A' at 4.75 km N, E-E' at 0.75 km E, and S-S' at 0.25 km E. There is a variation in anomaly amplitude, however, as the profile line direction changes with respect to the orientation of the telluric field ellipse. As has been demonstrated by numerical model studies in Part 1 of this report (Beyer, 1977a) some caution must be exercised in the orientation of E-field ratio telluric lines. Yet, Line D-D', which is nearly perpendicular to the observed principal telluric field axis yields data consistent with the other telluric profiles and with other types of geophysical data; the amplitude of anomalies appears to be exaggerated, however.

The telluric data are, for the most part, consistent with a reasonable interpretation of gravity, seismic and d.c. resistivity data. Over most of Grass Valley, measurements at only 0.05 Hz were made so that no depth discrimination was possible. In some areas where it is difficult to reconcile the 0.05 tellurics with d.c. resistivity results an

explanation could possible lie in the response of the telluric field to deeper structure than is observed by the resistivity methods. Along Line E-E' where both 8 and 0.05 Hz telluric data were recorded there is good agreement between the high frequency tellurics and the dipole-dipole resistivity data for small N-spacings.

Dipole-Dipole Resistivity

The dipole-dipole resistivity method, when performed with 500 meter or 1 kilometer dipoles to separations of N = 10, is exceptionally slow and expensive. In normal exploration it would not be used as extensively as was the case in Grass Valley. The intent, however, was to use the method as a basis for evaluating other electrical techniques. If a geologic strike direction is well defined, two-dimensional numerical modeling of a highly data-intensive method using a controlled source affords the possibility of detailed determination of the structure.

The process used to invert the field data was trial and error. At the present time, inversion of complex two-dimensional data by numerical estimation schemes is not tractable because there are too many variables. In the case of the computer code used by the author, the resistivity of every element in a 113 X 16 grid is a variable. The horizontal resolution, and the vertical resolution to a depth of two dipole lengths, is one-fourth of a dipole unit. At greater depths, the nodal separation increases to one-half, one, two, and more dipole lengths. The use of the human mind, rather than a numerical estimation technique, to invert data such as dipole-dipole resistivity pseudo-sections, has the advantages of incorporating reasonable determinations based upon other types of data, and allowing for a sophisticated weighting of various subtle factors observed in the data. The disadvantage, of course, is that

models based upon preconceived notions or biases of the interpreter may be developed while other reasonable possibilities are overlooked.

This relates to the problem of uniqueness. To what extent are models developed by trial and error unique? They are not. However, if there is a reasonable matching of the field data, and the interpretation is consistent with geological and other geophysical information, then the model derived by trial and error is certainly as valid as those arrived at by other means.

It was demonstrated in Part II of this report (Beyer, 1977b) that the study of modeled dipole-dipole response to numerous simple structures was essential to the proper conceptual interpretation of dipole-dipole pseudo-section data. In deriving the models presented as interpretations to the Grass Valley data is has been learned that modeling (inverting) dipole-dipole pseudo-sections using detailed two-dimensional models is an exceptionally difficult, time-consuming, and frustrating task. After an interpreter has devoted considerable effort to studying pseudo-sections for simple models and has attempted fitting field data, many characteristics in the pseudo-section which relate to actual structure will become evident. Yet, even at this point it may be difficult to obtain a close fit to the field data pseudo-section. The proper trends may be present in the model data, but the effects due to a particular portion of the structure may be undesirably dominant, with the result that contour lines do not resemble those in the field data. For near-surface model features, extensive juggling of the resistivity, thickness, and lateral boundary location may be required before a good fit can be obtained. For example, in the Grass Valley models presented the surface location of the bedrock-sediment contact is of supreme importance to all

apparent resistivities down-to-the-left and down-to-the-right from the dipole straddling the contact. It was found in modeling the dipole-dipole data on Line D-D' (see Figure III-20) that if the surface contact at 8.75 W was moved one-quarter dipole length to the right, all the apparent resistivities down-to-the-right from 8.5 W would be markedly increased. Furthermore, the apparent resistivity values down-to-the-right from 9.5 km W would be somewhat reduced.

Some of the models presented yield excellent fits to the observed dipole-dipole data. One of these, the model for Line A-A', was arrived at after six attempts. All others, however, required over a dozen attempts, and in the case of Line E-E', twenty. A satisfactory model fit was never obtained for Line B-B', possibly because of significant conductive structures adjacent to the survey line. On the other hand, the model for Line A-A', which yields such a good fit, is not completely consistent with other data in that the resistive mass at 3.25 N (Figure III-18) does not extend deep enough. The physical situation is clearly three-dimensional, yet in this case a two-dimensional model produces the desired result.

Clearly, the definition of anomalous structures is not precise. Certainly the detail displayed in the models at depth cannot be regarded as exact. However, if considered conceptually, the models appear to be valid in that they are generally consistent with other data and can be interpreted in terms of reasonable Basin and Range geologic structures.

CONCLUSIONS

No deep drilling and logging has been done in Grass Valley, Nevada, so ultimately it is impossible to assess either the relative values of the geophysical methods stressed in this report, or the validity of a geologic interpretation based on these or other data.

The only tests which remain to evaluate a technique are its internal consistency, its correlation with geological and other geophysical methods and its interpretability in terms of developing a reasonable geologic model.

Using these criteria the analysis of Grass Valley data indicates several points.

The bipole-dipole resistivity mapping method was the least useful of the electrical methods employed because of the shallow versus deep anomaly ambiguity for a single transmitter, and the different but uninterpretable anomaly patterns for multiple transmitters. The comparison of apparent resistivity and apparent conductance maps for Grass Valley gave ambiguous or contradictory results.

As a reconnaissance electrical exploration technique the E-field ratio telluric method appeared to be highly successful. The only regret was that 8 Hz data were not obtained along most of the survey lines. Every telluric profile was consistent with adjacent or intersecting profiles, and there was a high degree of correlation with gravity, P-wave delay, and resistivity data in terms of developing a reasonable model of Grass Valley. In areas where stations can be occupied along straight lines whose orientations can range from perpendicular to strike to parallel to the principle axis of the telluric ellipse, the method is very useful for estimating the resistivity structure with

respect to another area along the survey line (supplimentary geological and geophysical information is necessary of course). The greatest drawback of the method is that absolute values of apparent resistivity are not obtained; another technique is required to make this assessment.

The E-field ratio telluric method is suggested as a qualitative technique. A familiarity of the response from simple models is desirable (Beyer, 1977a), but detailed modeling seems inappropriate because the magnetic component of the magnetotelluric field is not measured. Furthermore, however, the two-dimensional modeling which was attempted indicated that at 0.05 Hz the basin and range structure in the vicinity of Leach Hot Springs can not be treated as two-dimensional. This also means that long period magnetotelluric data from Grass Valley cannot be correctly interpreted using two-dimensional modeling.

Two-dimensional modeling of the dipole-dipole resistivity pseudo-section data was generally successful at delineating geologically reasonable conceptual models of the Grass Valley resistivity structure, with, in many areas, a good estimate of the actual resistivity. The models developed are, for the most part consistent with the gravity and telluric data, but this may be because these methods were instrumental in the designing of the dipole-dipole models. The telluric and dipole-dipole resistivity data compliment one another particularly well.

In spite of yielding some very useful resistivity models, however, the dipole-dipole method must be regarded as at best, a very qualified success. When employed on a large scale (1 kilometer dipoles to a separation of N = 10) the method requires heavy and sophisticated equipment, and is very slow. Hence, it is exceptionally expensive. To probe to great depth in conductive valleys, enormous transmitter-receiver

separations must be employed. Invariably, major lateral resistivity contrasts will be traversed which make for difficulty in interpretation. Indeed, the severest drawback of the dipole-dipole method is that the pseudo-section data are exceptionally hard to interpret. The point must be strongly made that a geophysicist unfamiliar with dipole-dipole pseudo-section model results should never attempt to interpret a resistivity pseudo-section which shows evidence of lateral resistivity contrasts. Furthermore, even with such knowledge, it can be exceptionally difficult to obtain a close model fit to complex pseudo-section data.

RECOMMENDATIONS

1) For electrical reconnaissance exploration of several hundred square kilometer areas, use of the bipole-dipole resistivity mapping method is not advised.

2) For such exploration, the E-field ratio telluric method, employing both a high and a low frequency appropriate to the resistivity structure under investigation, is highly recommended.

3) An electrical method yielding apparent resistivity and which can be modeled to obtain absolute resistivities, should be used in conjunction with the E-field ratio telluric method at some locations.

4) For the dipole-dipole method employing large dipole separations to become useful for the structural delineation of local anomalies of interest, two-dimensional numerical inversion schemes must be developed. It may be possible to reduce significantly the number of variables in a two-dimensional model by first evaluating the significance of varying the resistivity of various mesh elements as a function of depth. Larger units at depth than have been used in this study could be assigned a uniform resistivity. Additionally, based upon the particular field data being inverted, the elements in various near-surface regions could be constrained to have equal resistivities, or even a fixed resistivity value. Extensive knowledge of pseudo-section modeling would be required to make this type of decision, however.

REFERENCES

Beyer, H., 1977a, Telluric and d.c. resistivity techniques applied to the geophysical investigation of Basin and Range geothermal systems, Part I: the E-field ratio telluric method, LBL-6325-1/3: Lawrence Berkeley Laboratory, University of California, Berkeley.

Beyer, H., 1977b, Telluric and d.c. resistivity techniques applied to the geophysical investigation of Basin and Range geothermal systems, Part II: A numerical model study of the dipole-dipole and Schlumberger resistivity methods, LBL-6325-2/3: Lawrence Berkeley Laboratory, University of California, Berkeley.

Beyer, H., Dey, A., Liaw, A., McEvilly, T.V., Morrison, H.F., and Wollenberg, H., 1976, Preliminary open file report: geological and geophysical studies in Grass Valley, Nevada, LBL-5262: Lawrence Berkeley Laboratory, University of California, Berkeley.

Dey, A., 1976, Resistivity modeling for arbitrarily shaped two-dimensional structures, Part II: User's guide to the FORTRAN algorithm RESIS2D, LBL-5283: Lawrence Berkeley Laboratory, University of California, Berkeley.

Dey, A., and Morrison, H.F., 1977, An analysis of the bipole-dipole method of resistivity surveying, LBL-6332: Lawrence Berkeley Laboratory, University of California, Berkeley. Also, submitted for publication to Geothermics.

Dey, A., and Morrison, H.F., 1976, Resistivity modeling for arbitrarily shaped two-dimensional structures, Part I: Theoretical formulation, LBL-5223: Lawrence Berkeley Laboratory, University of California, Berkeley.

Goldstein, N.E., Beyer, H., Corwin, R., di Somma, D.E., Majer, E., McEvilly, T.V., Morrison, H.F., Wollenberg, H.A., and Grannell, R., 1976, Open file geoscience studies in Buena Vista Valley, Nevada, LBL-5913: Lawrence Berkeley Laboratory, University of California, Berkeley.

Hallof, P., 1957, On the interpretation of resistivity and induced polarization results: unpublished Ph.D. thesis, Massachusetts Institute of Technology, Cambridge.

Keller, G.V., Furgerson, R., Lee, C.Y., Harthill, N., and Jacobson, J.J., 1975, The dipole mapping method: Geophysics, v. 40, no. 3, p. 451-472.

Marshall, D.J., and Madden, T.R., 1959, Induced polarization, a study of its causes: Geophysics, v. 24, no. 4, p. 790-816.

Morrison, H.F., 1975, The up-down counter: a synchronous signal averager for earth resistivity measurements, in The study of temporal resistivity variations on the San Andreas Fault: Technical progress report on U.S.G.S. grant # 14-08-0001-G-124, period ending February 1, 1975; Engineering Geoscience, University of California, Berkeley.

Morrison, H.F., McEvilly, T.V., Wollenberg, H.A., and Goldstein, N.E., 1977, (Final report on the geothermal assessment of three sites in north central Nevada. Report in preparation.) Lawrence Berkeley Laboratory, University of California, Berkeley.

Noble, D.C., 1975, Geologic history and geothermal potential of the Leach Hot Springs area, Pershing County, Nevada: a preliminary report to the Lawrence Berkeley Laboratory.

Olmsted, F.H., Glancy, P.A., Harrill, J.R., Rush, F.E., and Vandenburgh, A.S., 1975, Preliminary hydrogeologic appraisal of selected hydrothermal systems in northern and central Nevada: U.S. Geol. Surv. open file report 75-56.

Ryu, J., 1971, Low frequency electromagnetic sounding: unpublished Ph.D. thesis, University of California, Berkeley.

Sass, J.H., Lachenbruch, A.H., Munroe, R.J., Greene, G.W., and Moses, T.H., 1971, Heat flow in the western United States: JGR, v. 67, no. 26, p. 6376-6413.

Sass, J.H., Olmsted, F.H., Sorey, M.L., Lachenbruch, A.H., Munroe, R.J., Galomis, S.P., Jr., and Wollenberg, H.A., 1976, Geothermal data from test wells drilled in Grass Valley and Buffalo Valley, Nevada; LBL-4489: Lawrence Berkeley Laboratory, University of California, Berkeley.

(for numbering sequence only)

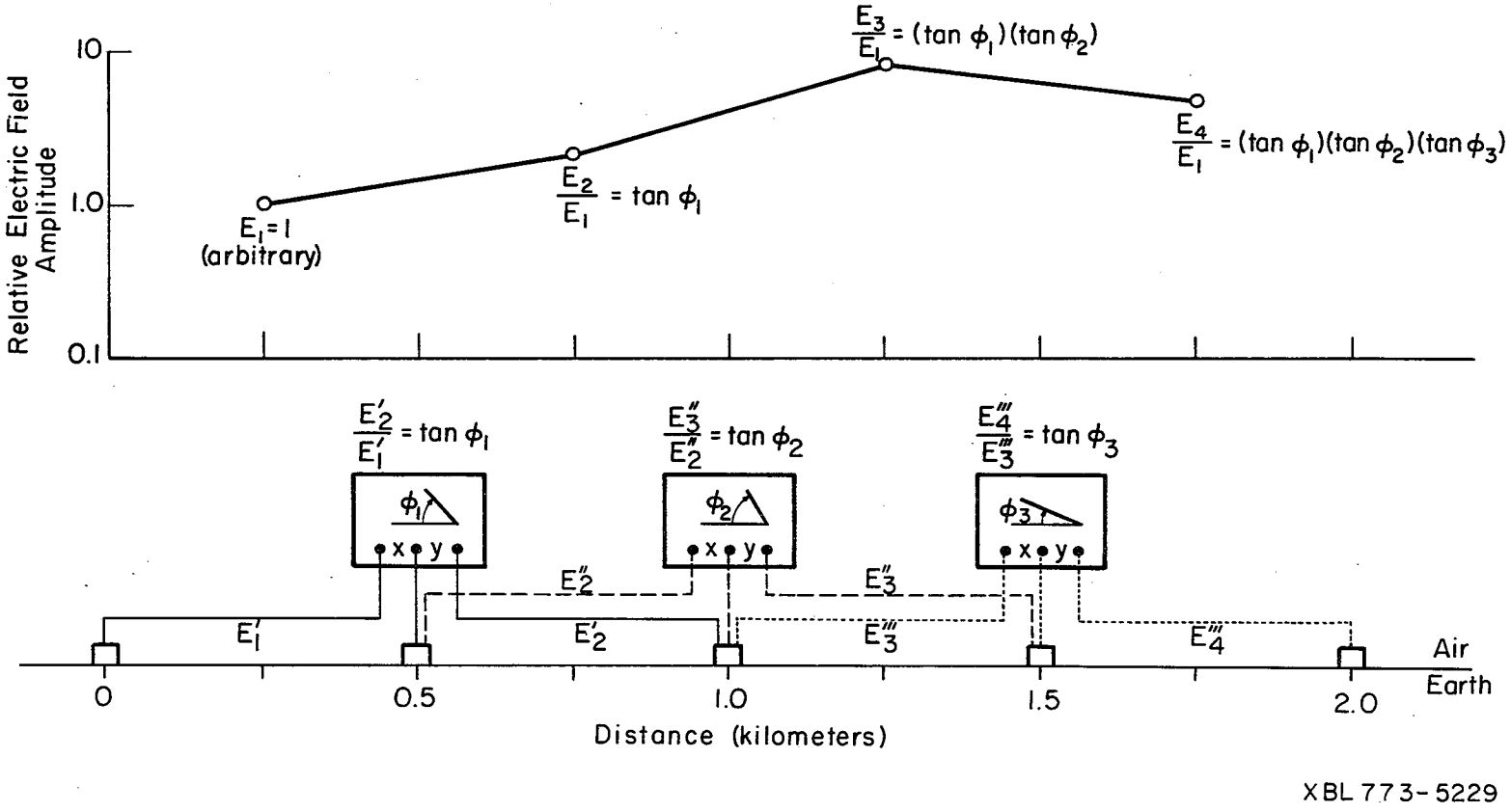

Figure III-1. Three successive E-field ratio telluric receiver stations and data plotting method.

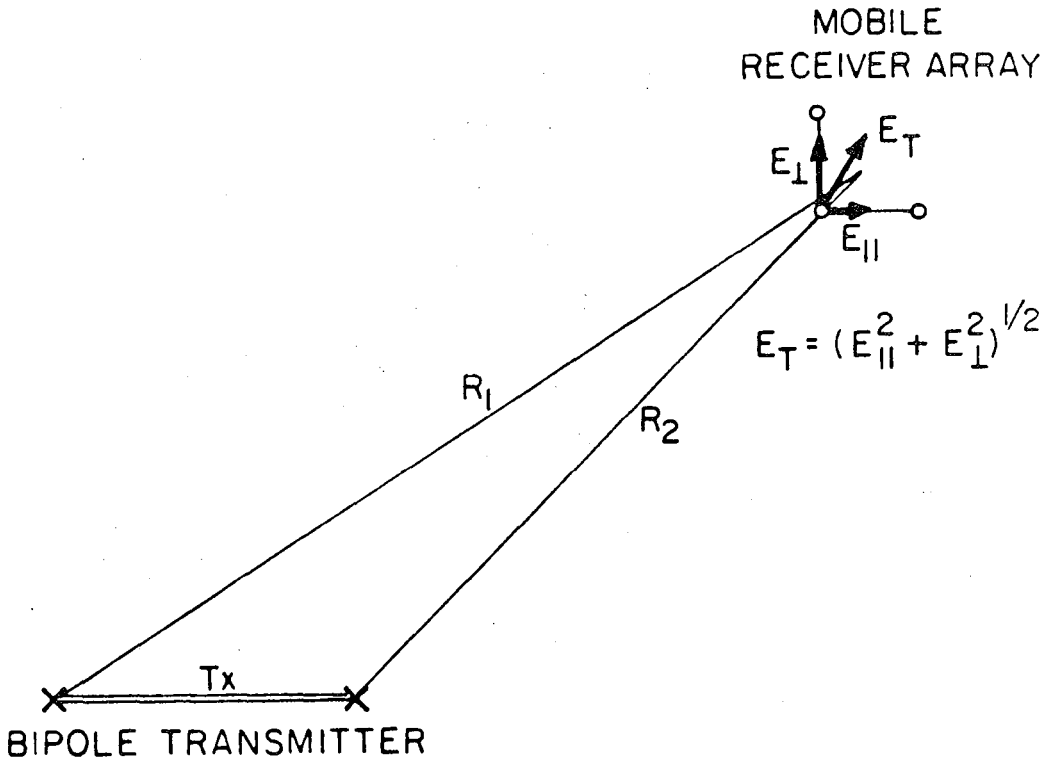

Figure III-2. Plan view of the bipole-dipoel resistivity mapping array.

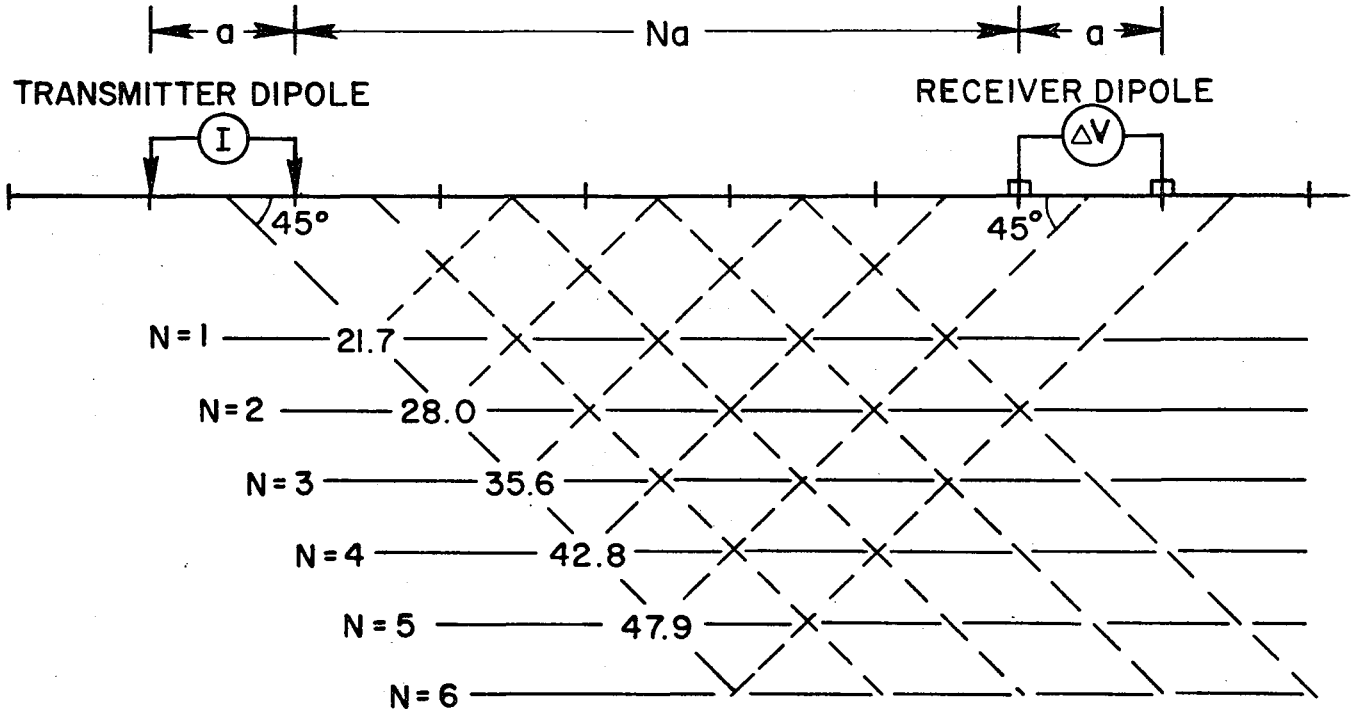

$$\rho_a = k\frac{\Delta V}{I} \quad \text{WHERE GEOMETRIC FACTOR, } k = \pi a N(N+1)(N+2), \text{ AND } N = 1,2,3,\ldots$$

Figure III-3. The dipole-dipole electrode configuration and the construction of the apparent resistivity pseudo-section. The particular transmitter and receiver dipole locations shown are separated by (N =) 5 dipole lengths, and are used to calculate the apparent resistivity, ρ_a=47.9.

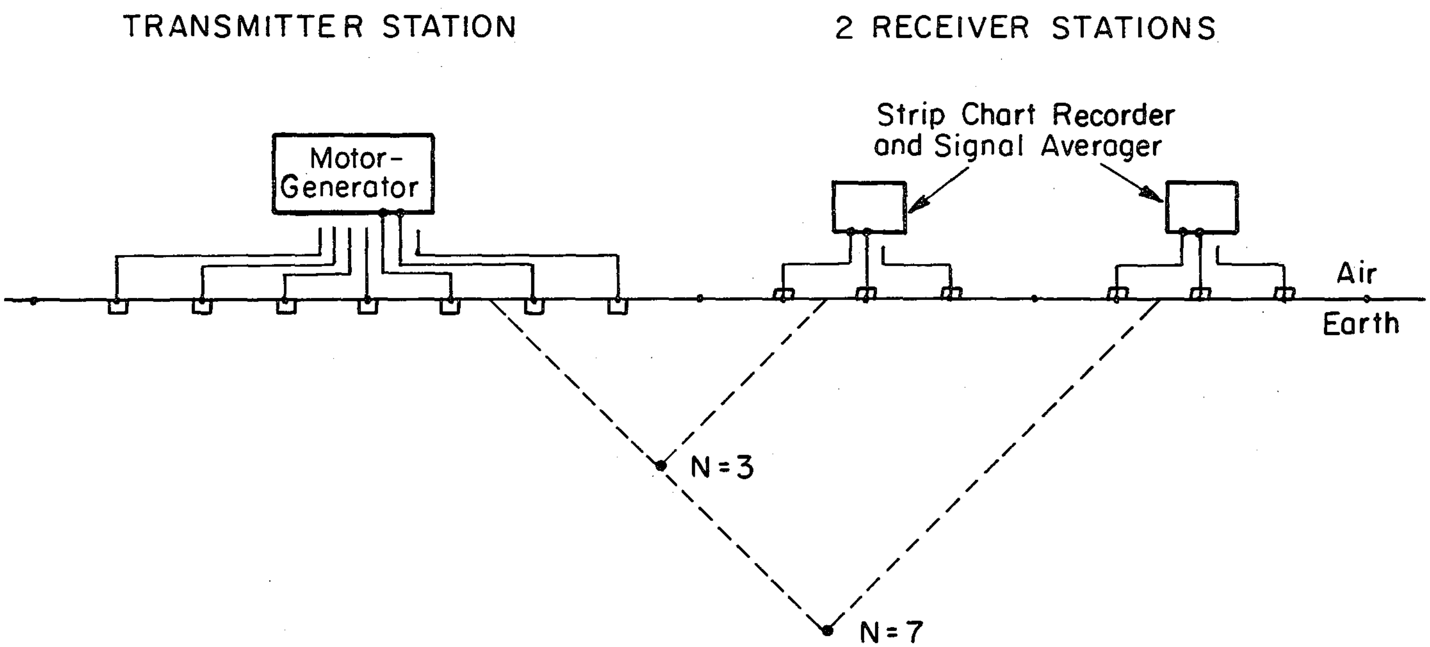

XBL 776-9367

Figure III-4. Diagram of multiple dipole-dipole transmitter and receiver locations used by LBL field crew for 1 km long dipoles. The generator and receiver instruments are connected to dipoles for which apparent resistivity values can be calculated at N = 3 and N = 7 in the pseudo-section.

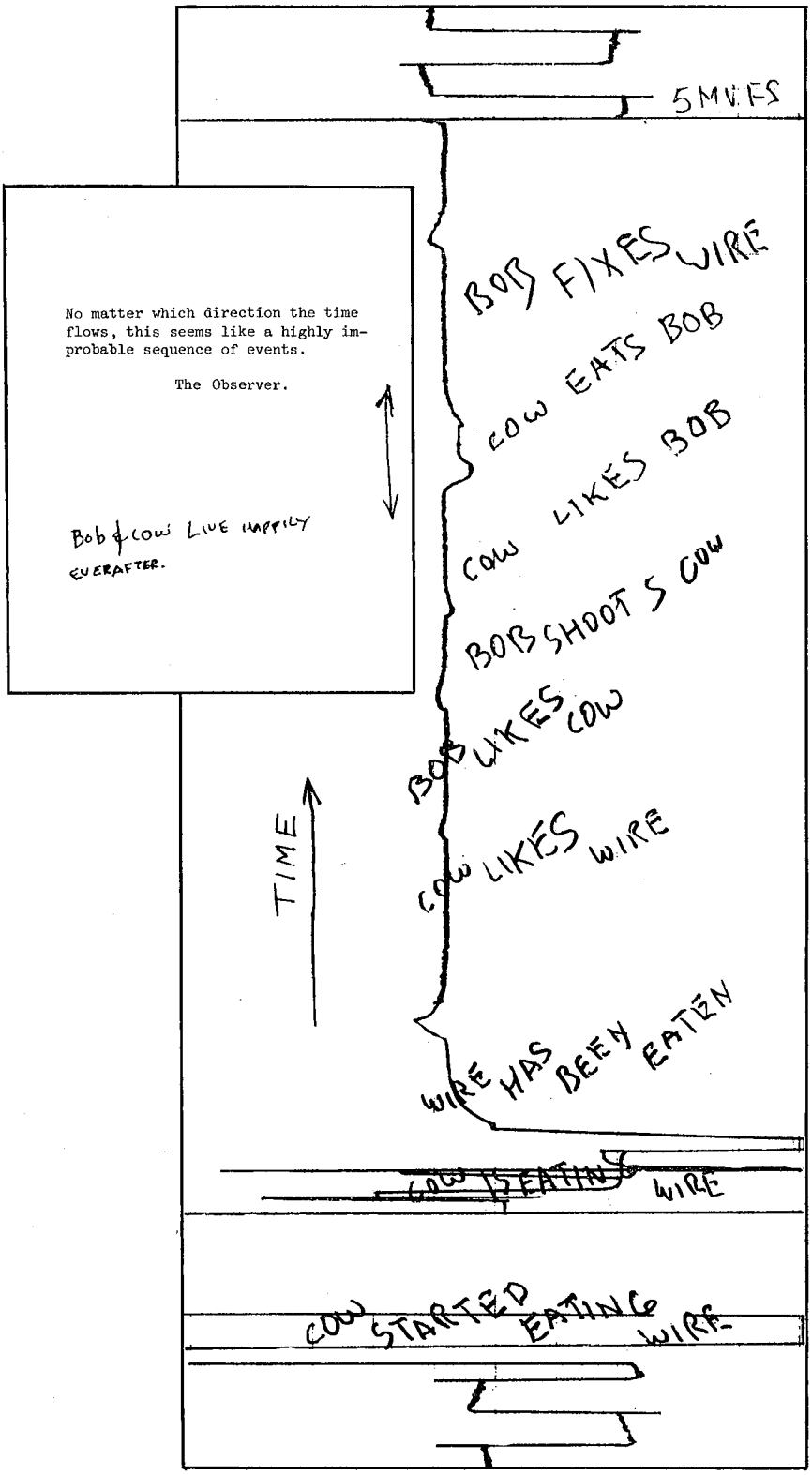

Figure III-5. An encounter between an LBL field crewman and a member of the bovine persuasion over the proper use of a long receiver wire, as recorded on the receiver strip chart record. Additional graffiti appeared after the record segment was posted as a warning to others destined for field work in Nevada.

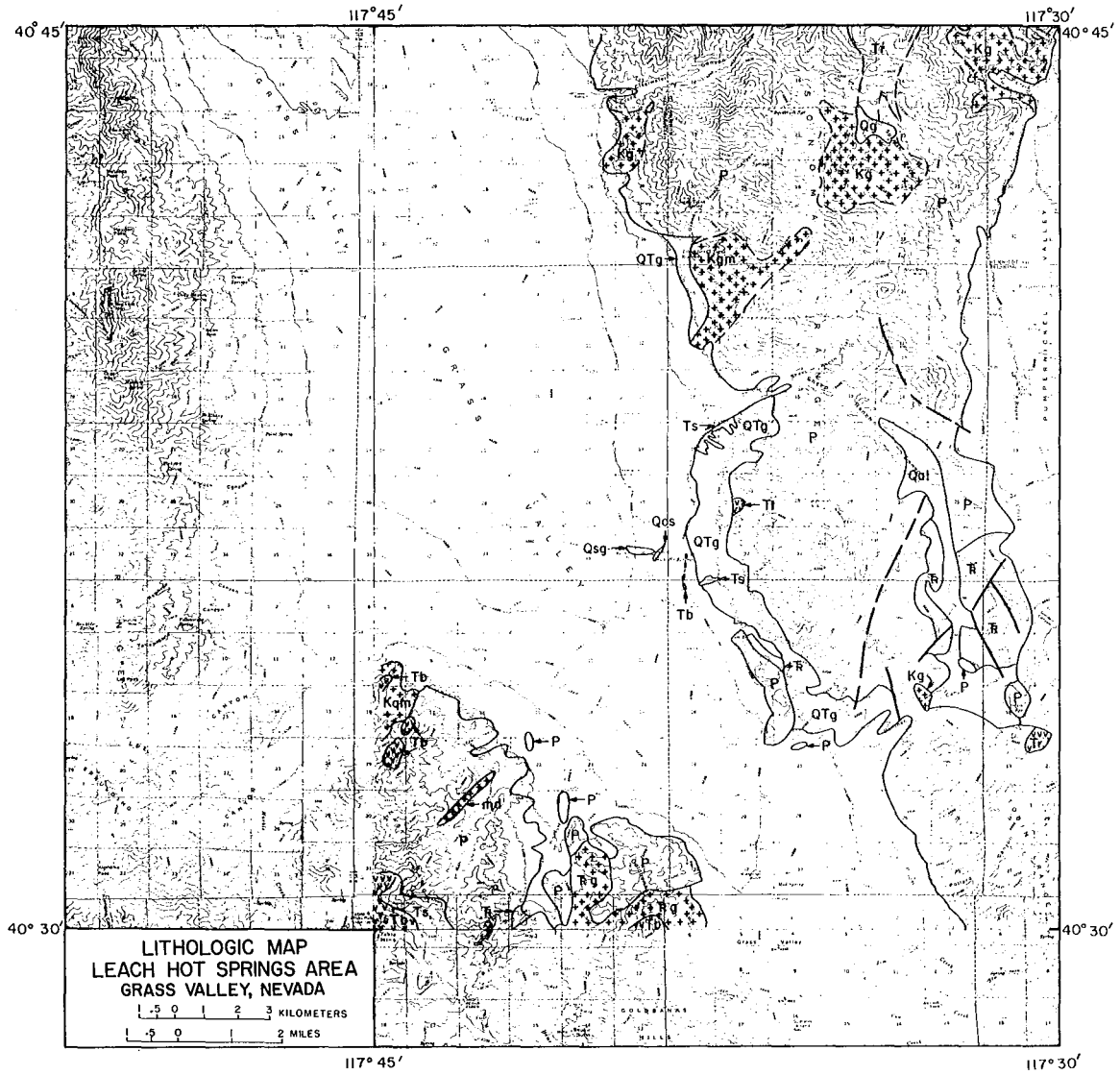

Figure III-6. Lithologic map, Leach Hot Springs area. Qal: alluvium, Qos: older sinter deposits, Qsg: sinter gravels, QTg: Quaternary-Tertiary gravels and fanglomerates, Tb: Tertiary basalt, Tr: Tertiary rhyolite, Tt: tuff, Ts: Tertiary sedimentary rocks, Kqm: quartz monzonite, Kg: granitic rock, md: mafic dike, TRg: Triassic granitic rocks, TR: undifferentiated Triassic sedimentary rocks, P: undifferentiated Paleozoic sedimentary rocks.

XBL 776-9117

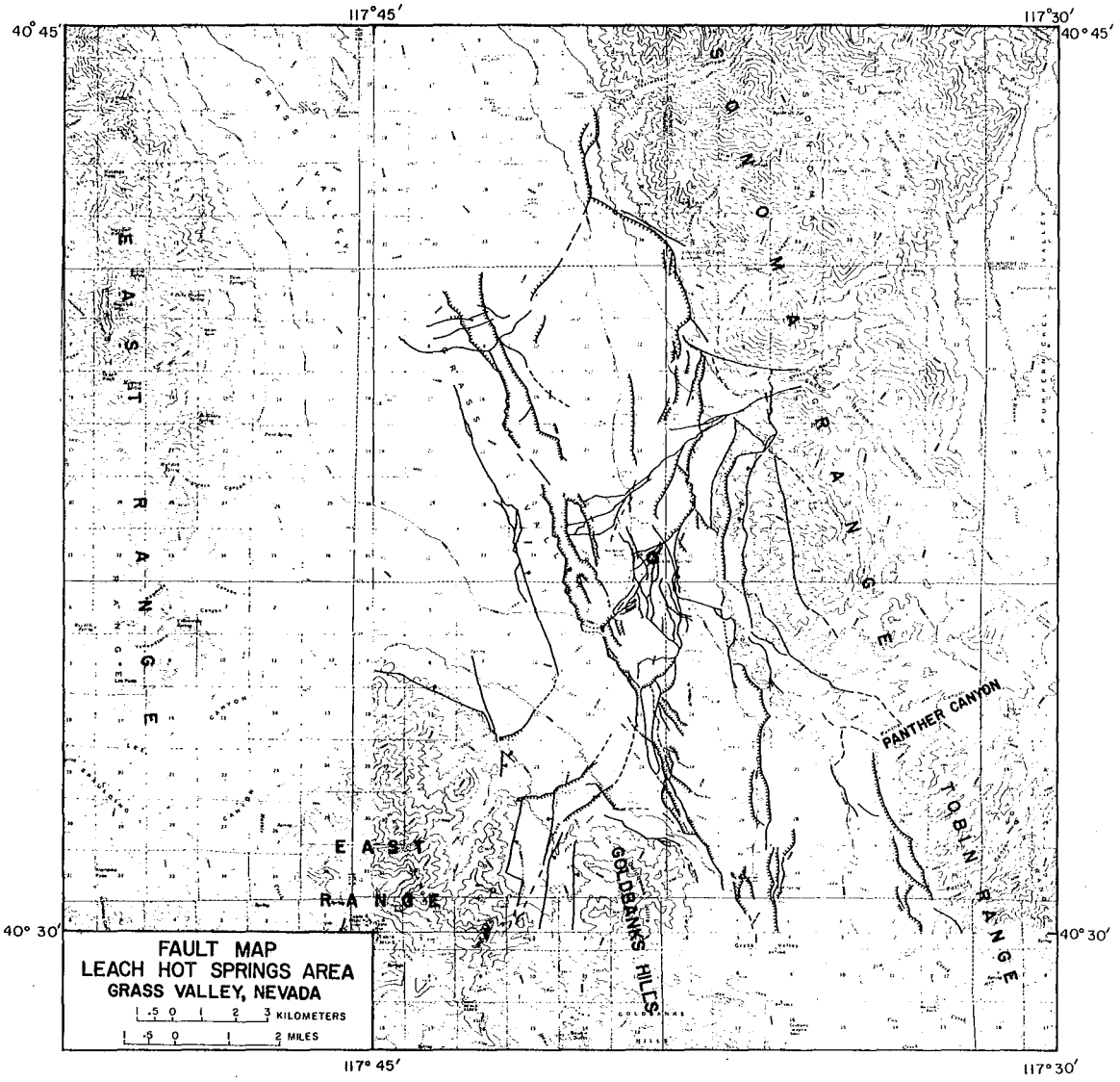

Figure III-7. Fault map of the Leach Hot Springs area. Hachured lines indicate down-faulted sides of scarplets; ball symbol indicates downthrown side of other faults. Leach Hot Springs is denoted by a small circle near the center of the map, and Hot Springs passes through it to the northeast and southwest. ED7769116

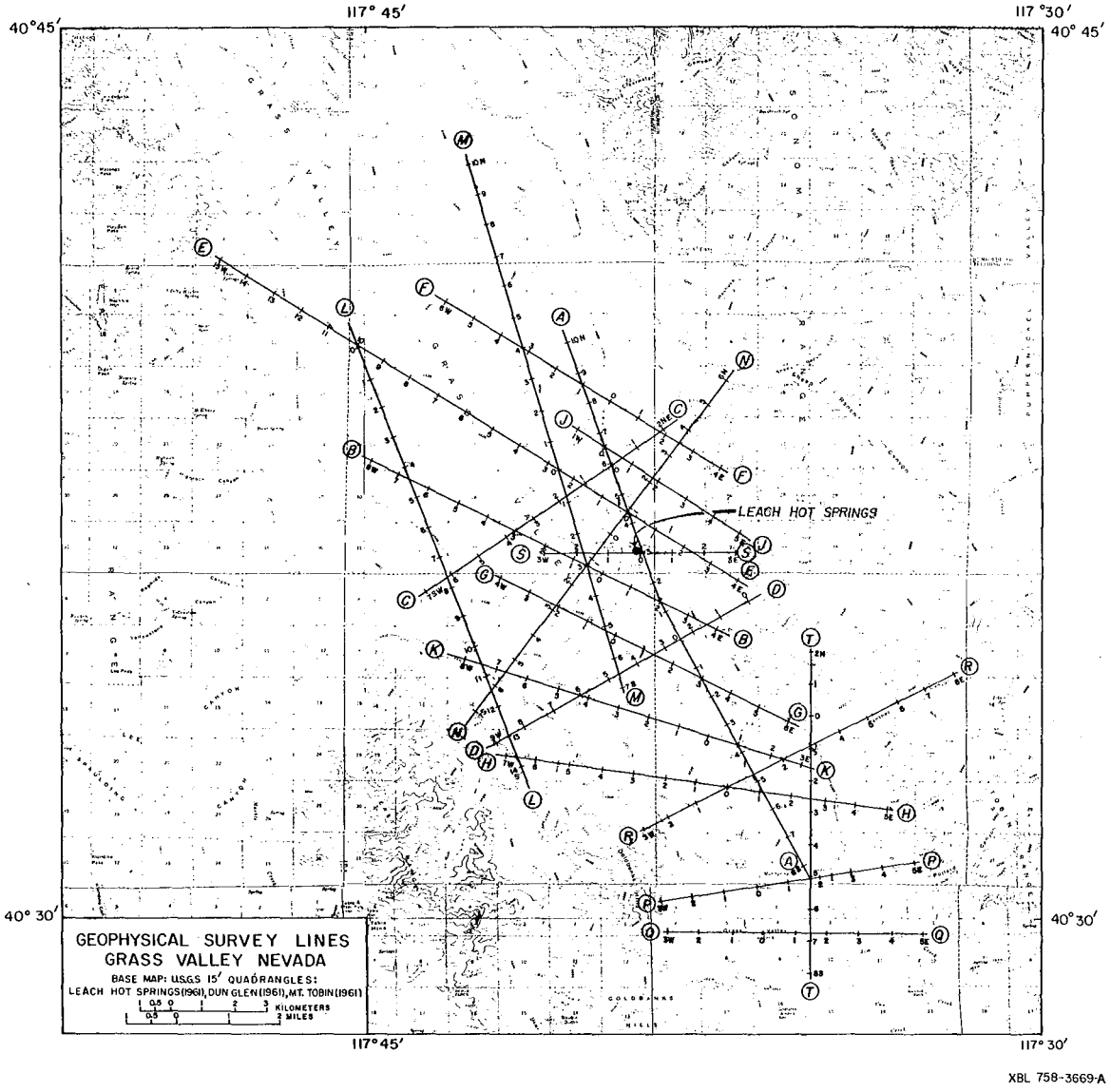

Figure III-8. Geophysical survey lines in Grass Valley, Nevada.

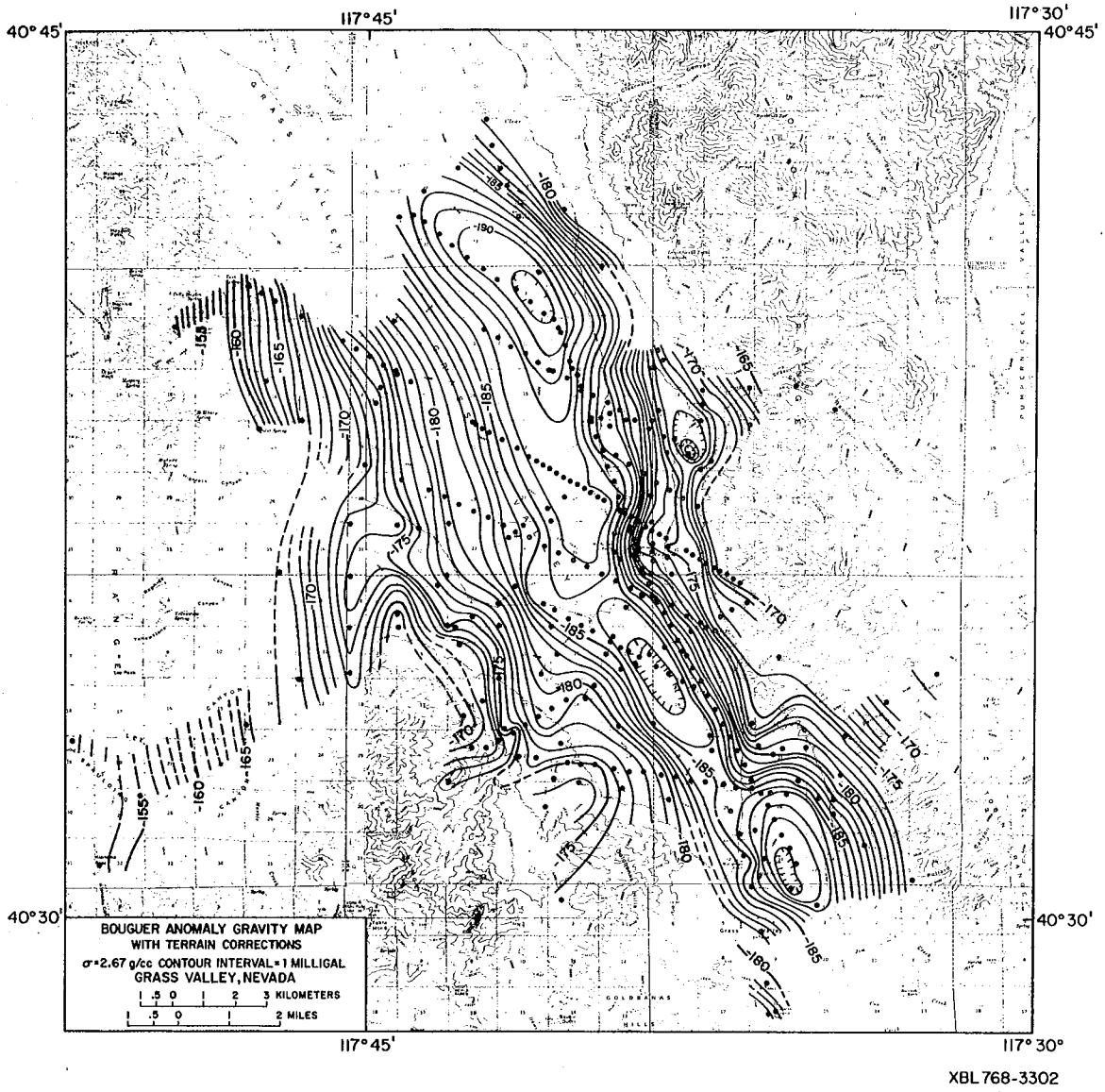

Figure III-9. Complete Bouguer anomaly gravity map, Grass Valley, Nevada.

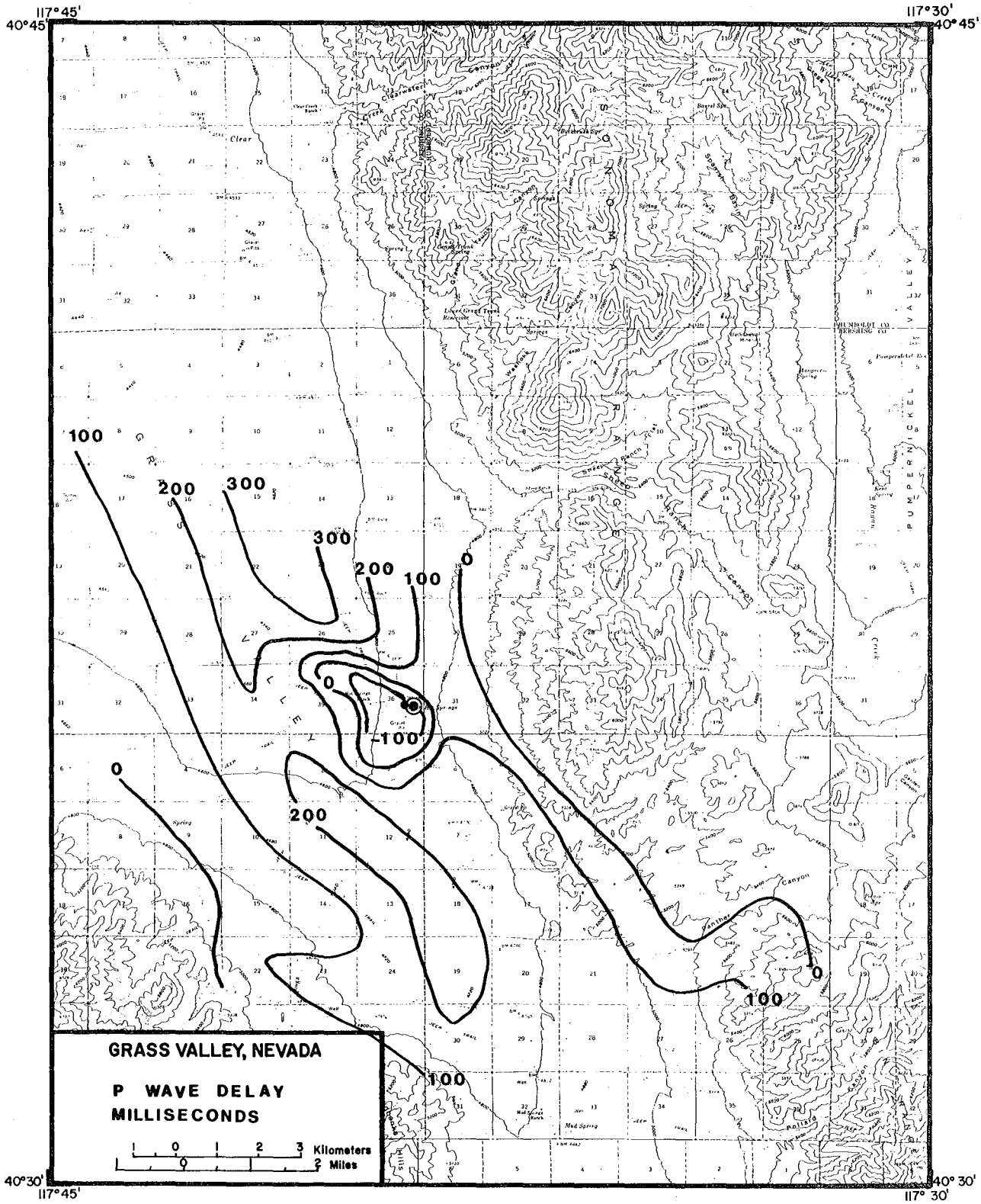

Figure III-10. Normalized P-wave delay, in milliseconds, for southern Grass Valley. Symbol shows location of Leach Hot Springs, an area of strong negative delays. XBL 768-10125

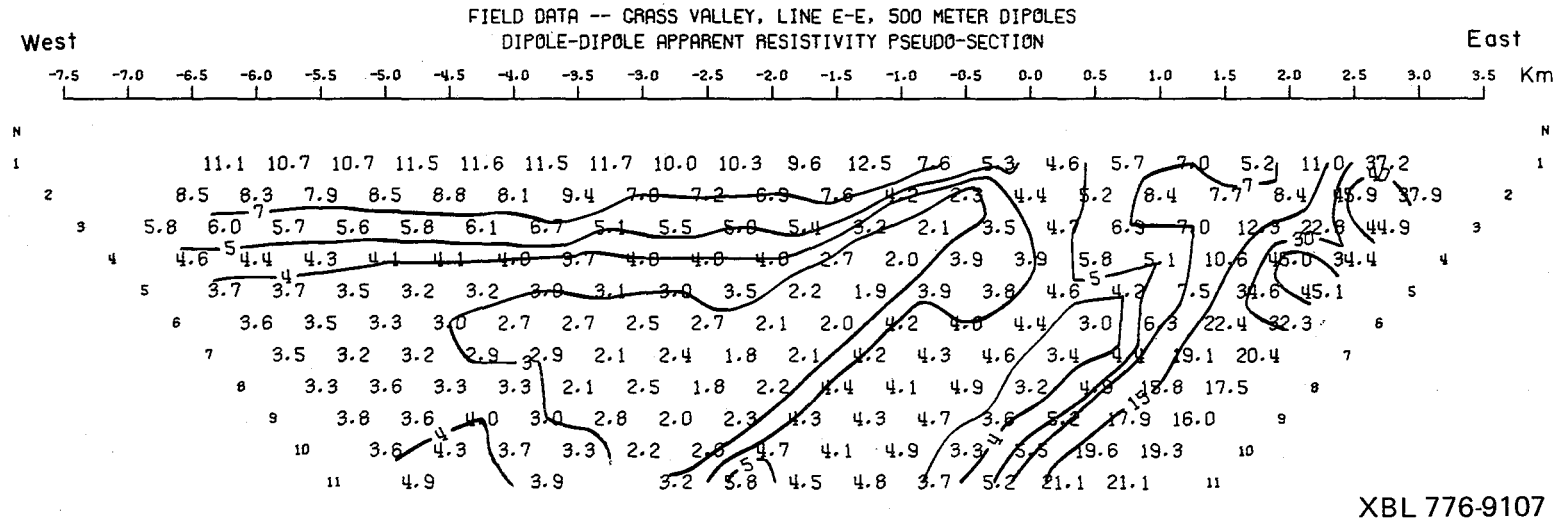

Figure III-11. Field data dipole-dipole apparent resistivity pseudo-section for 500-meter dipoles along Line E-E'.

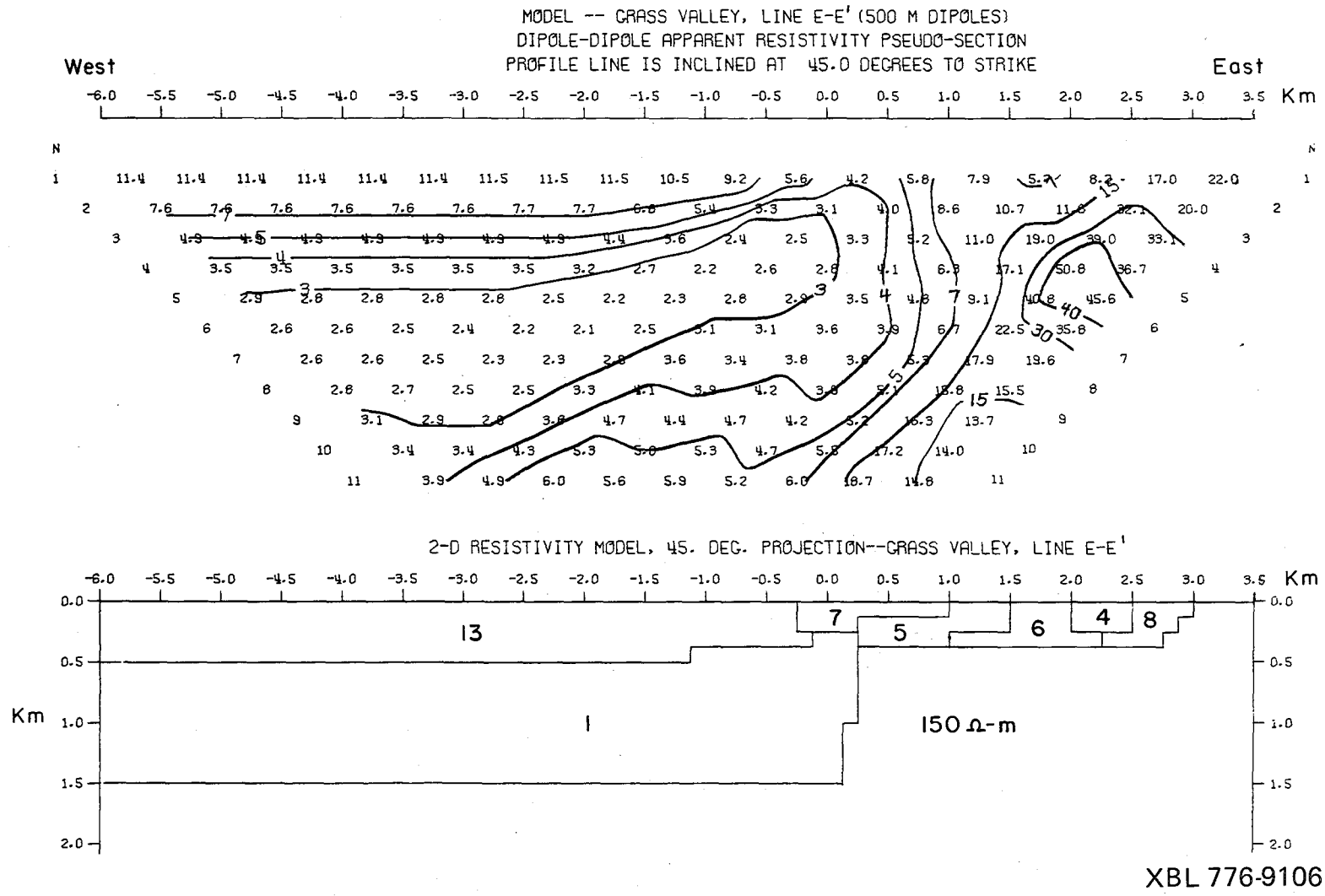

XBL 776-9106

Figure III-12. Two-dimensional resistivity model (projection in the profile line direction at 45° to strike) and resultant dipole-dipole apparent resistivity pseudo-section for 500-meter dipoles along Line E-E'. Basement resistivity is 150 ohm-meters.

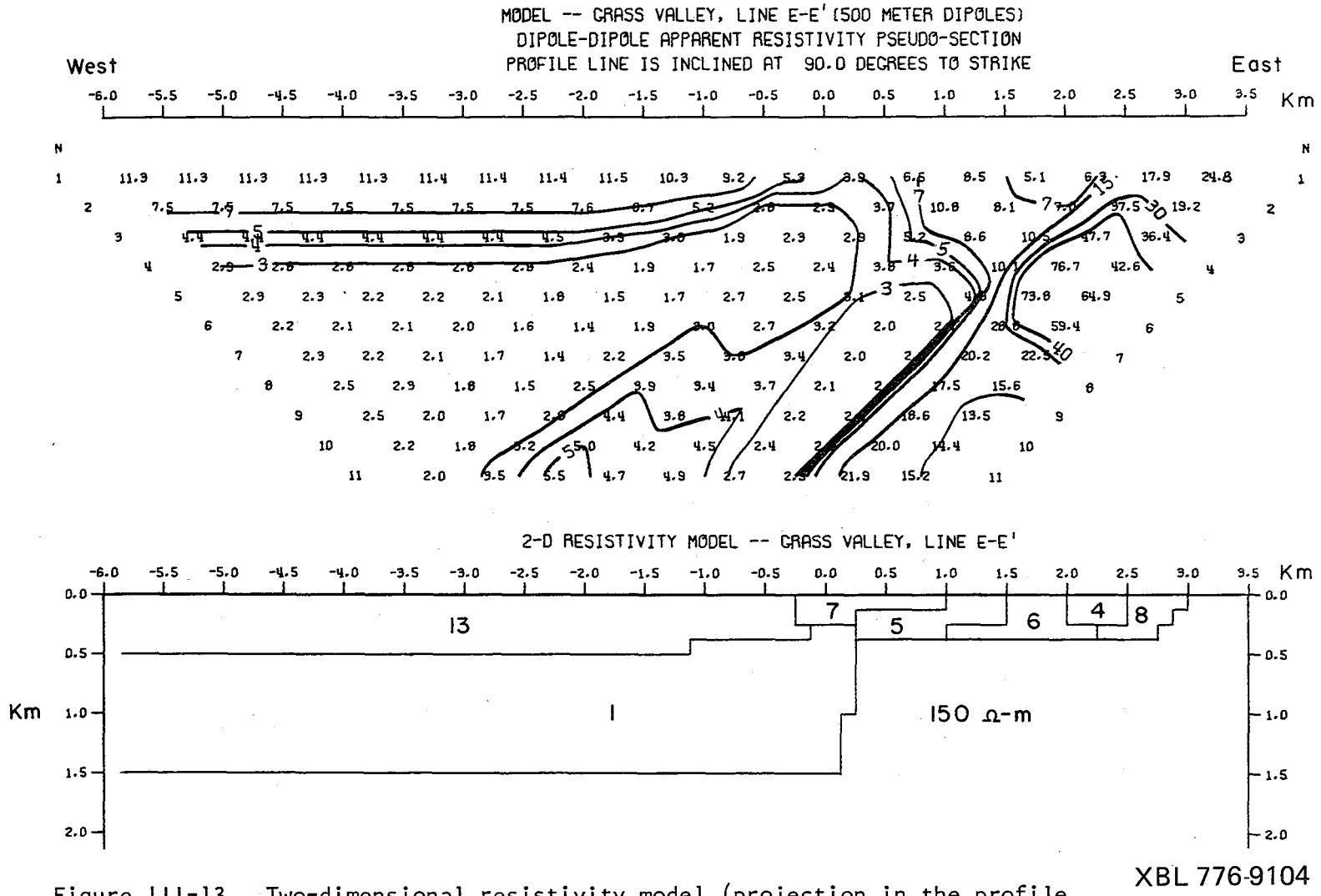

XBL 776-9104

Figure III-13. Two-dimensional resistivity model (projection in the profile line direction perpendicular to strike) and resultant dipole-dipole apparent resistivity pseudo-section for 500-meter dipoles along Line E-E'.

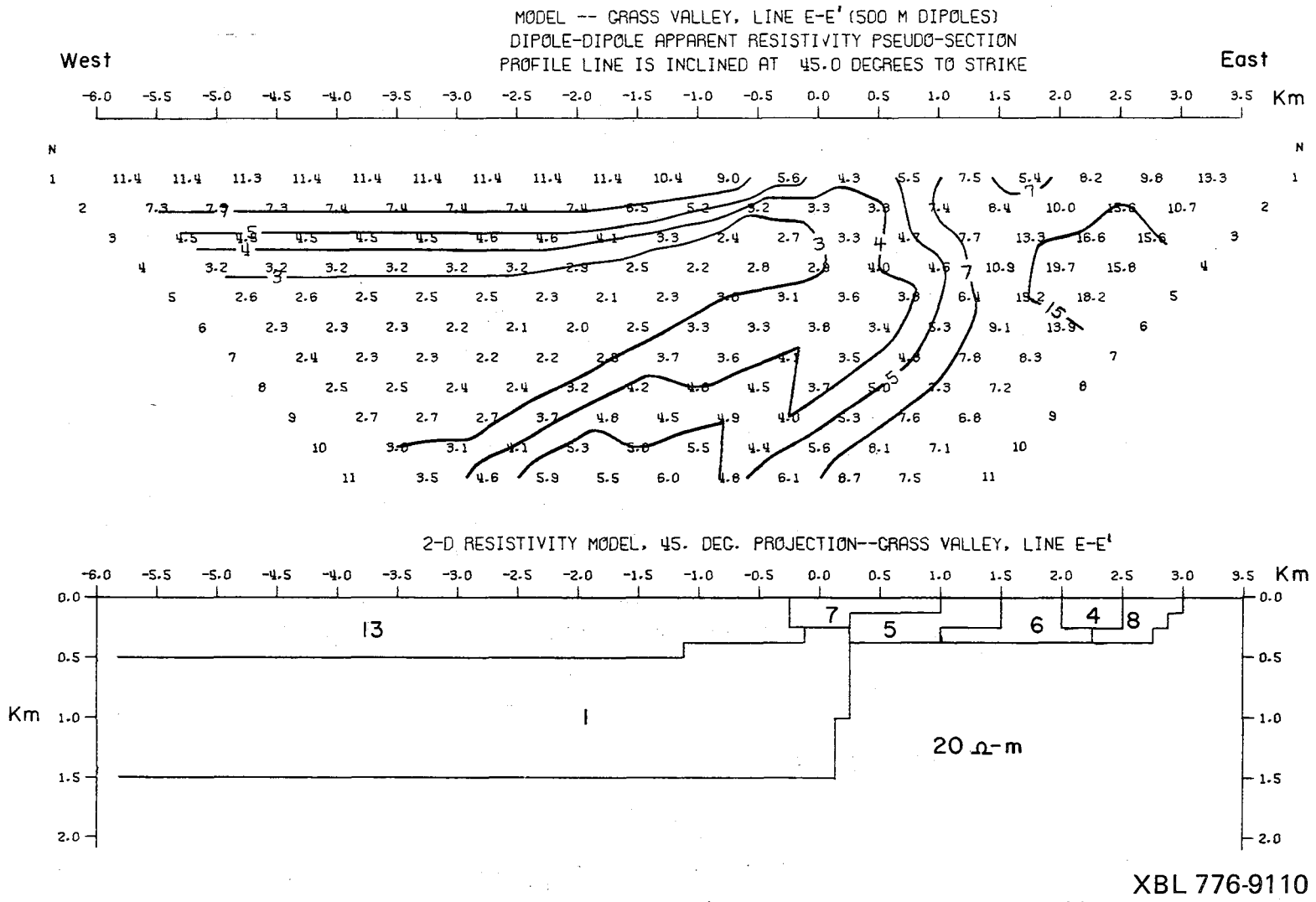

Figure III-14. Two-dimensional resistivity model (projection in the profile line direction at 45° to strike) and resultant dipole-dipole apparent resistivity pseudo-section for 500-meter dipoles along Line E-E'. Basement resistivity is 20 ohm-meters.

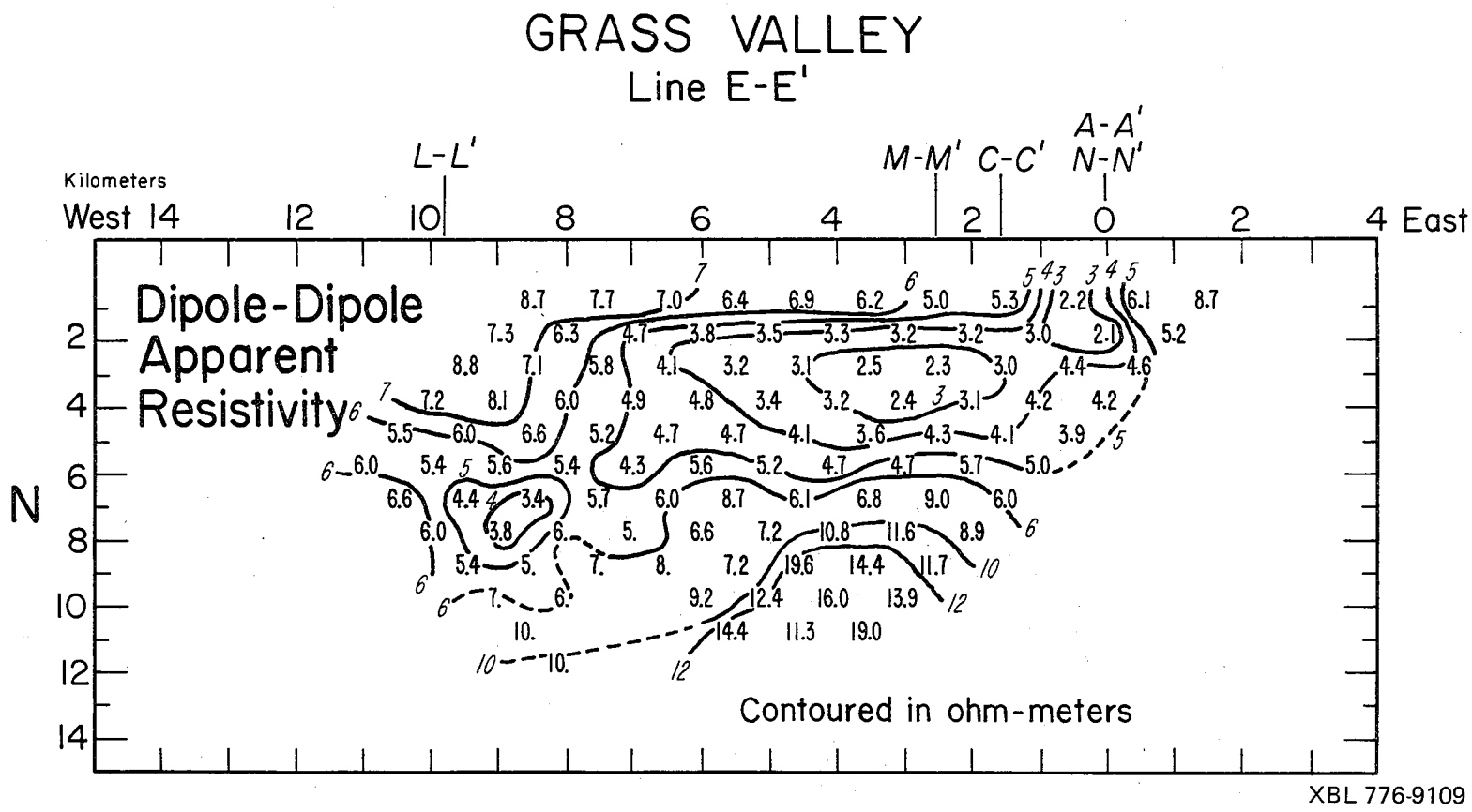

Figure III-15. Field data dipole-dipole apparent resistivity pseudo-section for 1 km dipoles along Line E-E'.

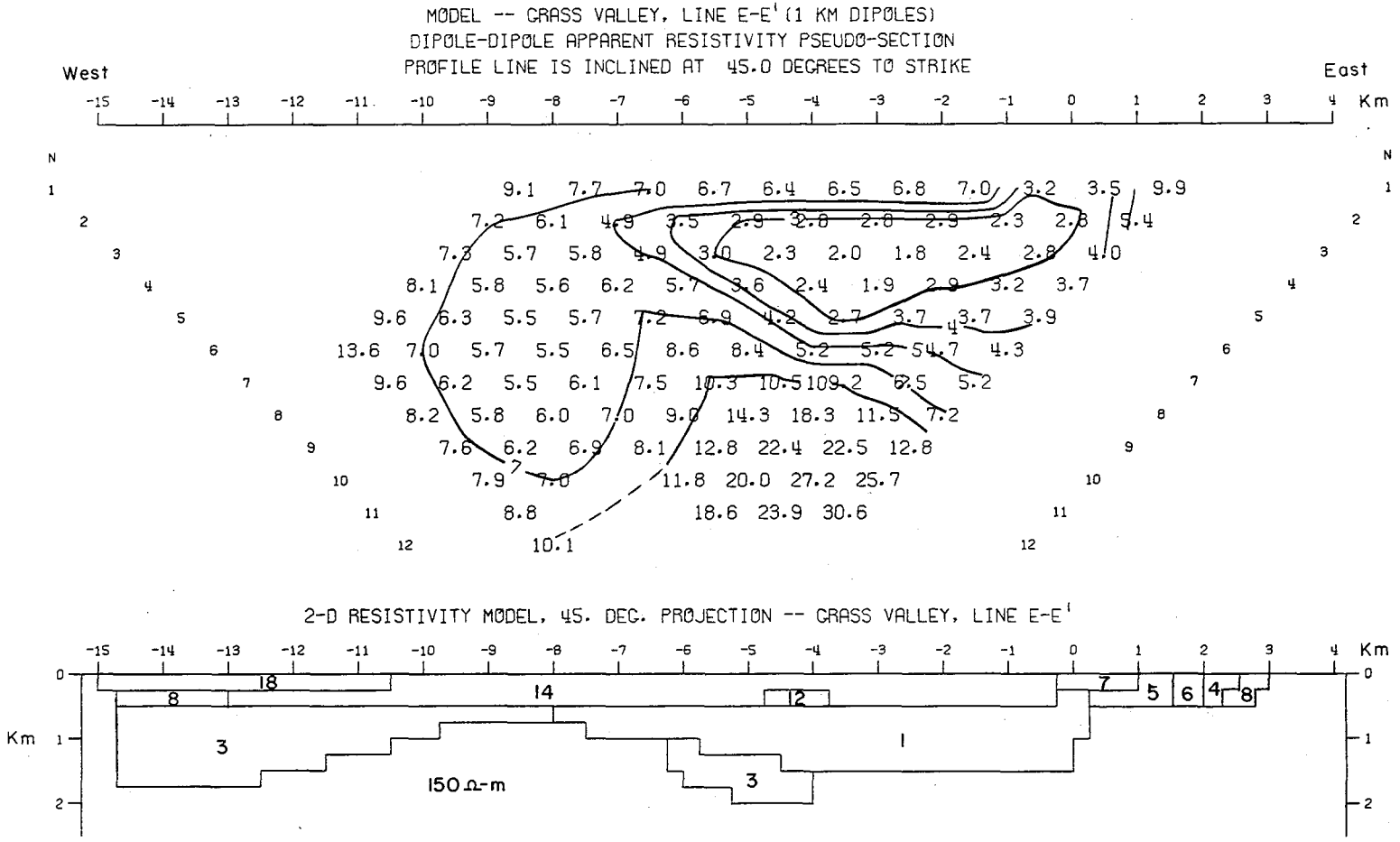

Figure III-16. Two-dimensional resistivity model (projection in the profile line direction at 45° to strike) and resultant dipole-dipole apparent resistivity pseudo-section for 1 km dipoles along Line E-E'.

XBL 776-9111

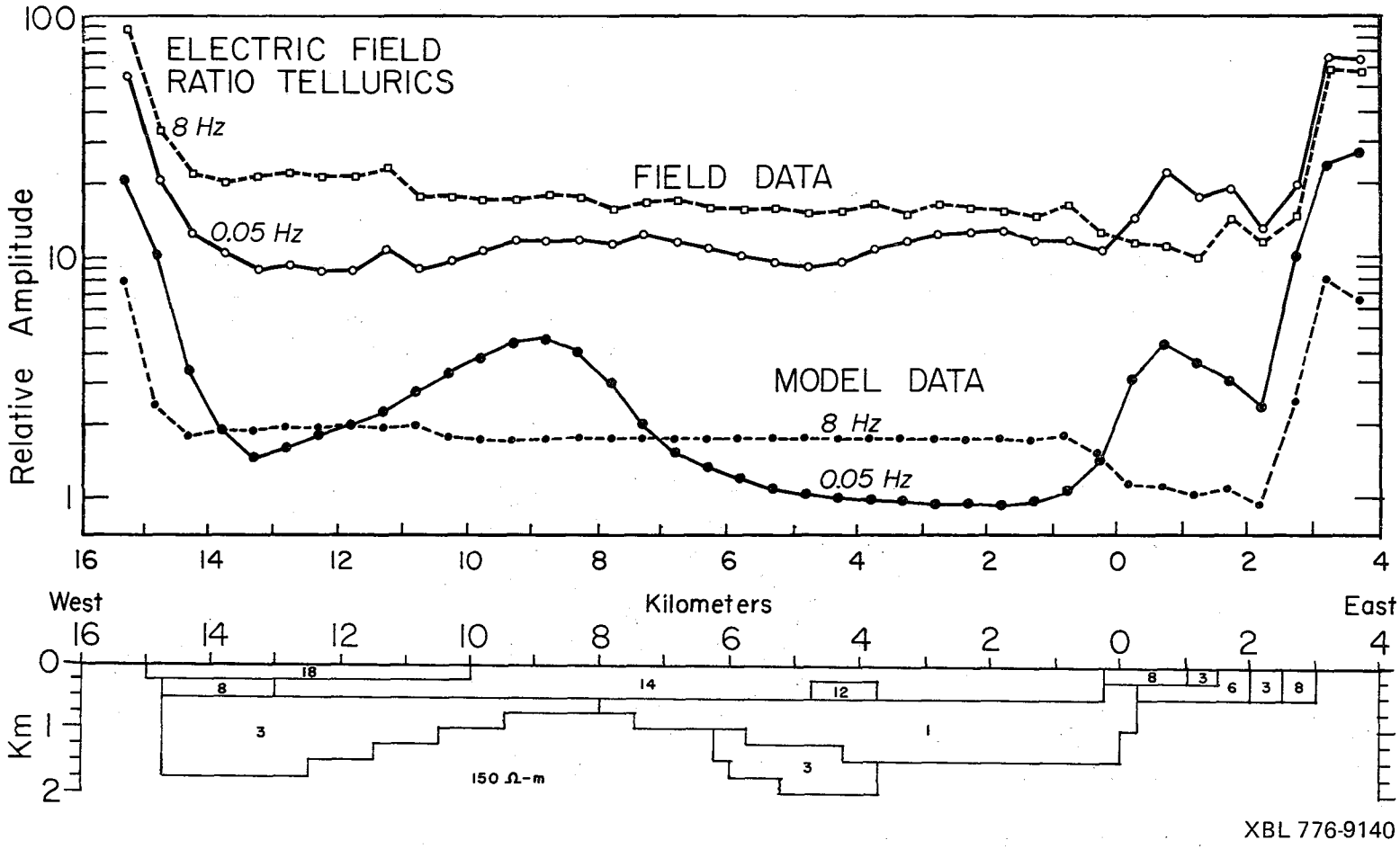

Figure III-17. Modeled E-field ratio telluric response at 0.05 and 8 Hz for the Line E-E' resistivity structure developed on the basis of dipole-dipole resistivity modeling. Telluric profile data can be shifted up or down to any position on the "relative amplitude" axis.

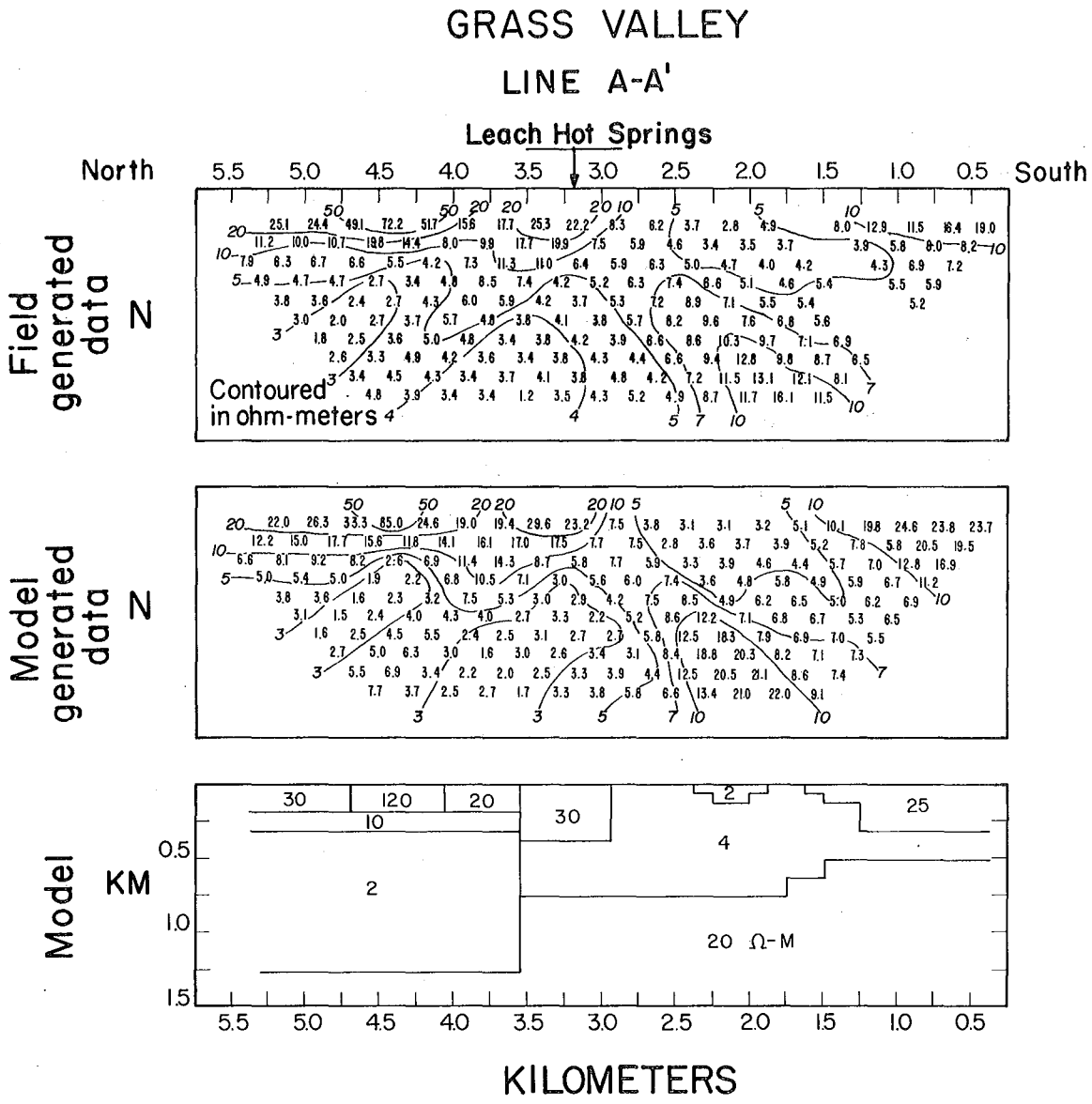

XBL 762-589

Figure III-18. Dipole dipole apparent resistivity pseudo-section for 250-meter dipoles along Line A-A': field data, model generated data, and two-dimensional resistivity model.

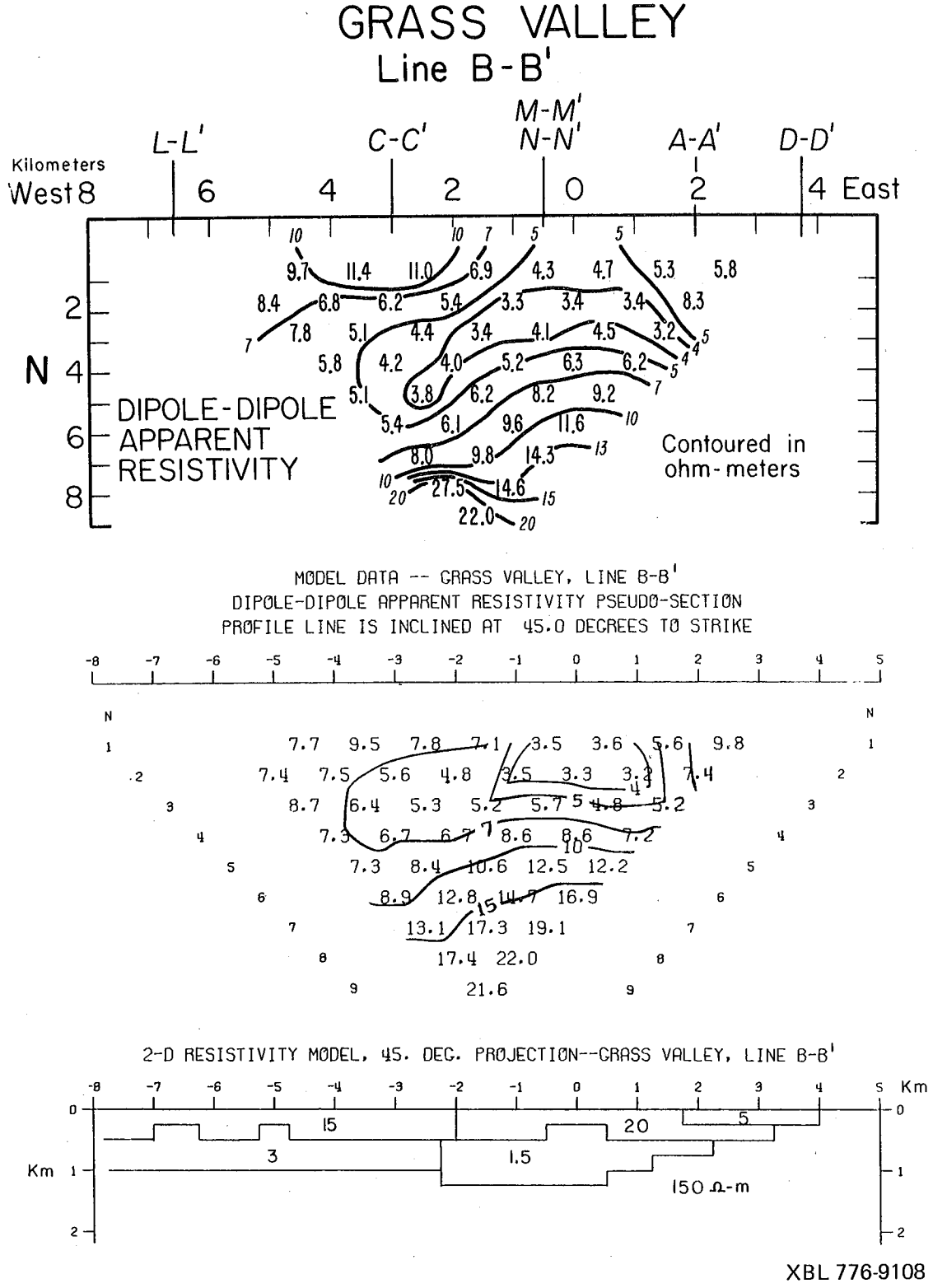

Figure III-19. Dipole-dipole apparent resistivity pseudo-section for 1 km dipoles along Line B-B': field data, model generated data, and two-dimensional resistivity model.

GRASS VALLEY
Line D-D'

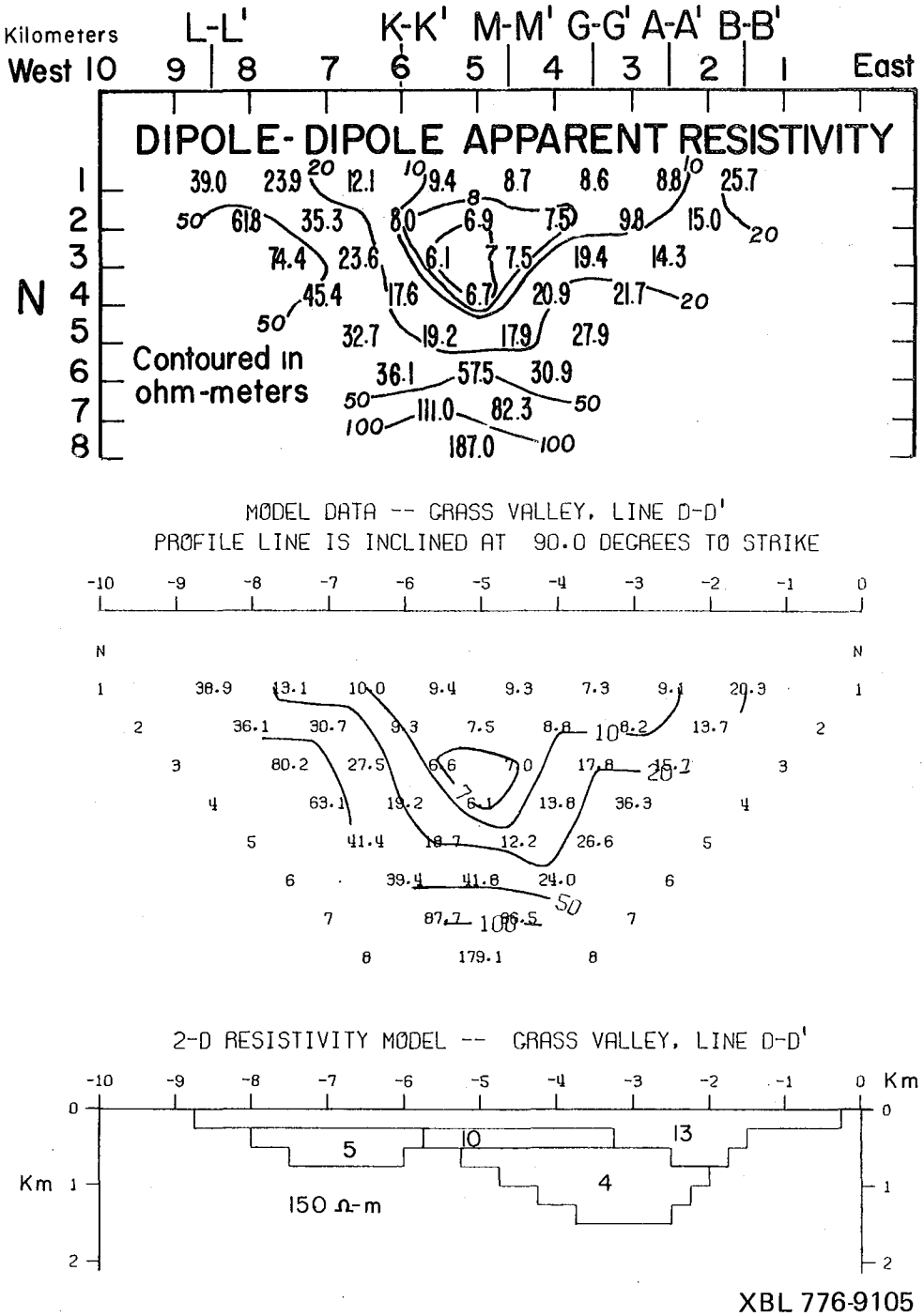

Figure III-20. Dipole-dipole apparent resistivity pseudo-section for 1 km dipoles along Line D-D': field data, model generated data, and two-dimensional resistivity model.

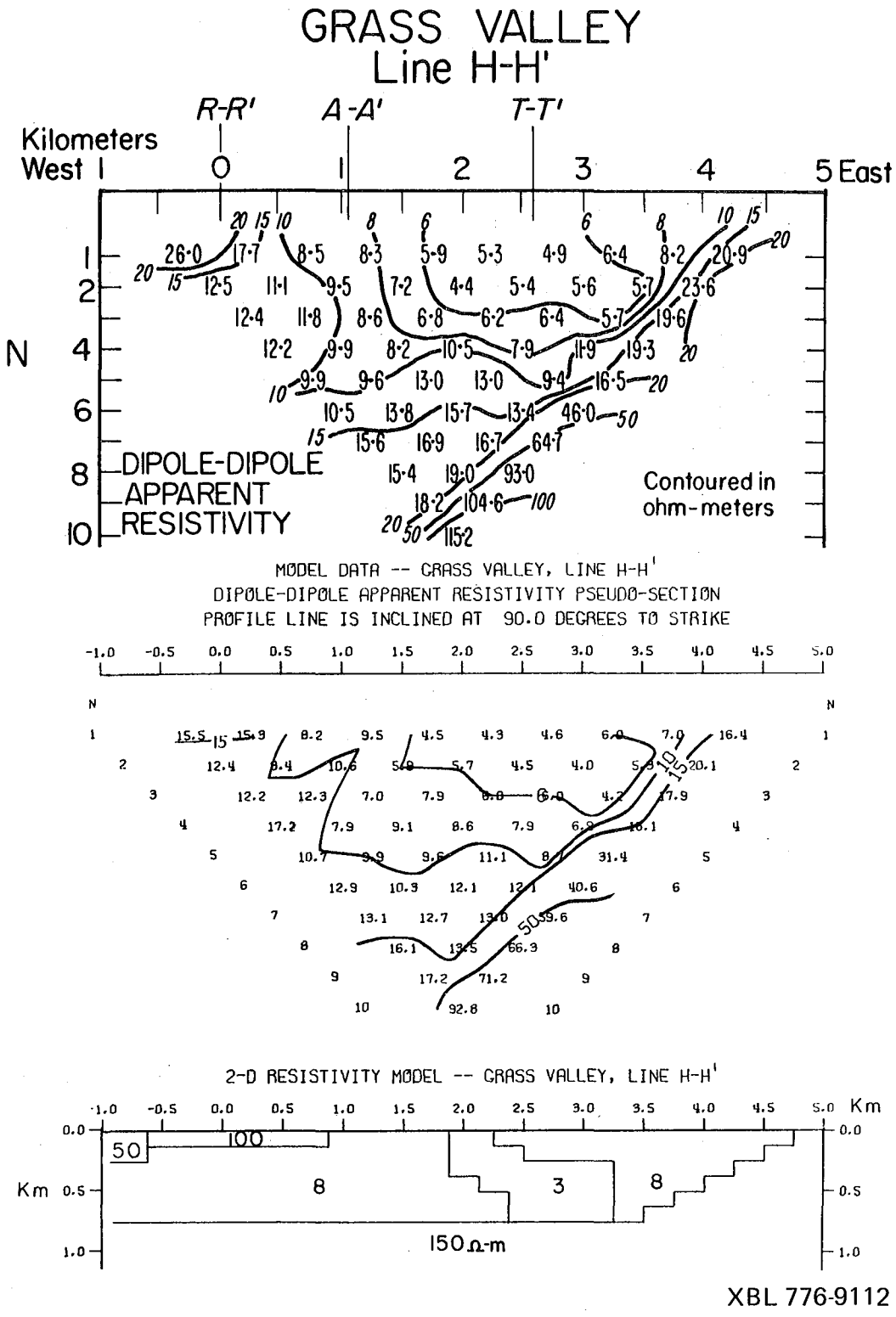

Figure III-21. Dipole-dipole apparent resistivity pseudo-section for 1 km dipoles along Line H-H': field data, model generated data, and two-dimensional resistivity model.

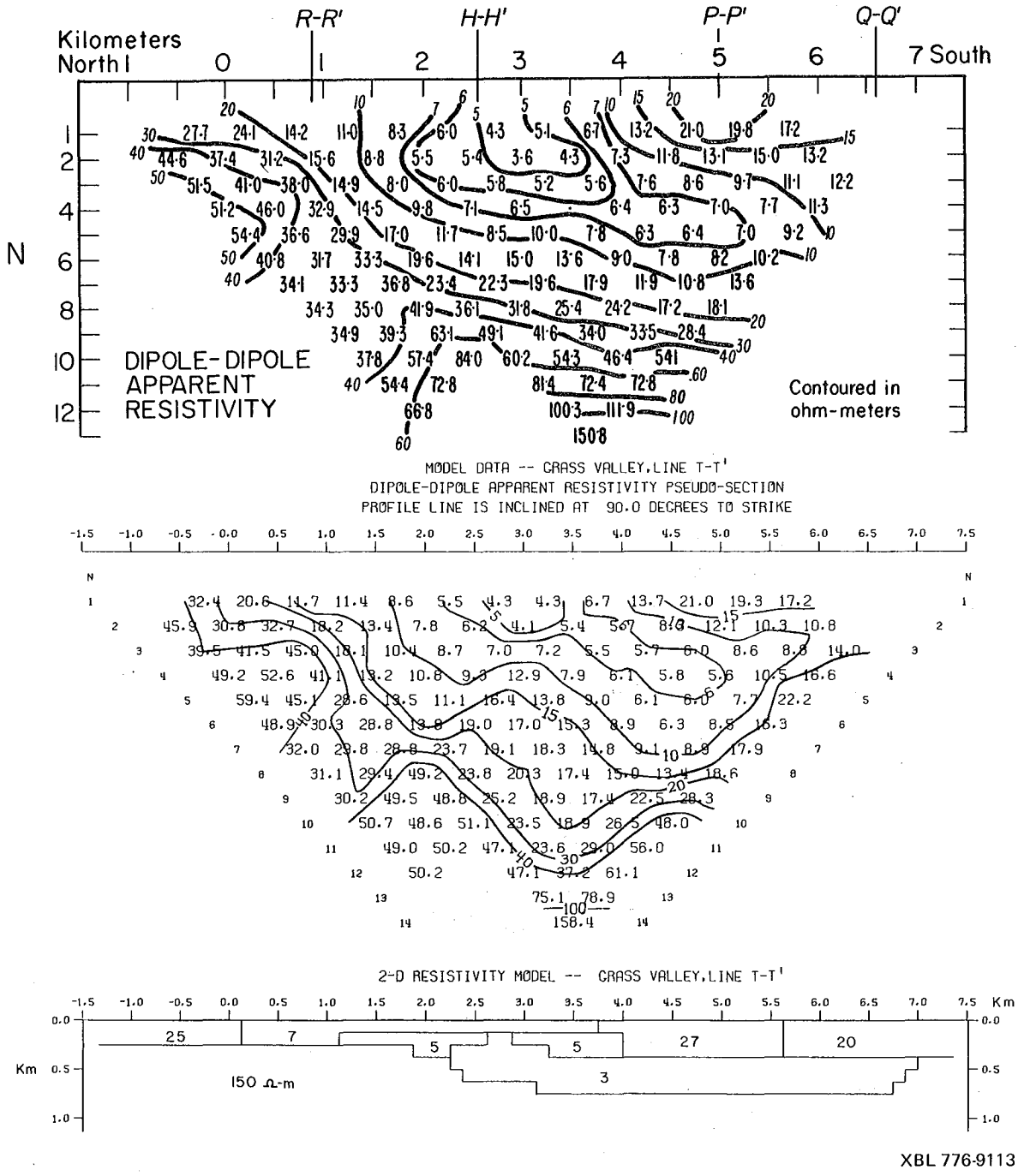

Figure III-22. Dipole-dipole apparent resistivity pseudo-section for 1 km dipoles along Line T-T': field data, model generated data, and two-dimensional resistivity model.

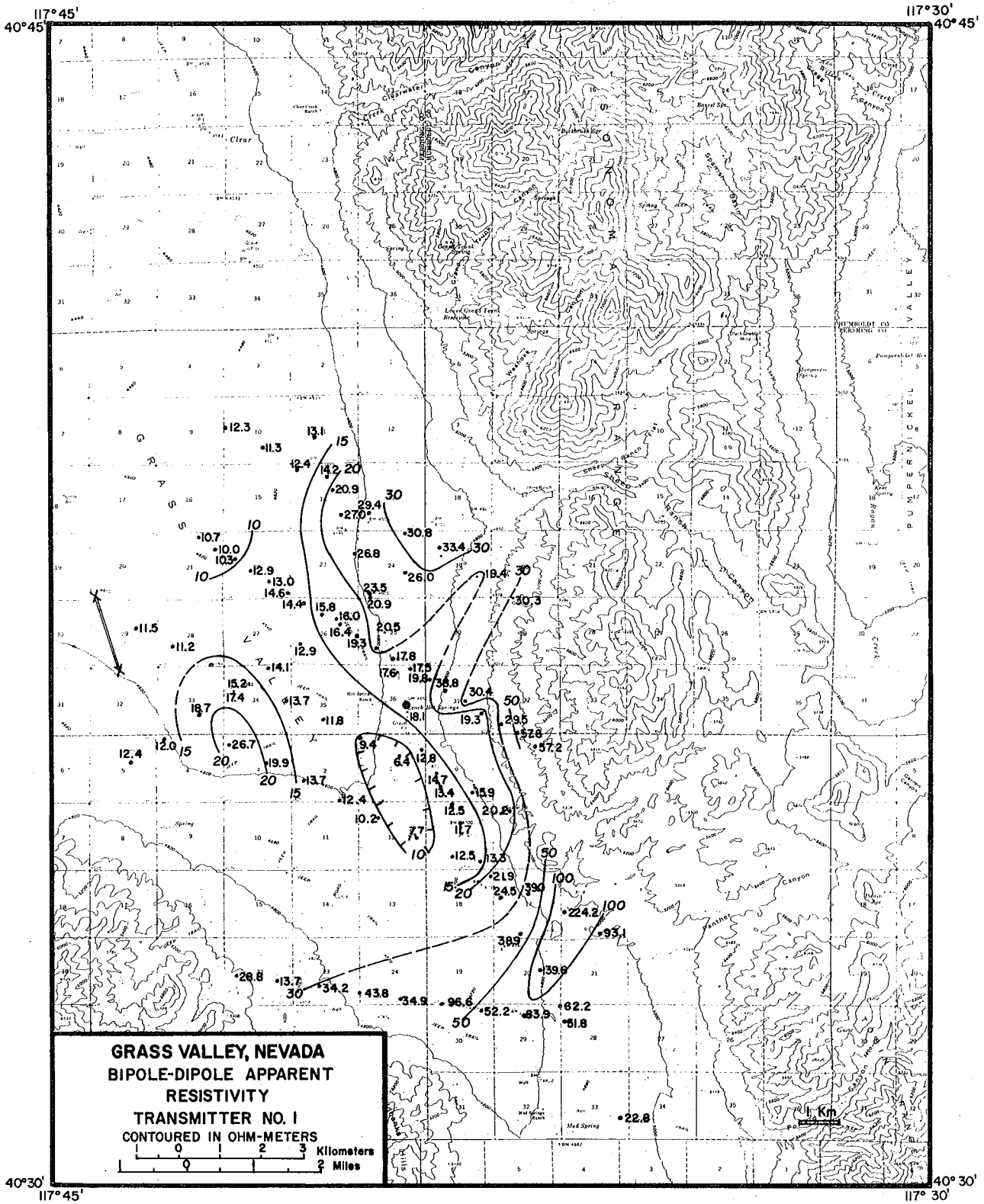

Figure III-23. Bipole-dipole apparent resistivity map for transmitter no. 1.

XBL 768-10090

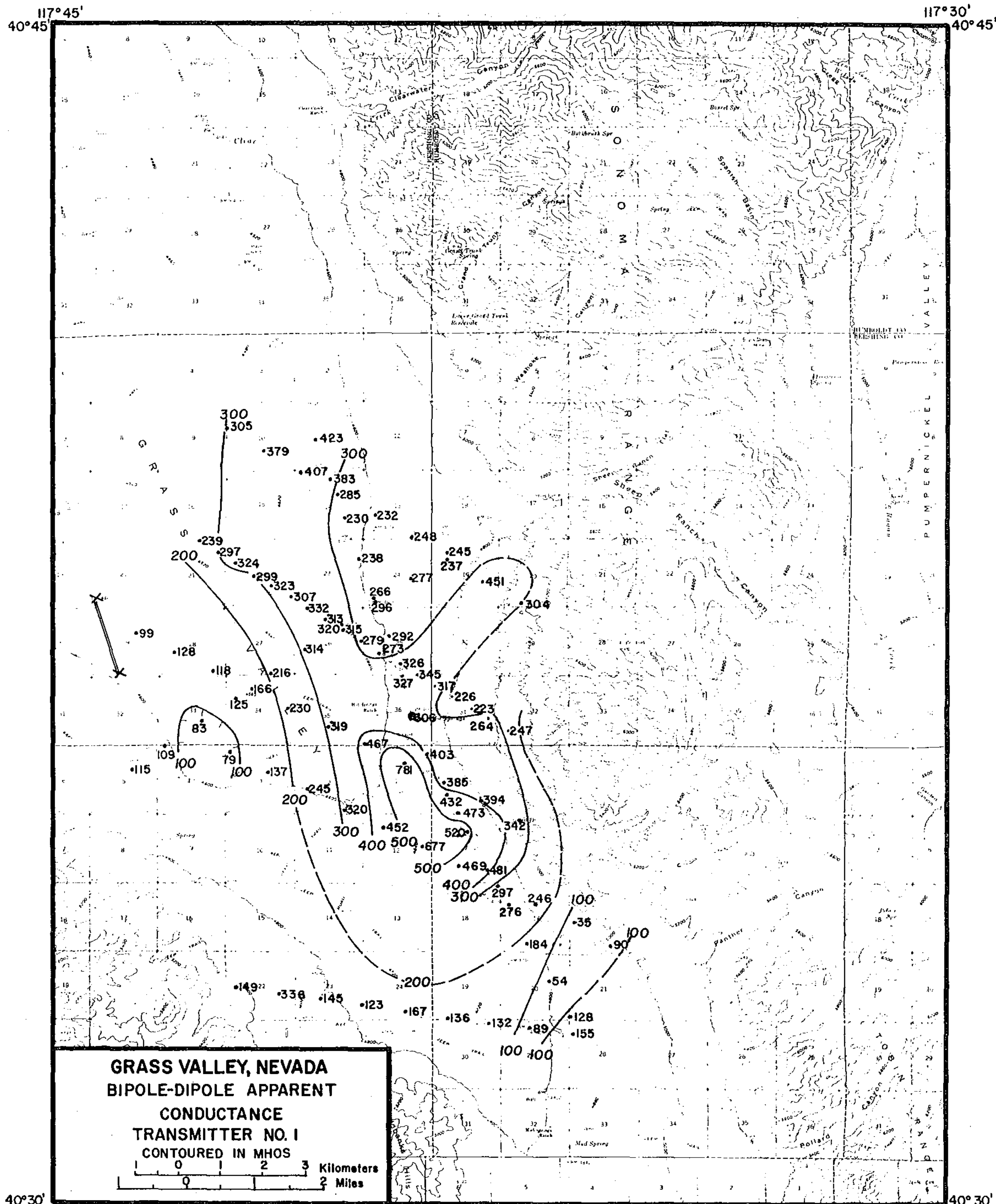

Figure III-24. Bipole-dipole apparent conductance map for transmitter no. 1.

XBL 768-10086

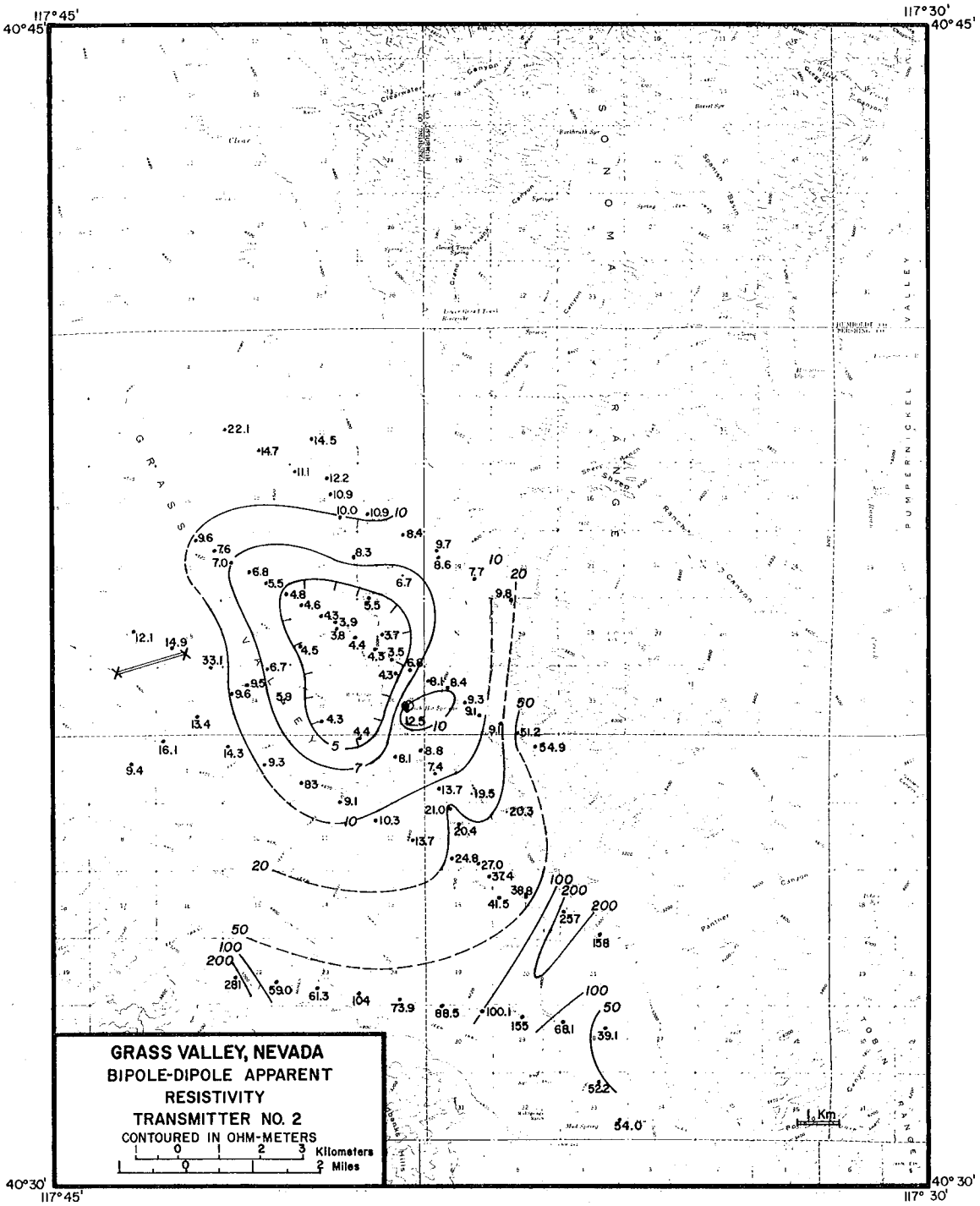

Figure III-25. Bipole-dipole apparent resistivity map for transmitter no. 2.

XBL 768-10087

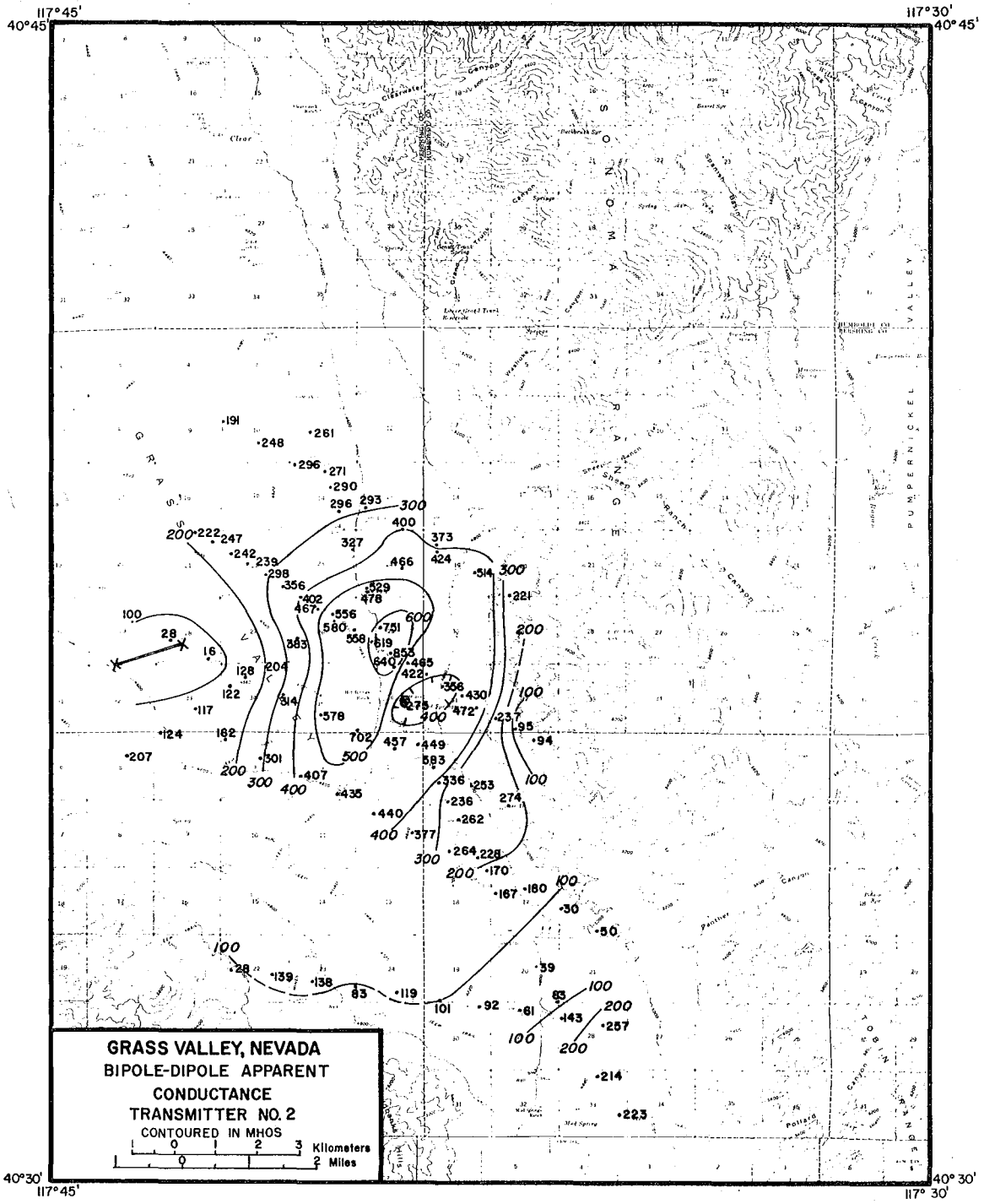

Figure III-26. Bipole-dipole apparent conductance map for transmitter no. 2.

XBL 768-10084

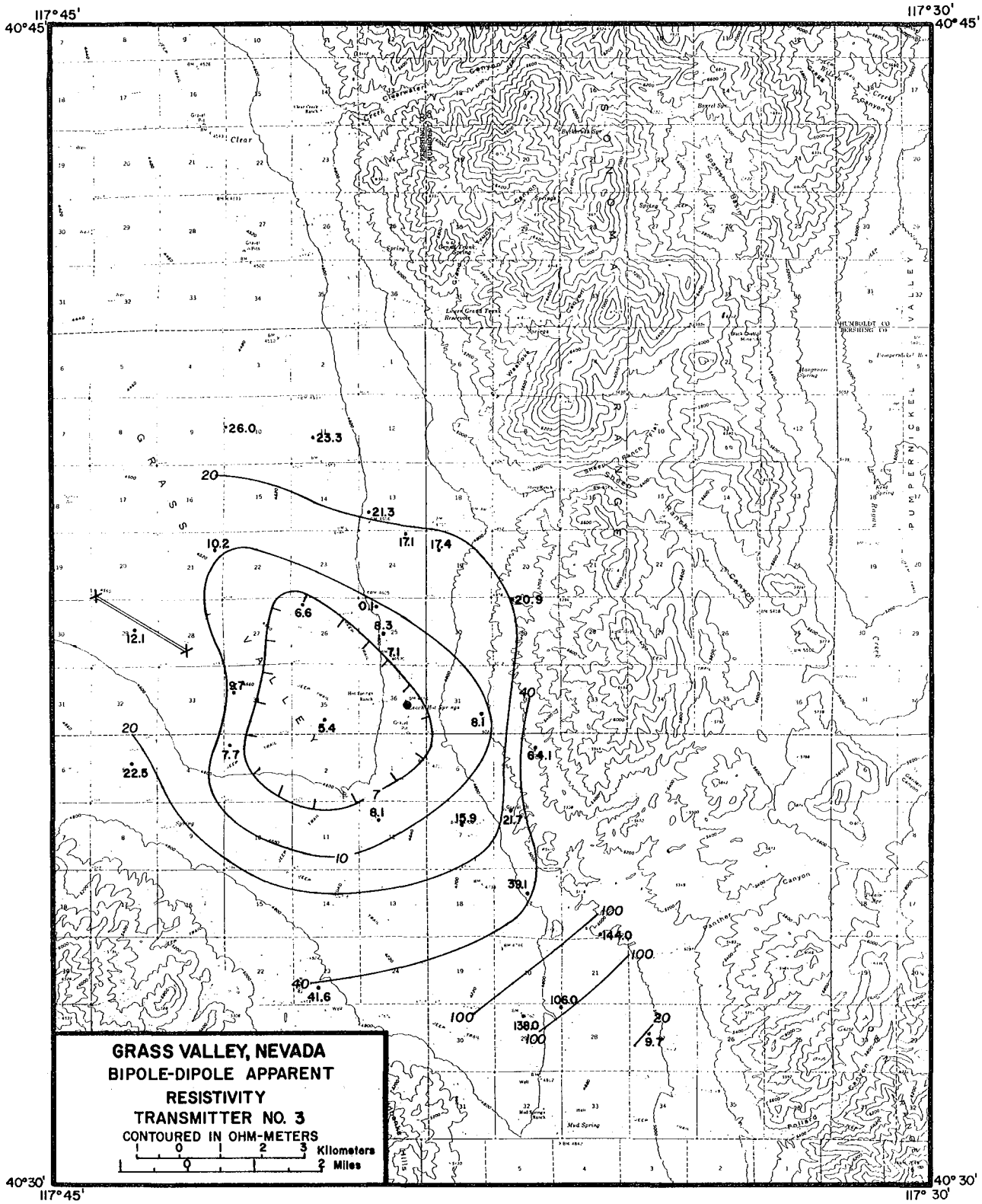

Figure III-27. Bipole-dipole apparent resistivity map for transmitter no. 3.

XBL 768-10092

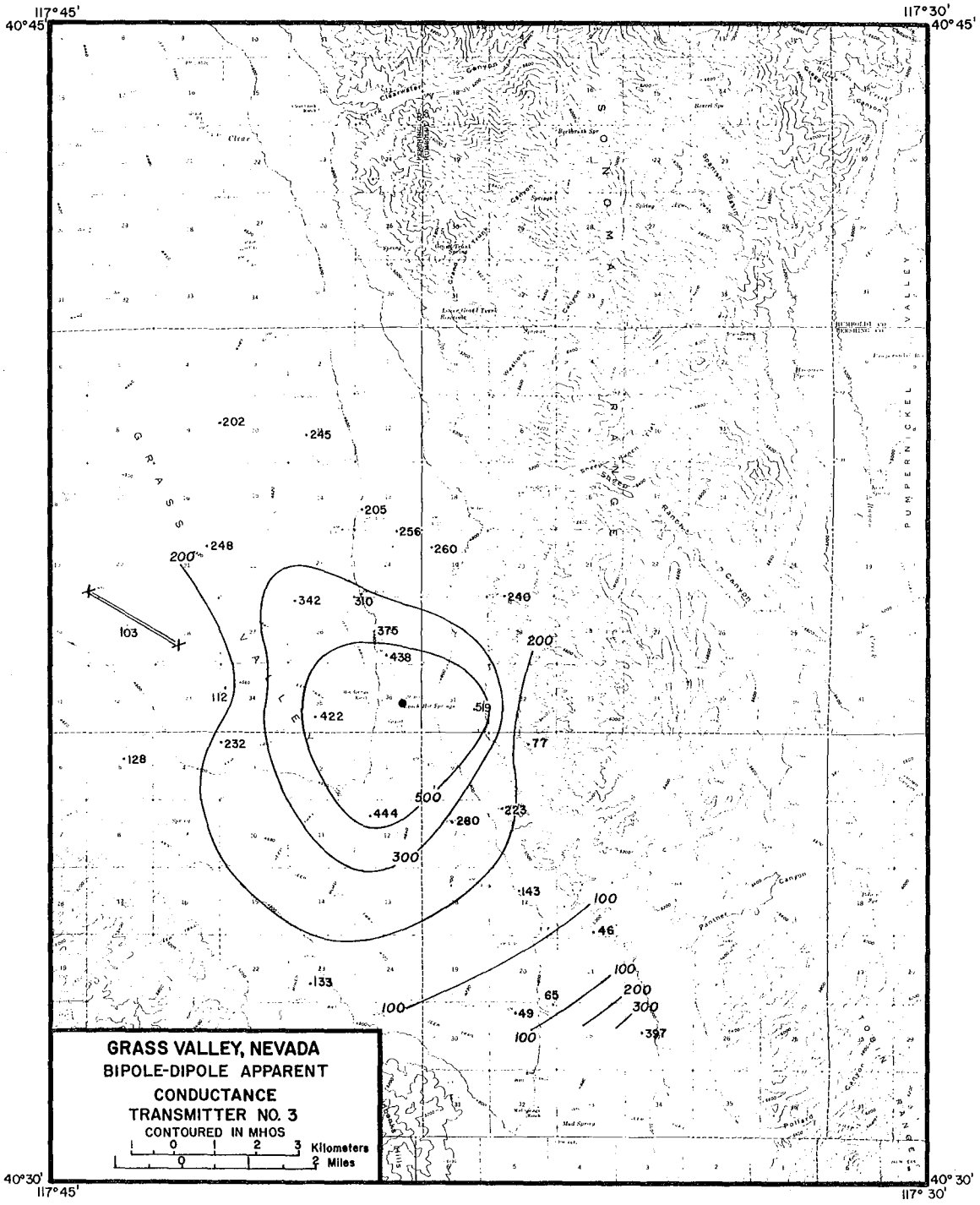

Figure III-28. Bipole-dipole apparent conductance map for transmitter no. 3.

XBL 768-10091

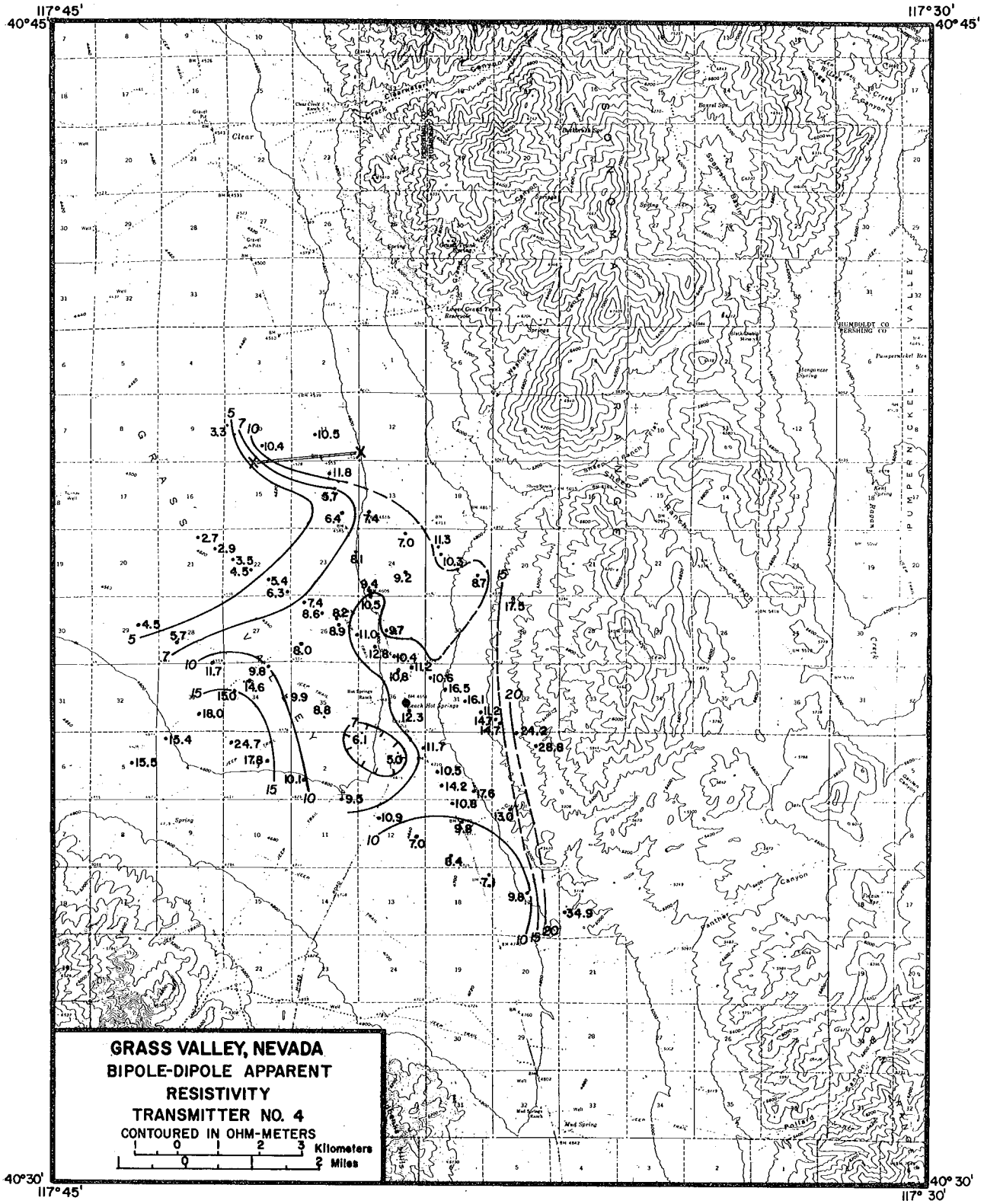

Figure III-29. Bipole-dipole apparent resistivity map for transmitter no. 4.

XBL 768-10088

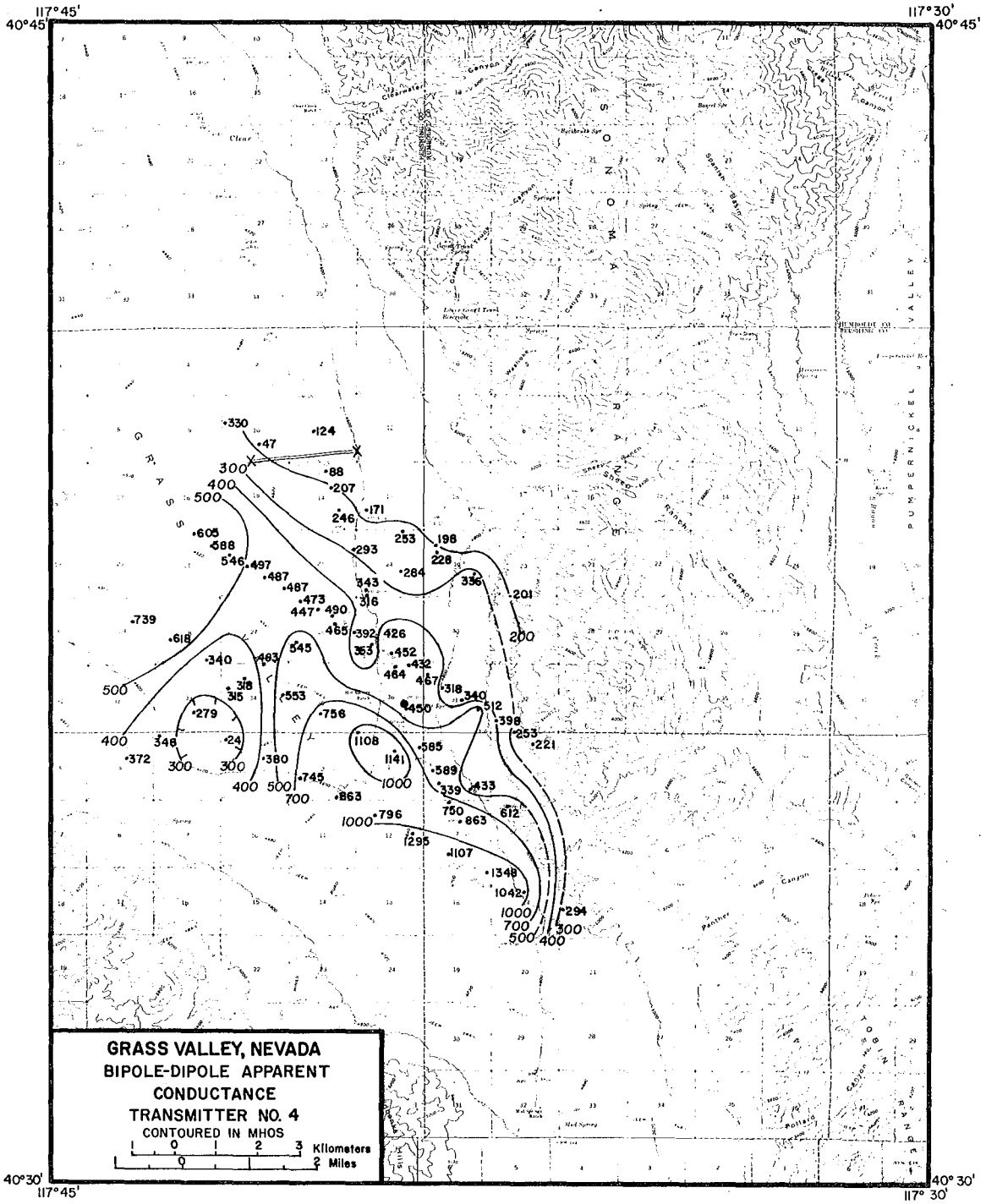

Figure III-30. Bipole-dipole apparent conductance map for transmitter no. 4.

XBL 768-10089

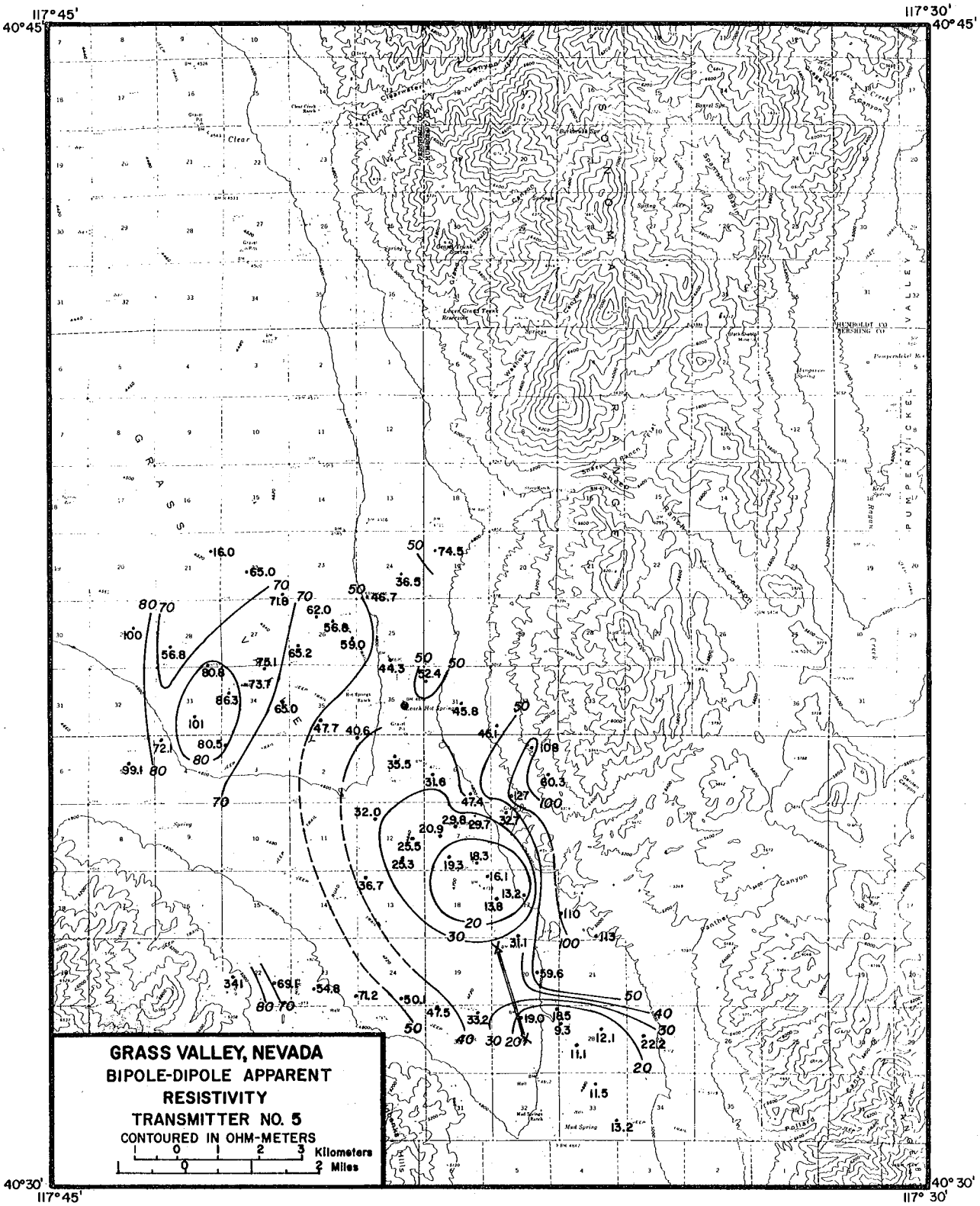

Figure III-31. Bipole-dipole apparent resistivity map for transmitter no. 5.

XBL 768-10085

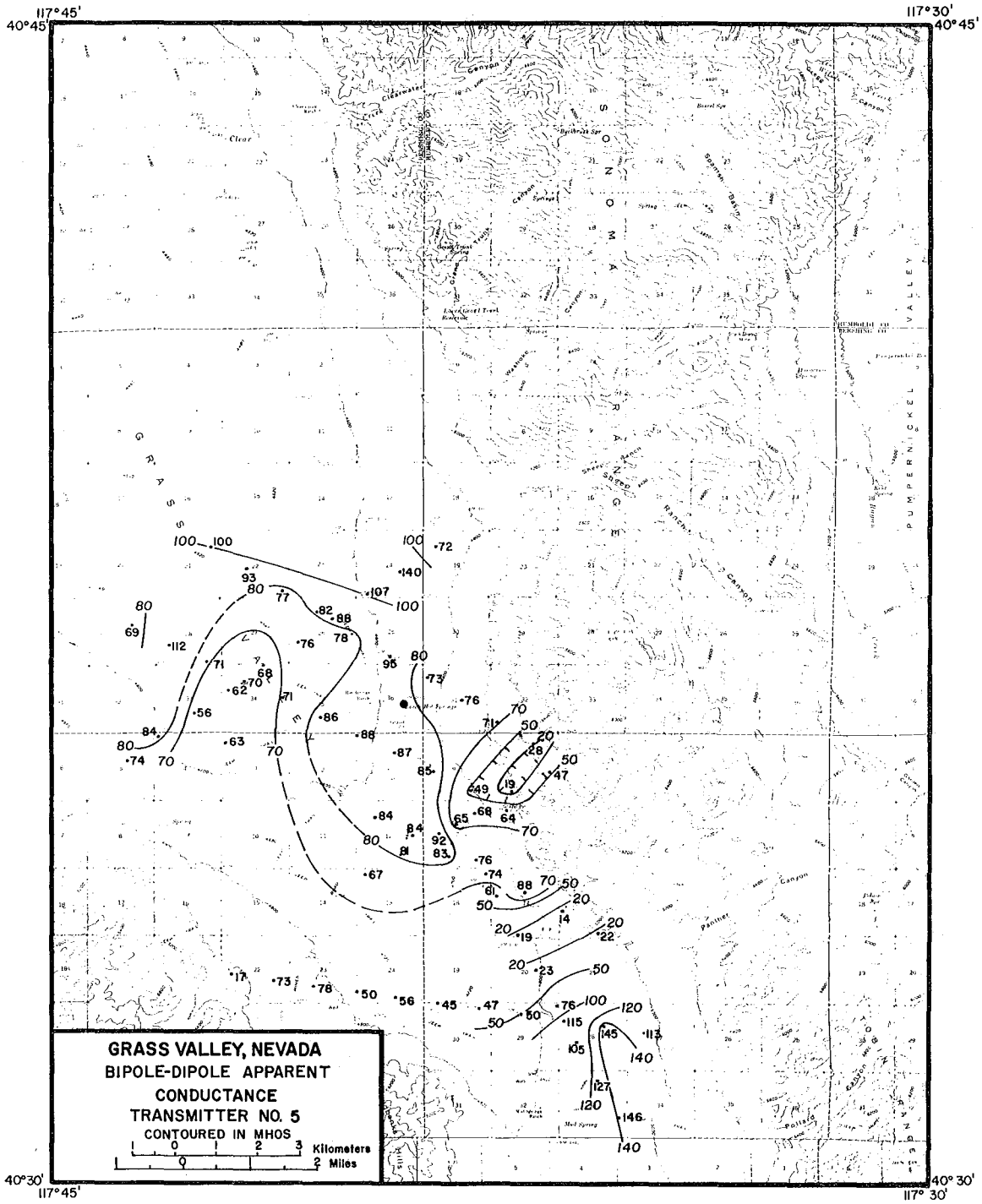

Figure III-32. Bipole-dipole apparent conductance map for transmitter no. 5.

XBL 768-10093

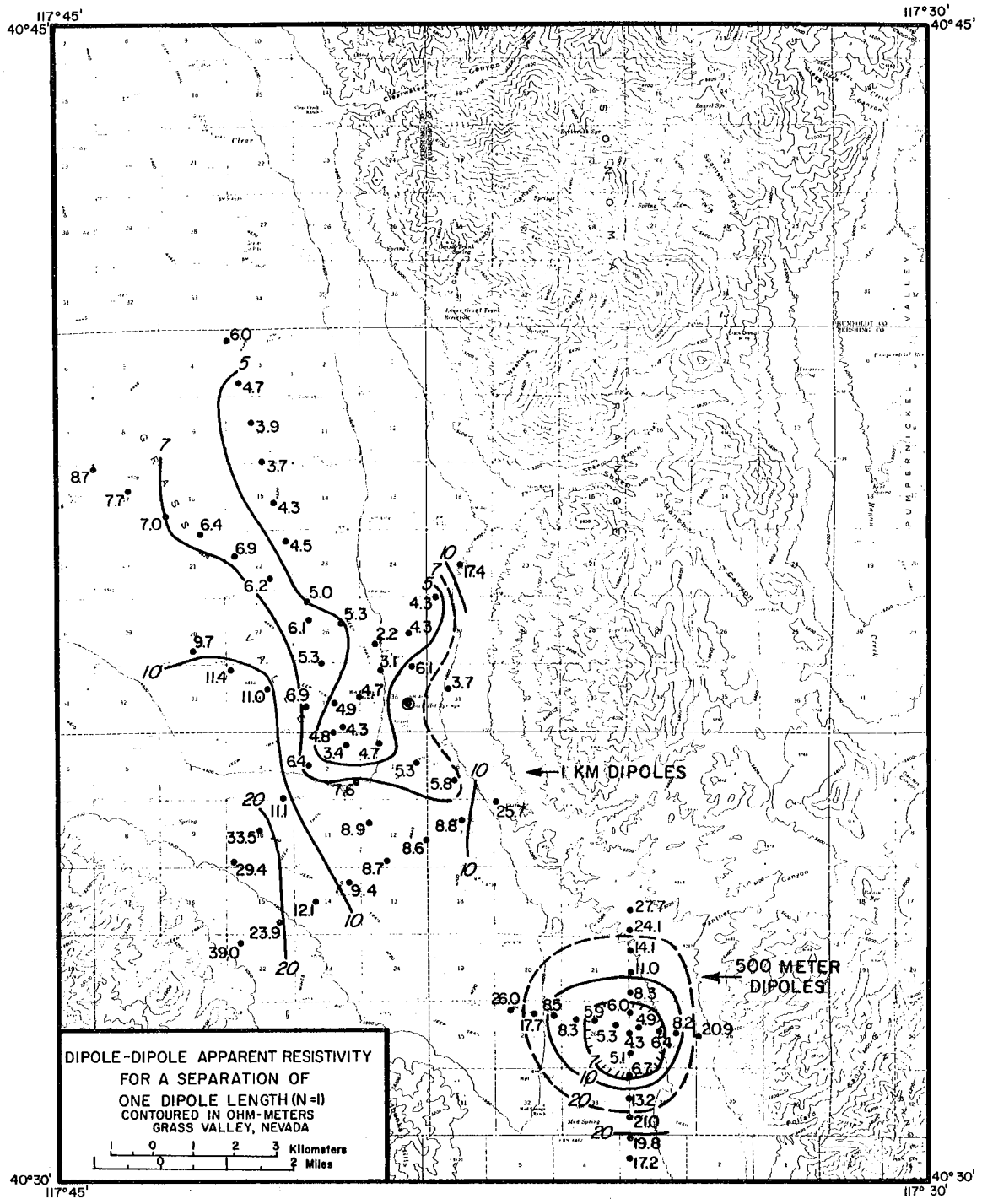

Figure III-33. Map of the near-surface apparent resistivity as observed by the dipole-dipole surveys at a separation of N = 1. Grass Valley, Nevada.

XBL 776-9114

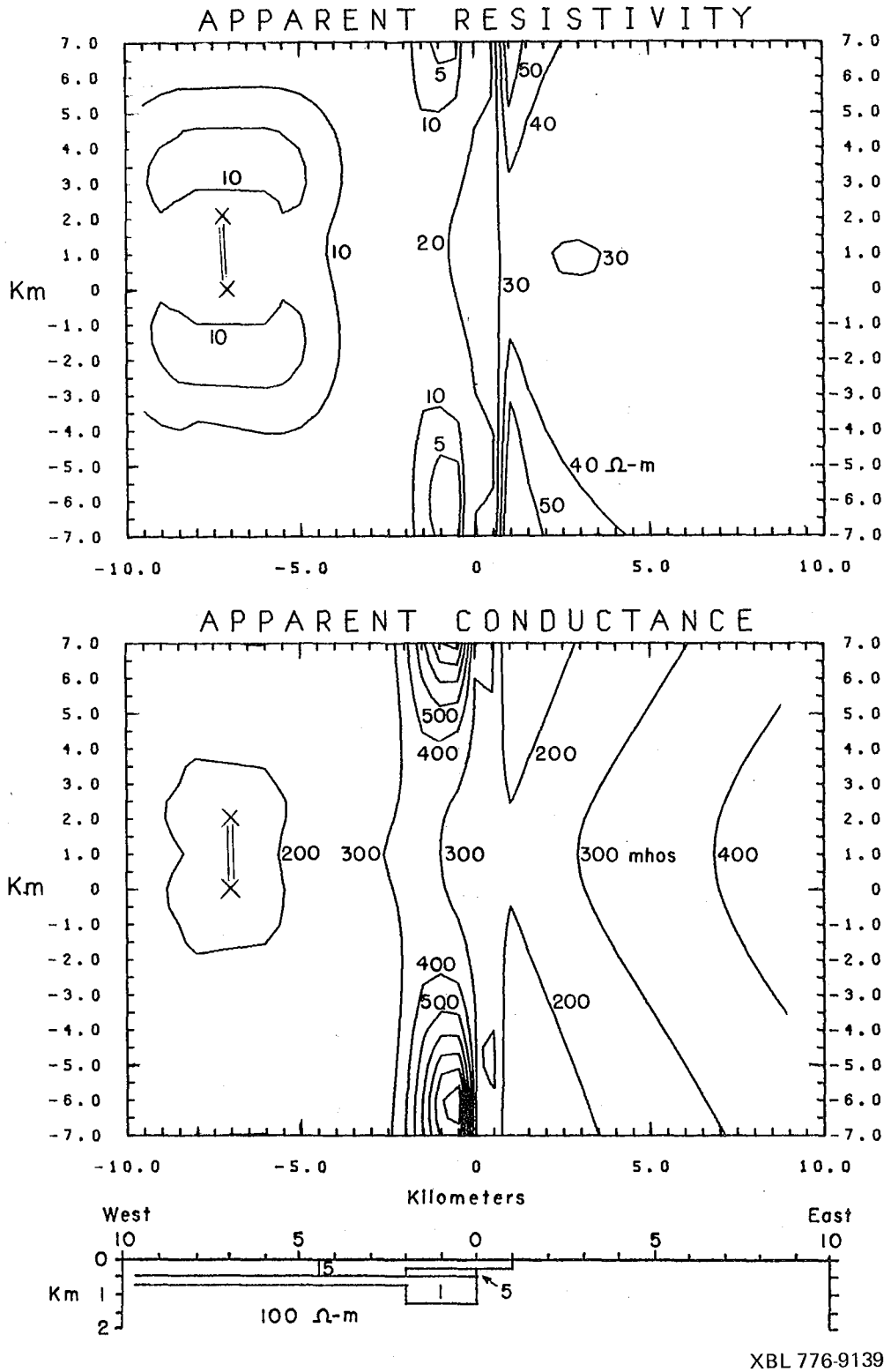

Figure III-34. Modeled bipole-dipole apparent resistivity and apparent conductance maps for a two-dimensional structure resembling Grass Valley in the vicinity of Leach Hot Springs. The bipole transmitter is parallel to strike, similar to transmitter no. 1.

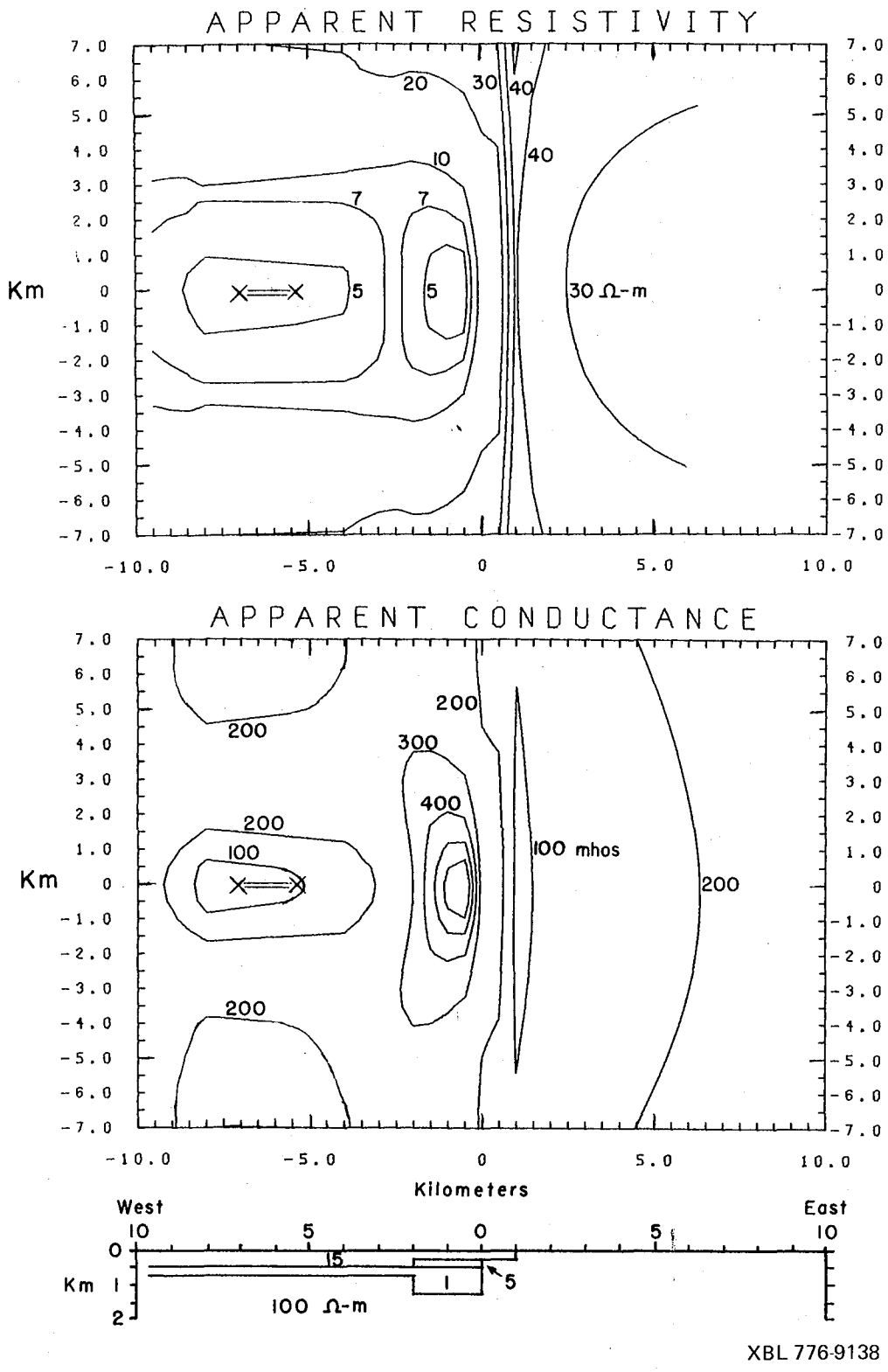

Figure III-35. Modeled bipole-dipole apparent resistivity and apparent conductance maps for a two-dimensional structure resembling Grass Valley in the vicinity of Leach Hot Springs. The bipole transmitter is perpendicular to strike, similar to transmitter no. 2.

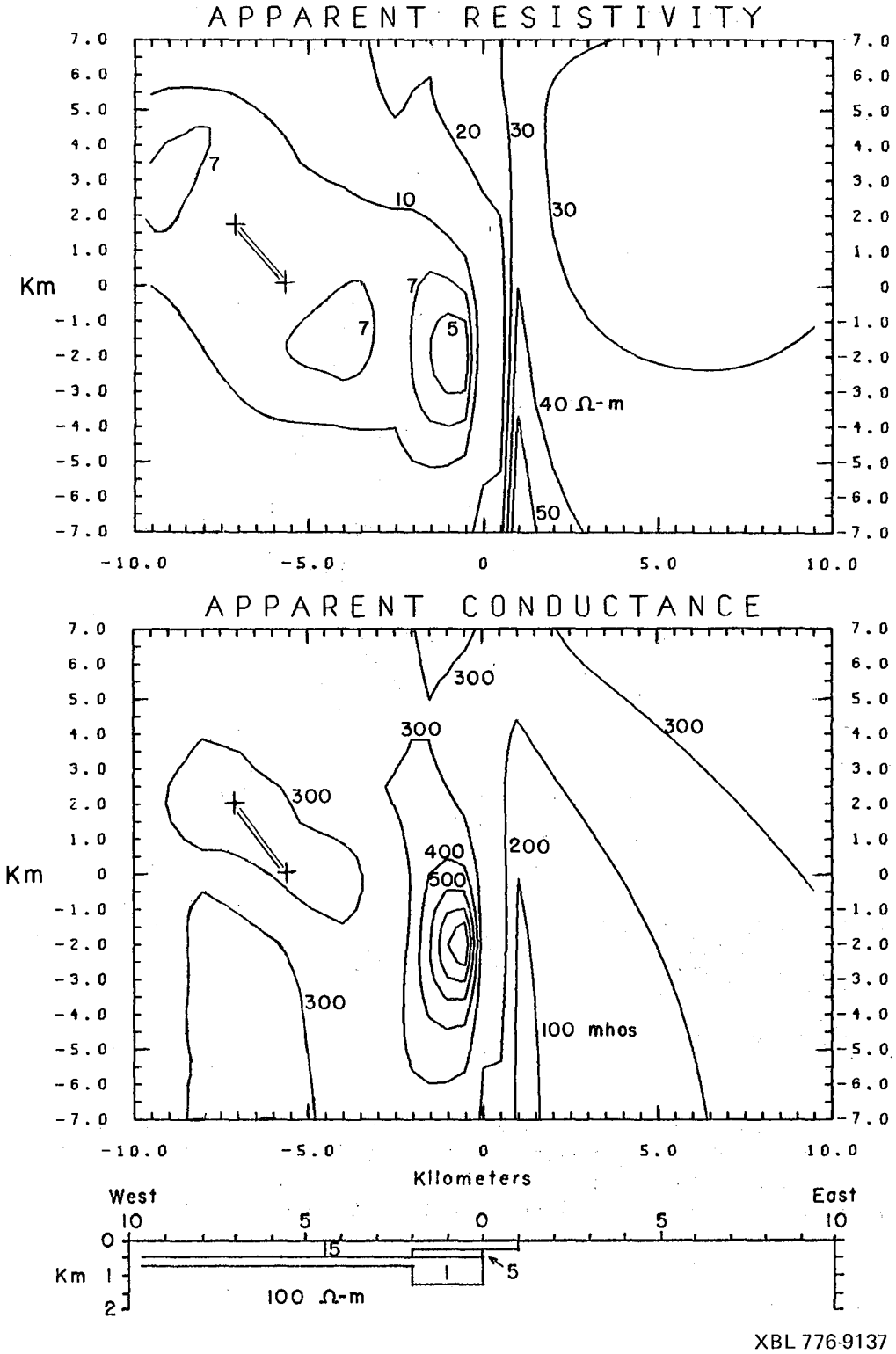

Figure III-36. Modeled bipole-dipole apparent resistivity and apparent conductance maps for a two-dimensional structure resembling Grass Valley in the vicinity of Leach Hot Springs. The bipole transmitter is at 45° to strike, similar to transmitter no. 3.

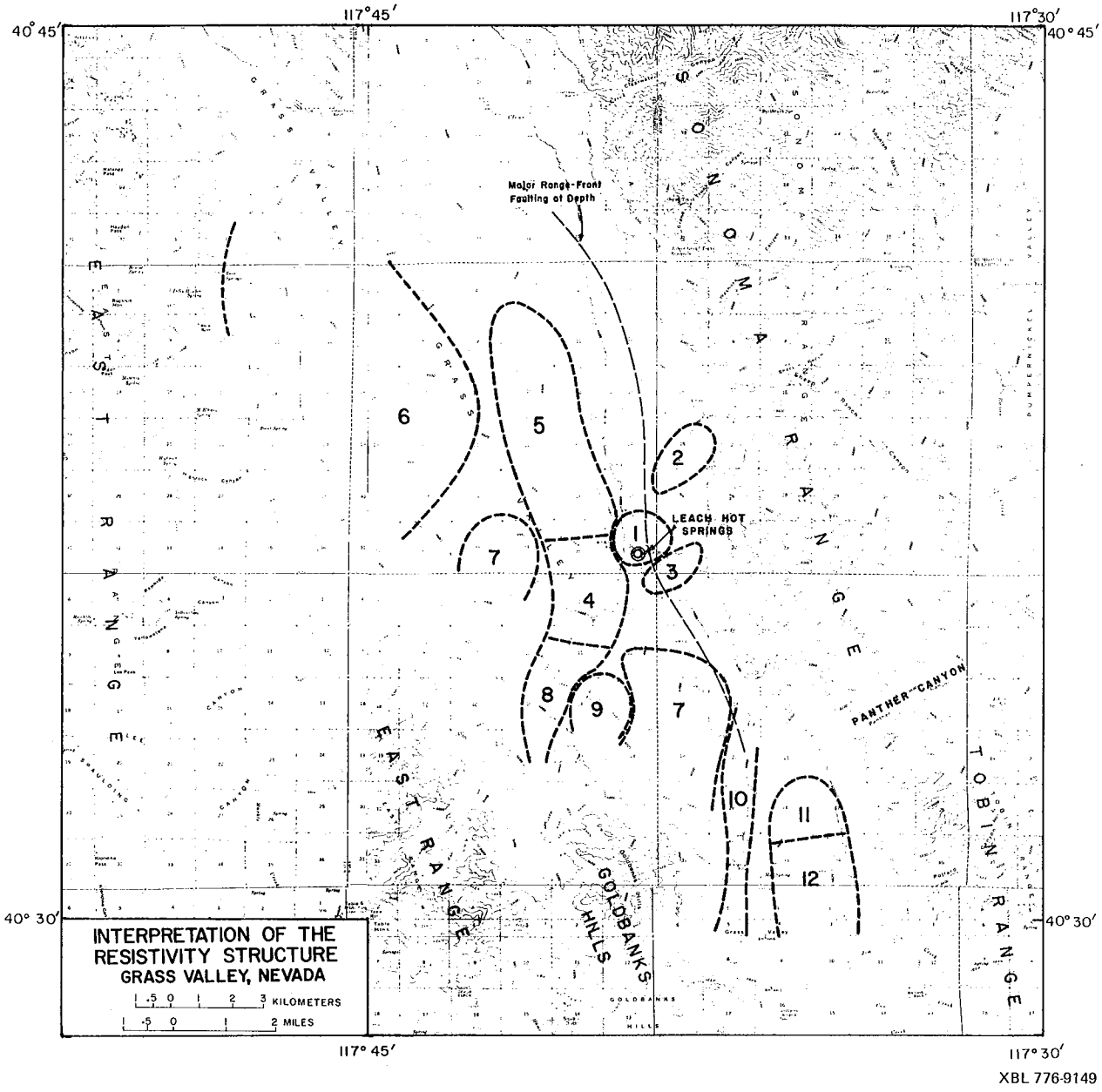

Figure III-37. Structural regions in Grass Valley, Nevada, delineated on the basis of the interpretation of telluric and d.c. resistivity data, in conjunction with gravity, seismic, and geological data. The numbered areas are discussed in the section entitled "The Resistivity Structure of Grass Valley."

APPENDIX III-A

Geophysical Data Profile Composites

Grass Valley, Nevada

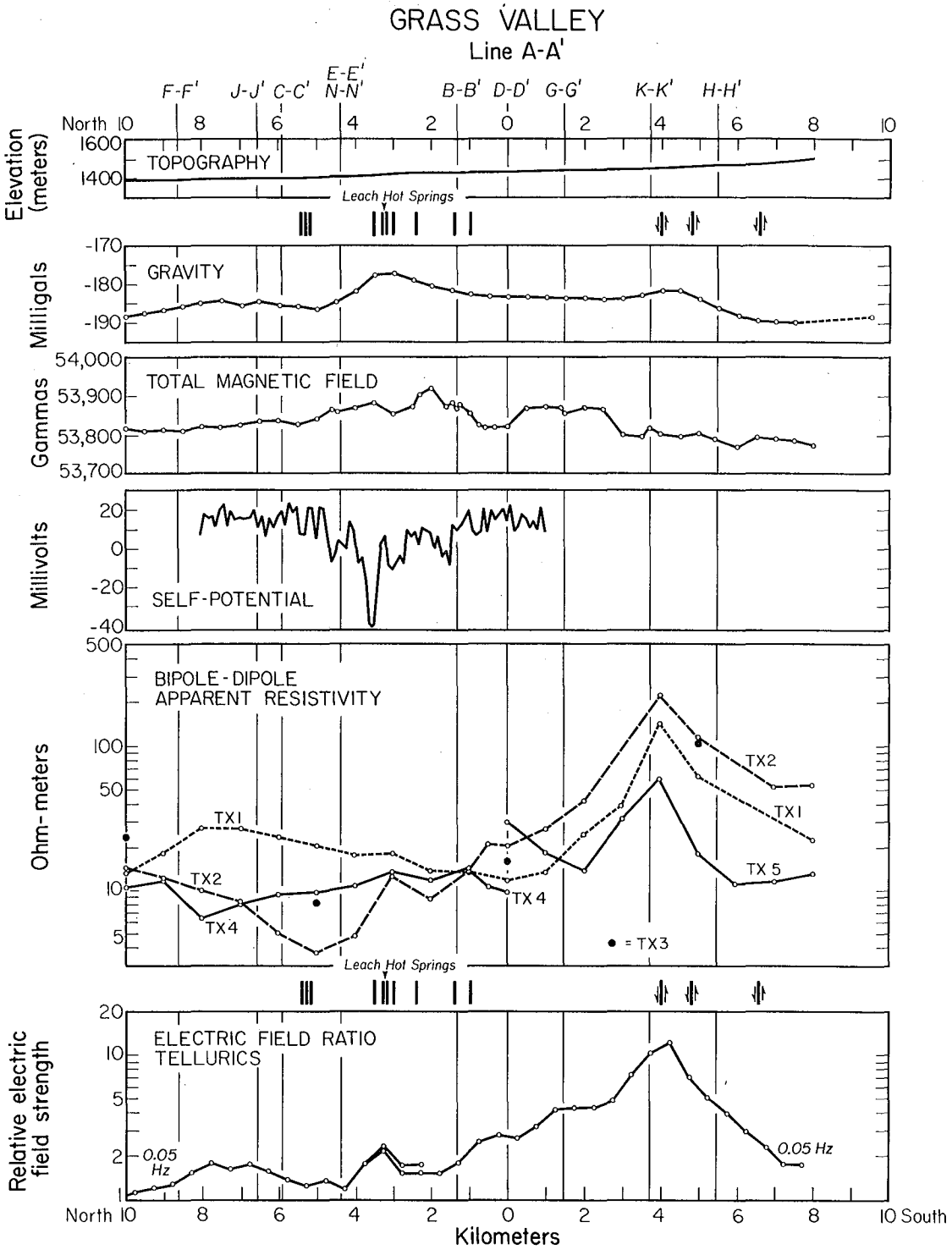

XBL 7512-9585

Figure III-A1. Geophysical data profile composite for Line A-A'.

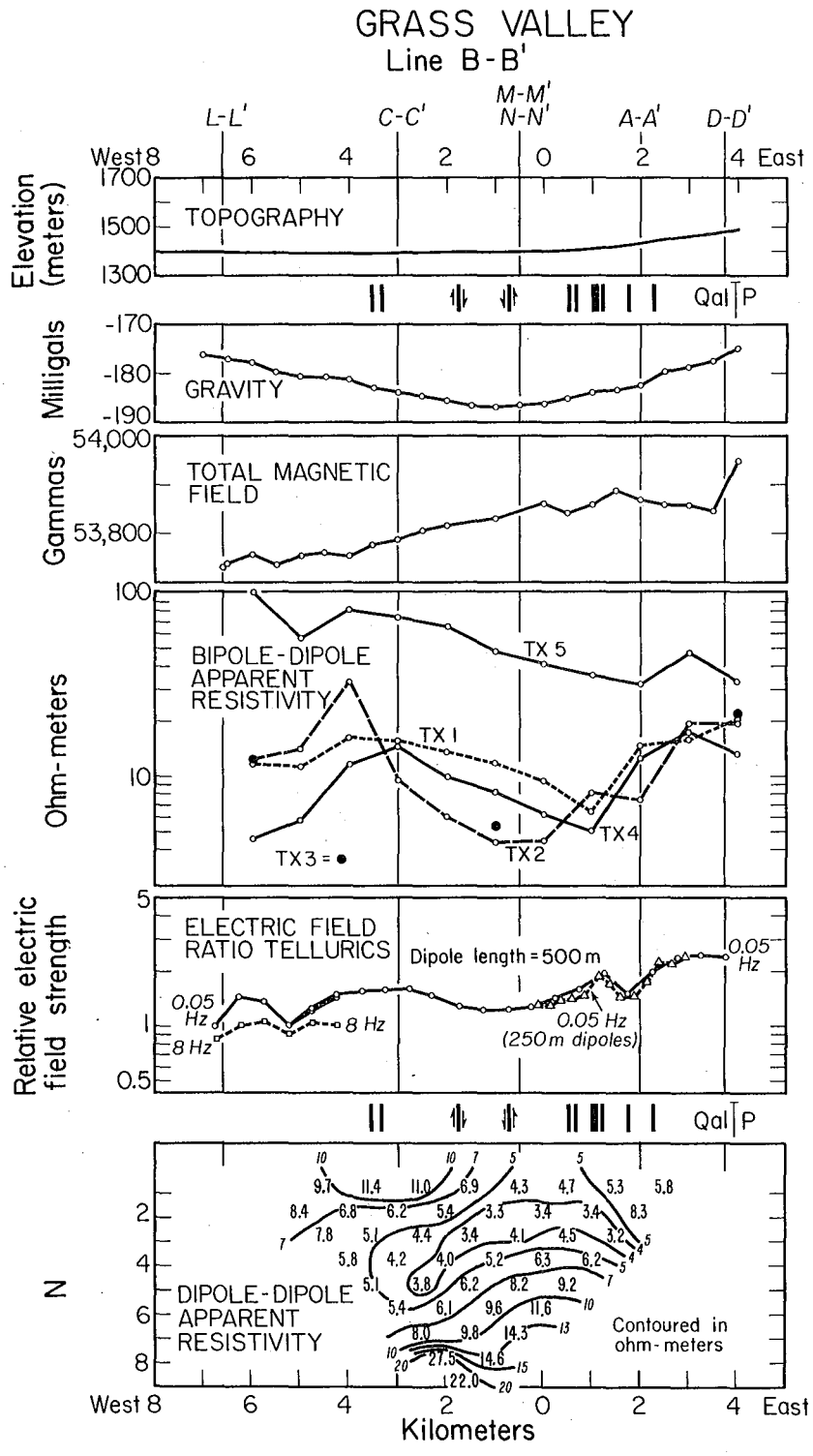

XBL 7512-9586

Figure III-A2. Geophysical data profile composite for Line B-B'.

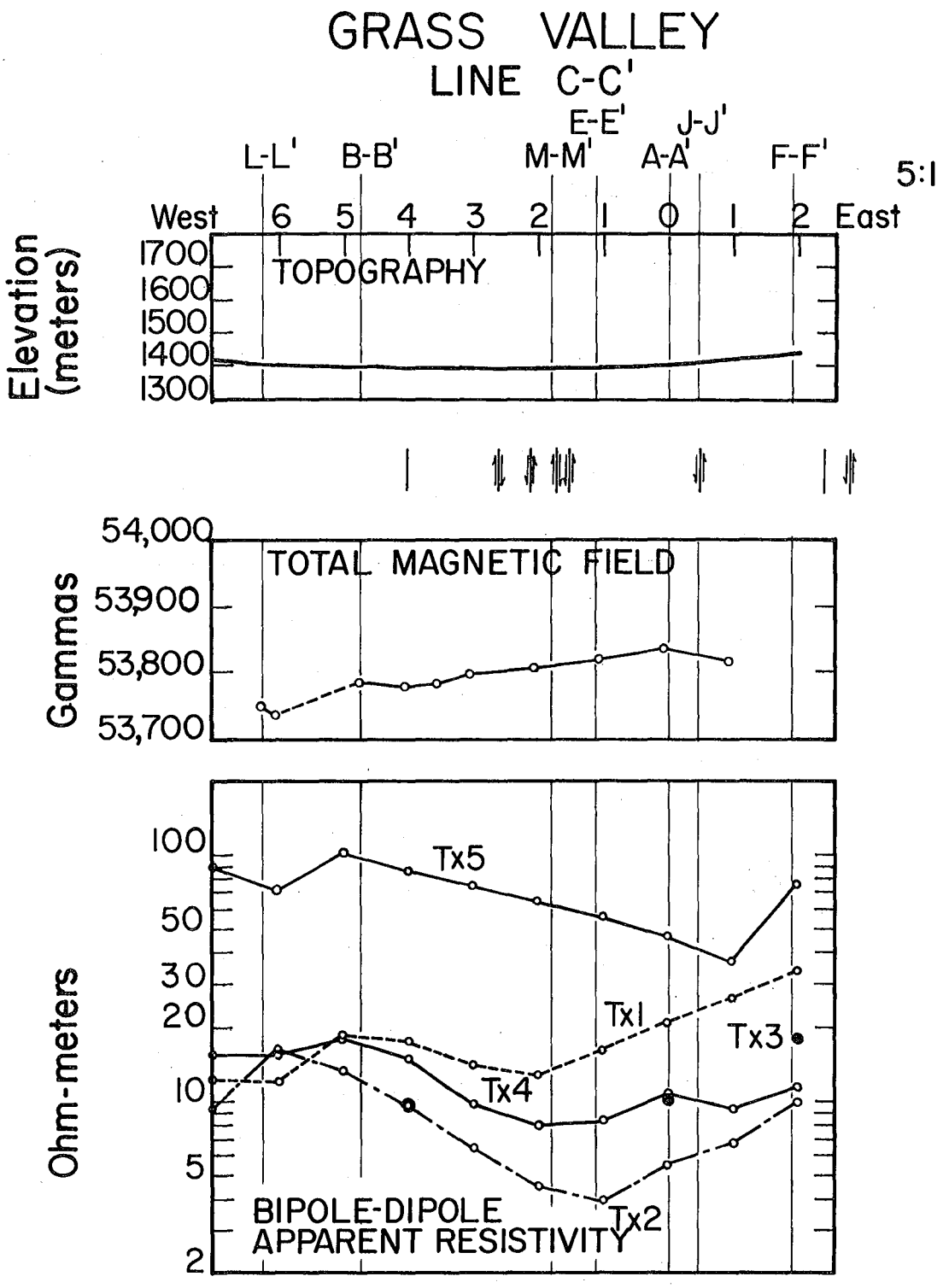

XBL 762-542

Figure III-A3. Geophysical data profile composite for Line C-C'.

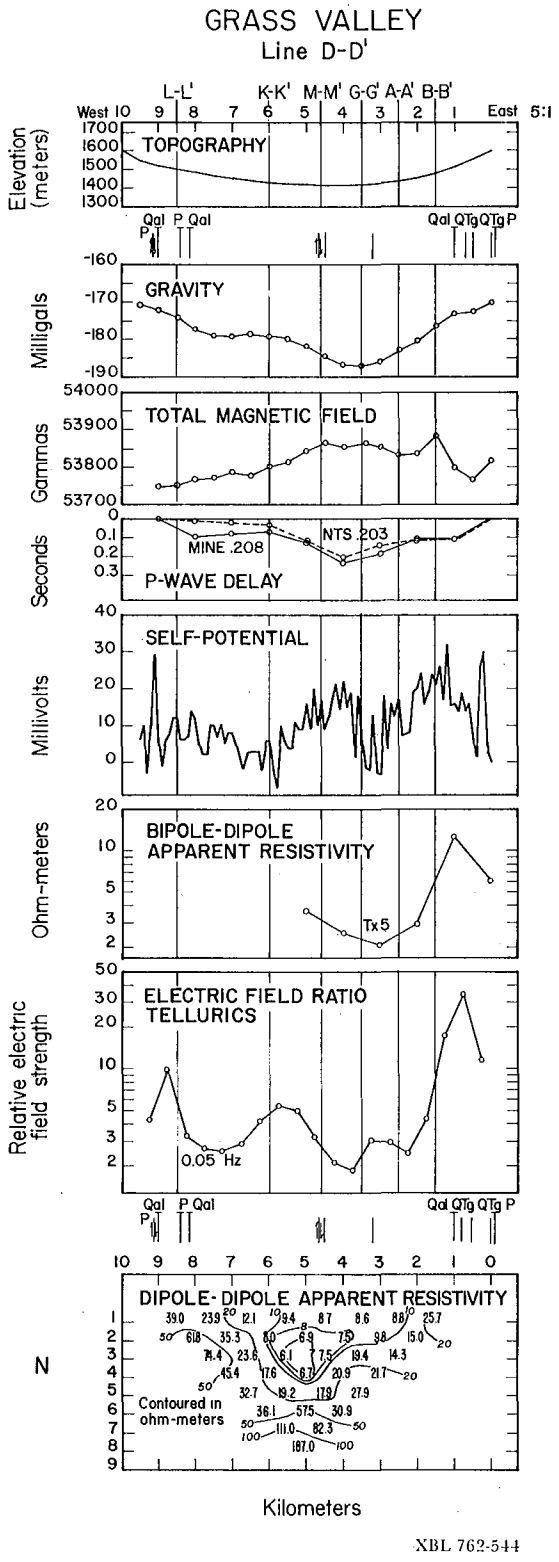

Figure III-A4. Geophysical data profile composite for Line D-D'.

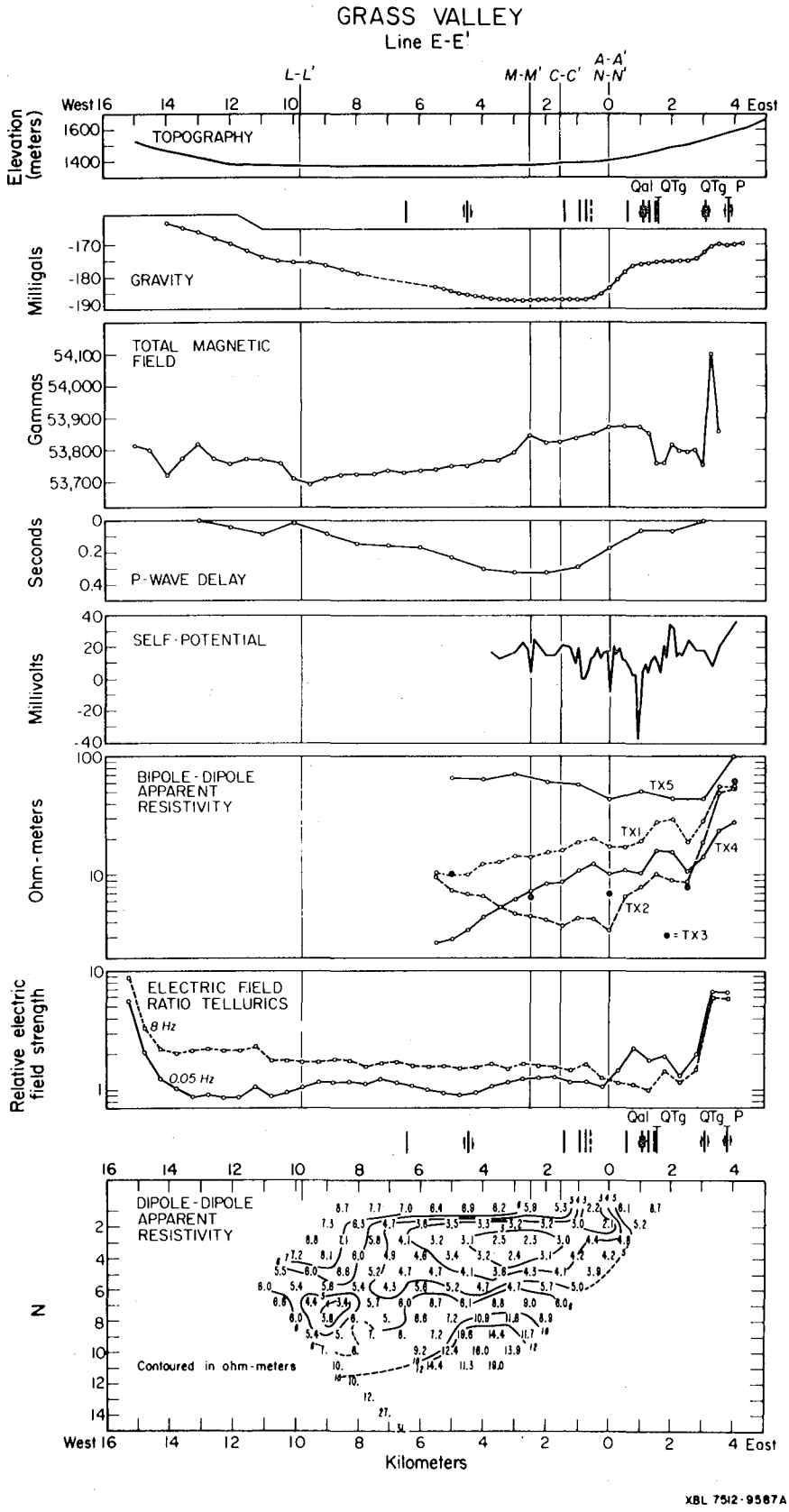

Figure III-A5. Geophysical data profile composite for Line E-E'.

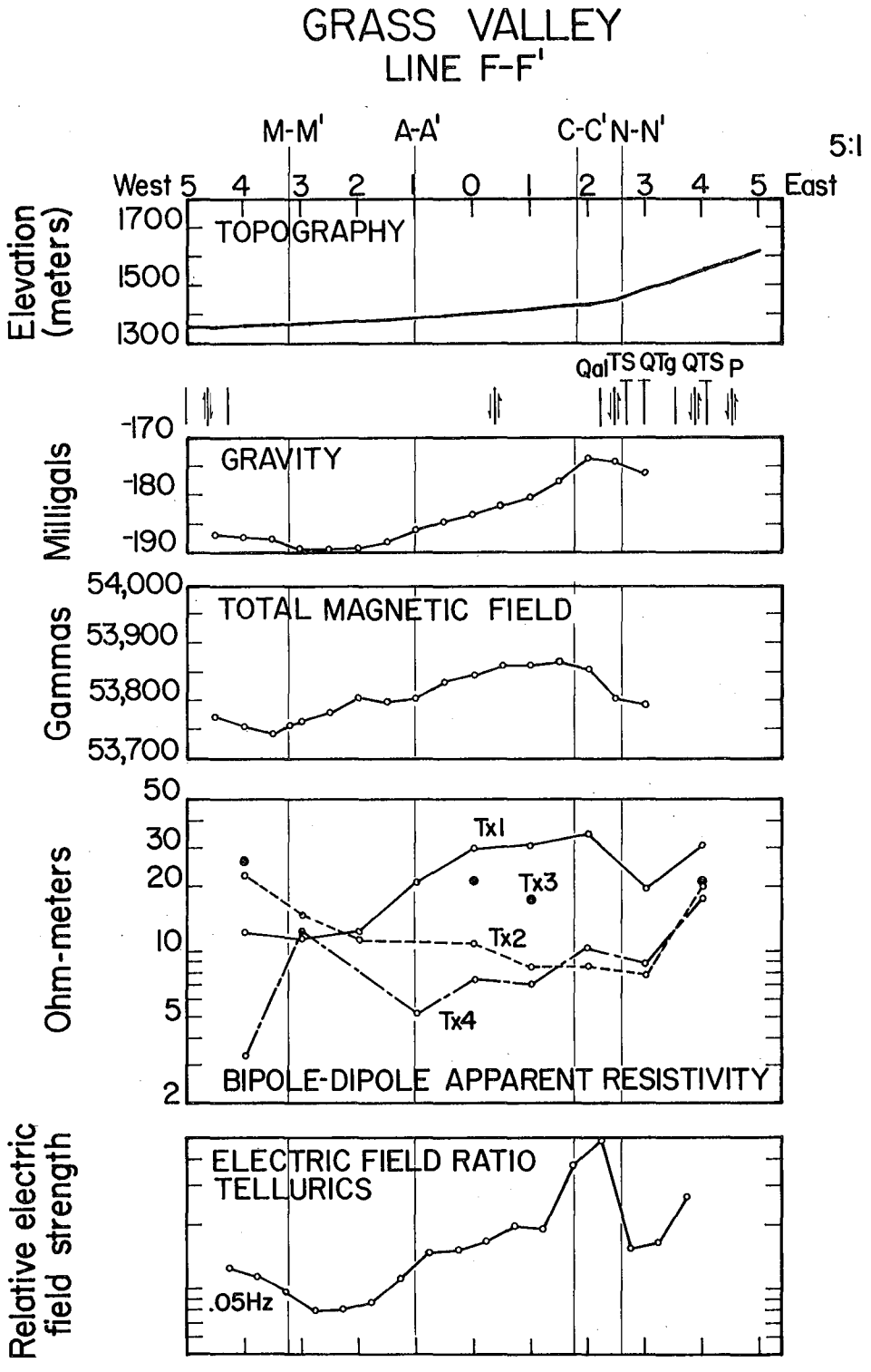

XBL 762-543

Figure III-A6. Geophysical data profile composite for Line F-F'.

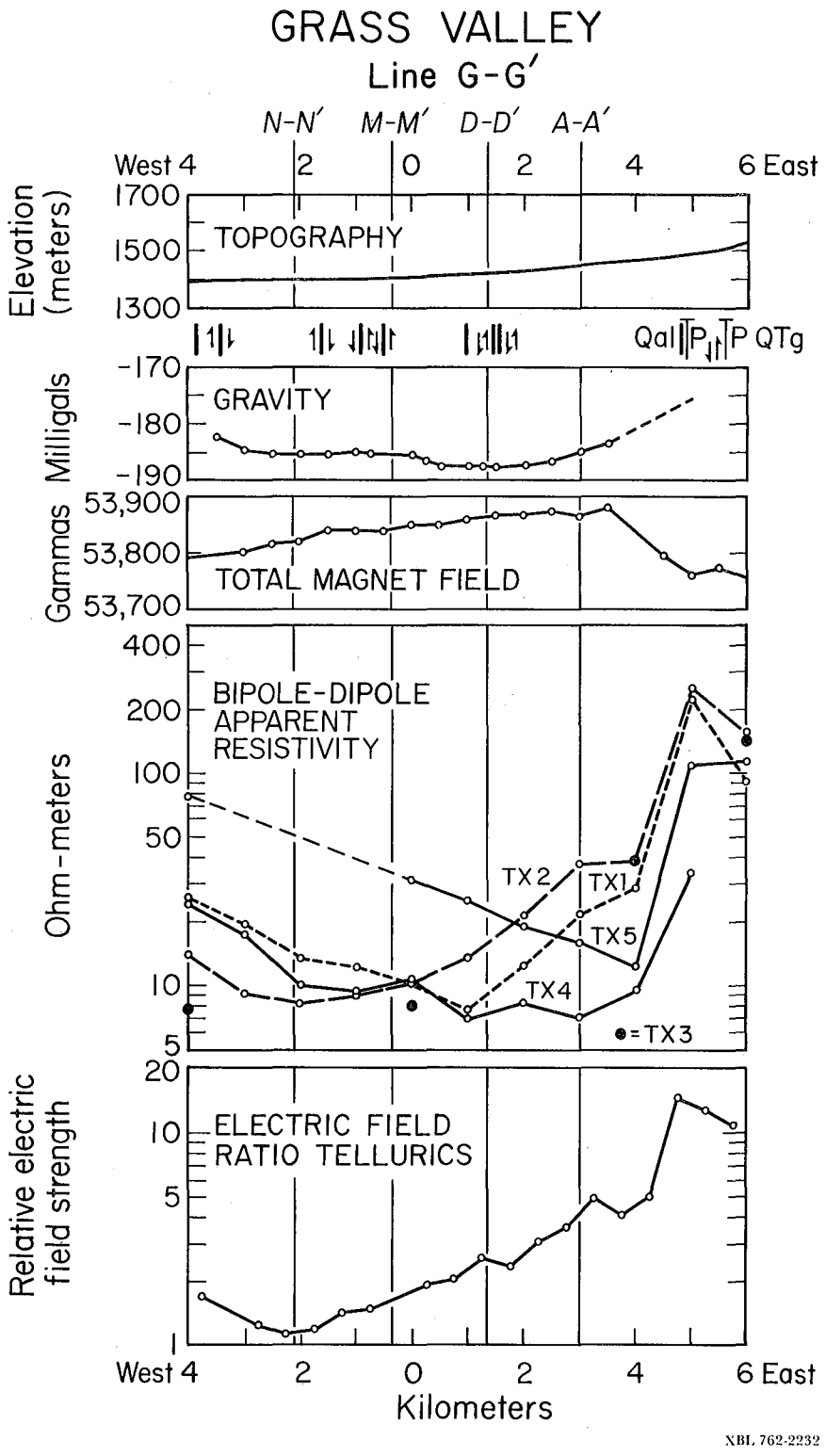

Figure III-A7. Geophysical data profile composite for Line G-G'.

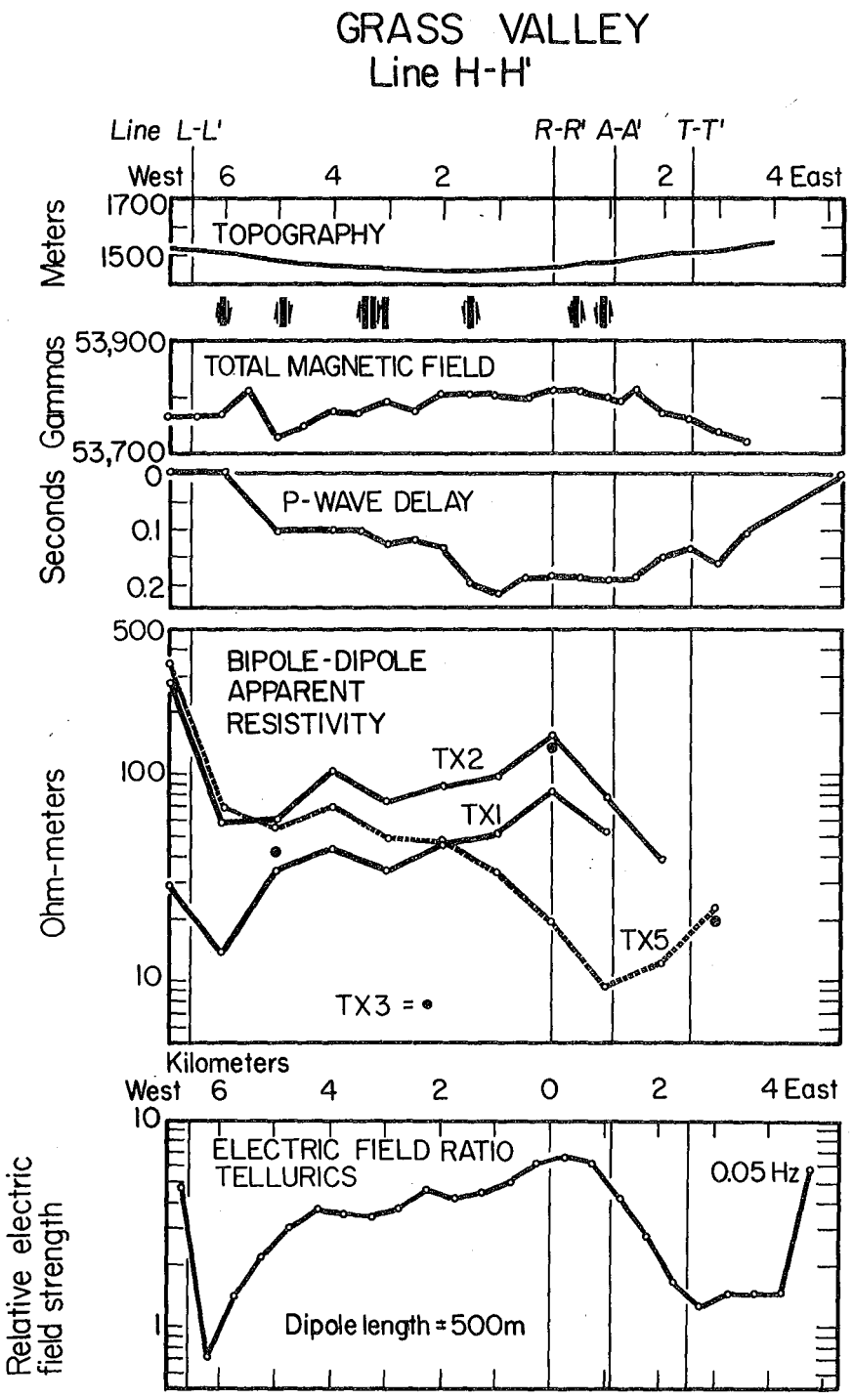

Figure III-A8. Geophysical data profile composite for Line H-H'.
XBL 7512-9825

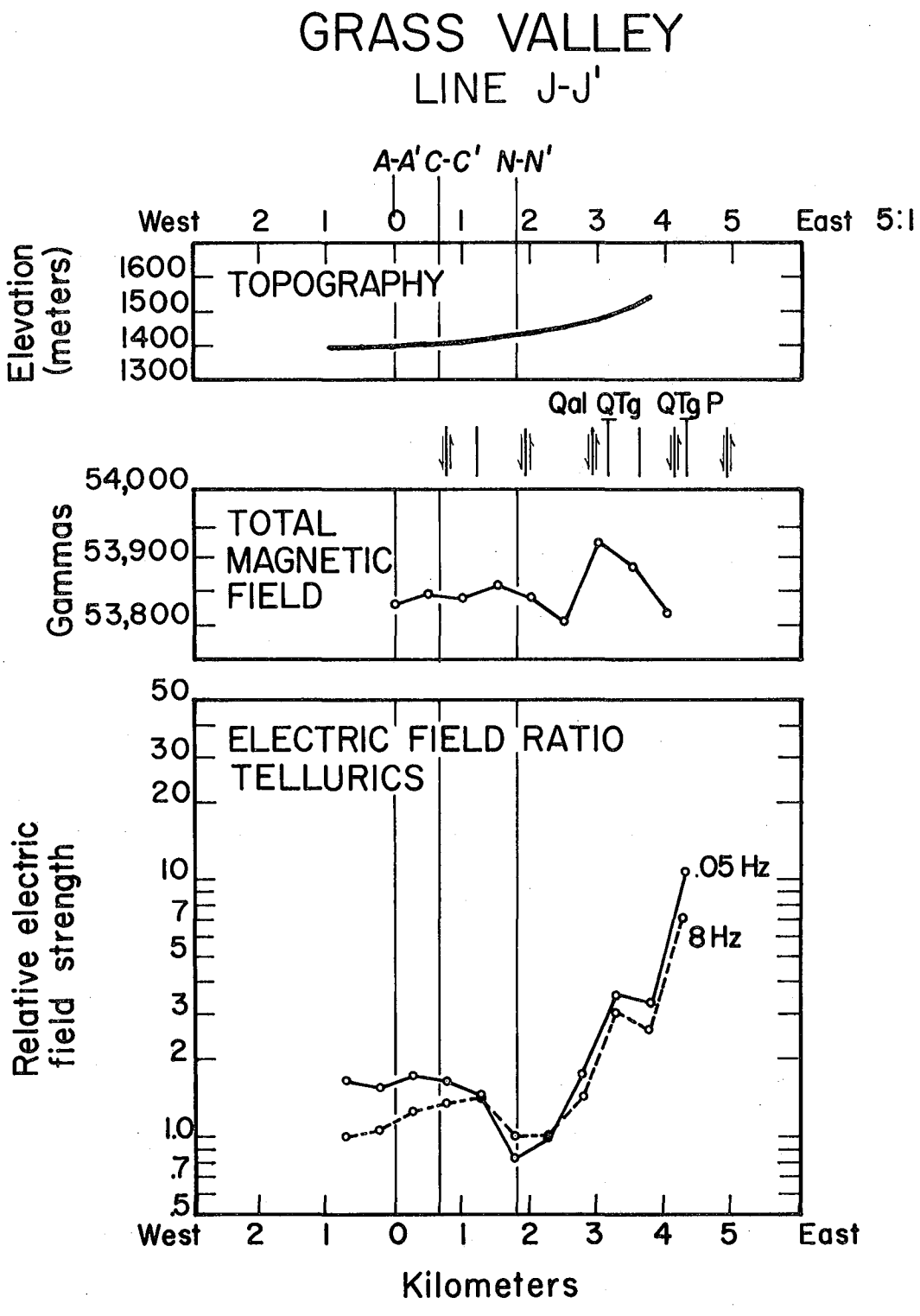

XBL 762-571

Figure III-A9. Geophysical data profile composite for Line J-J'.

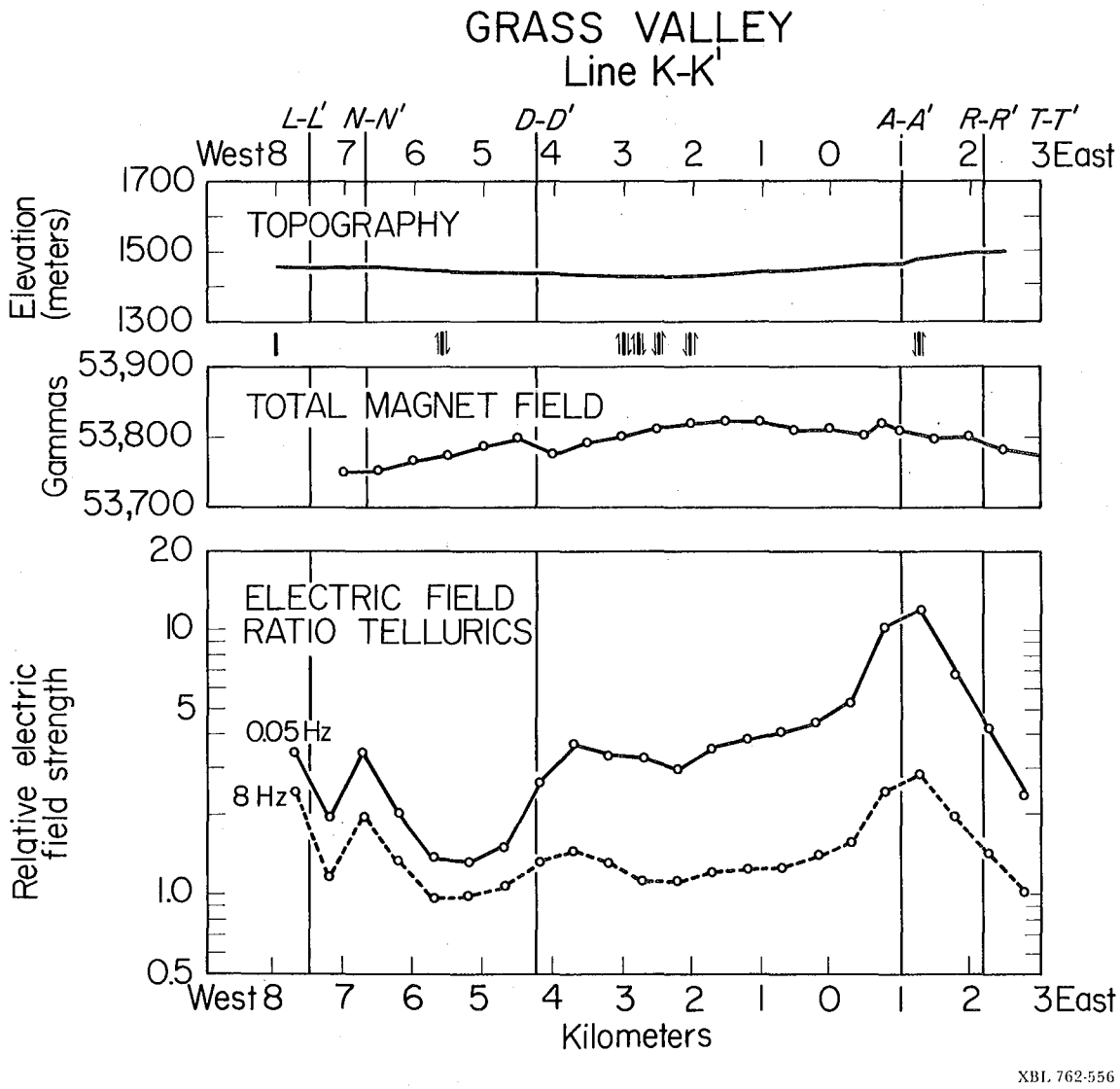

Figure III-A10. Geophysical data profile composite for Line K-K'.

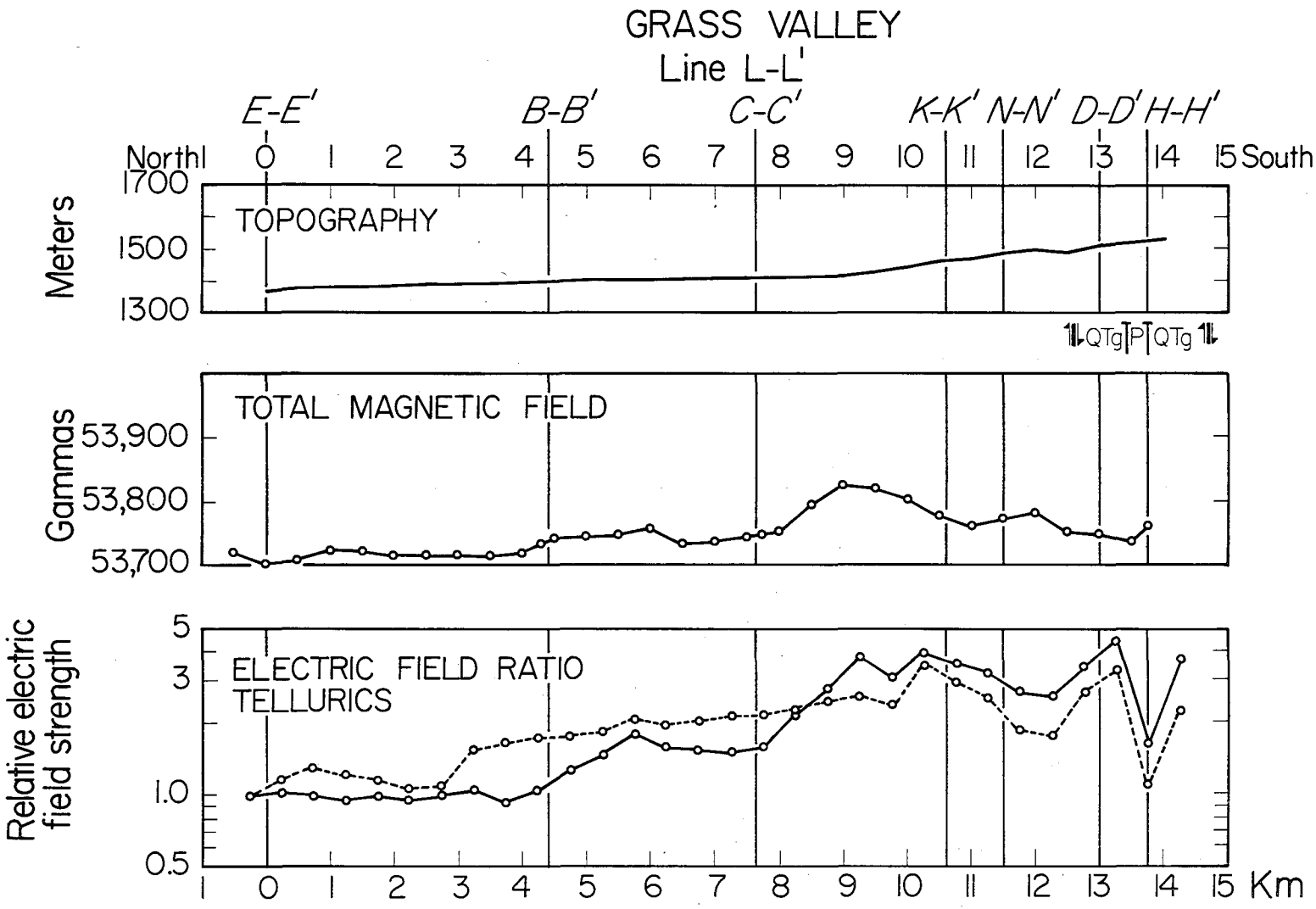

Figure III-A11. Geophysical data profile composite for Line L-L'.

XBL 762-555

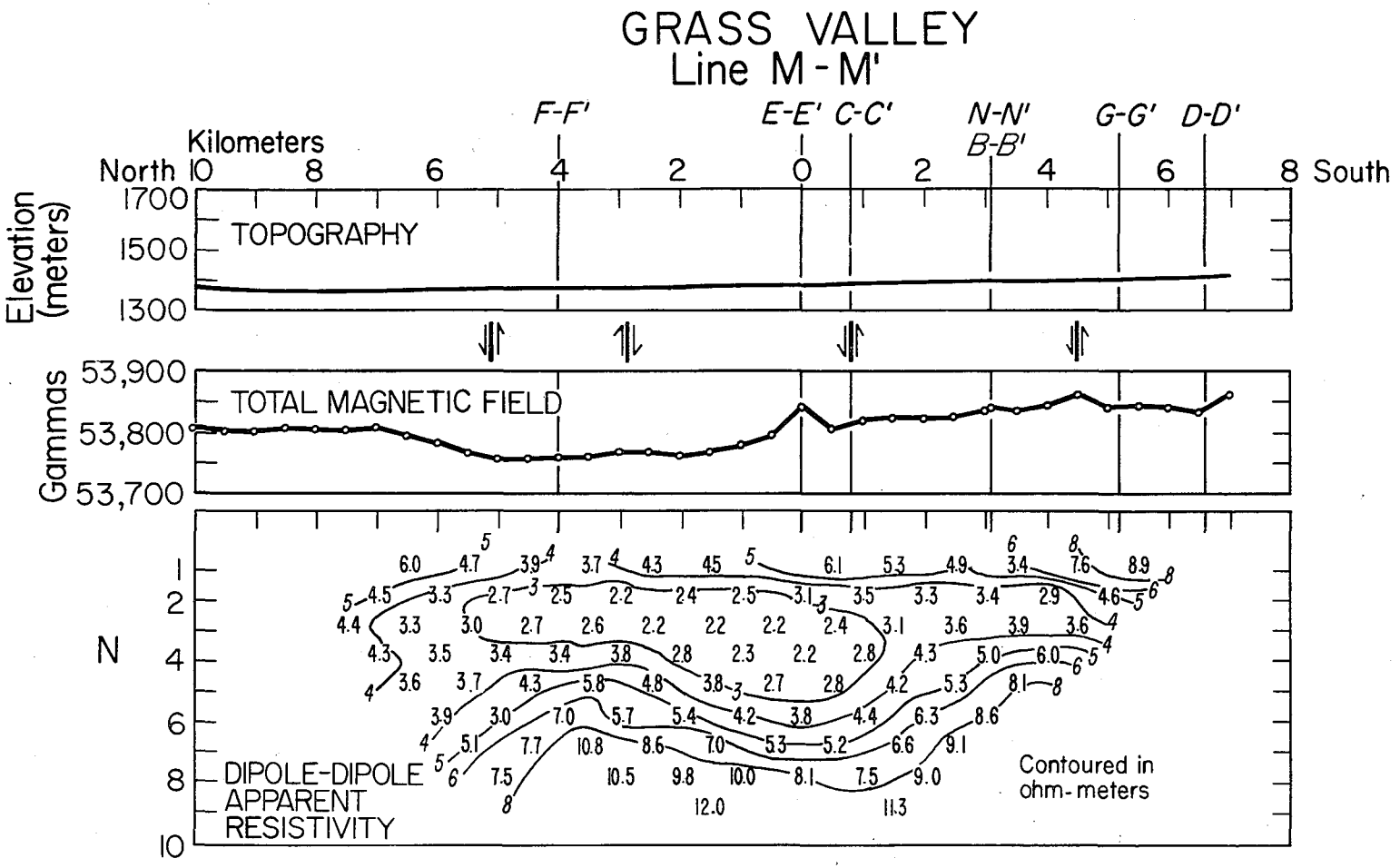

Figure III-A12. Geophysical data profile composite for Line M-M'.

XBL 763-619

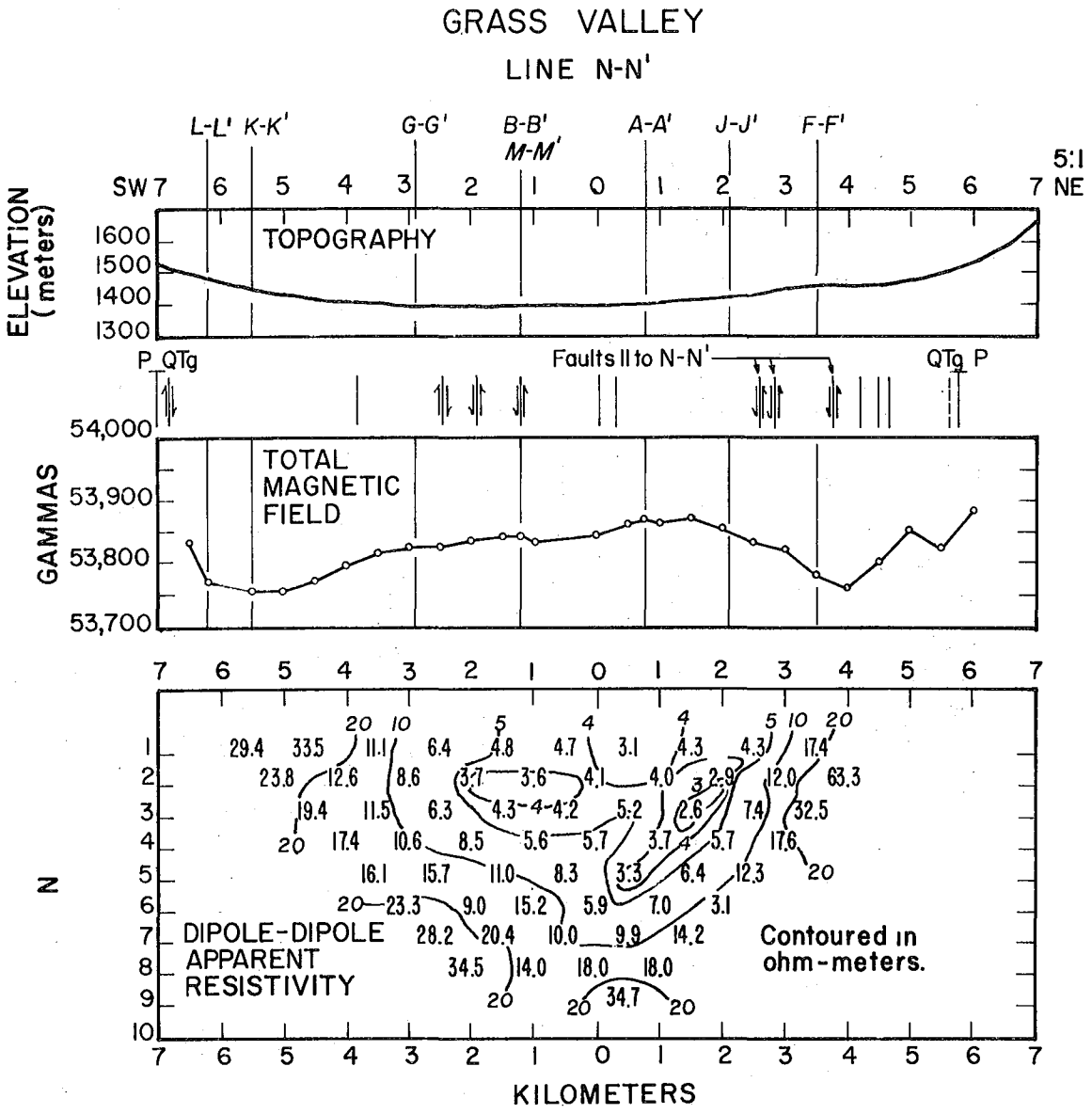

XBL 763-618

Figure III-A13. Geophysical data profile composite for Line N-N'.

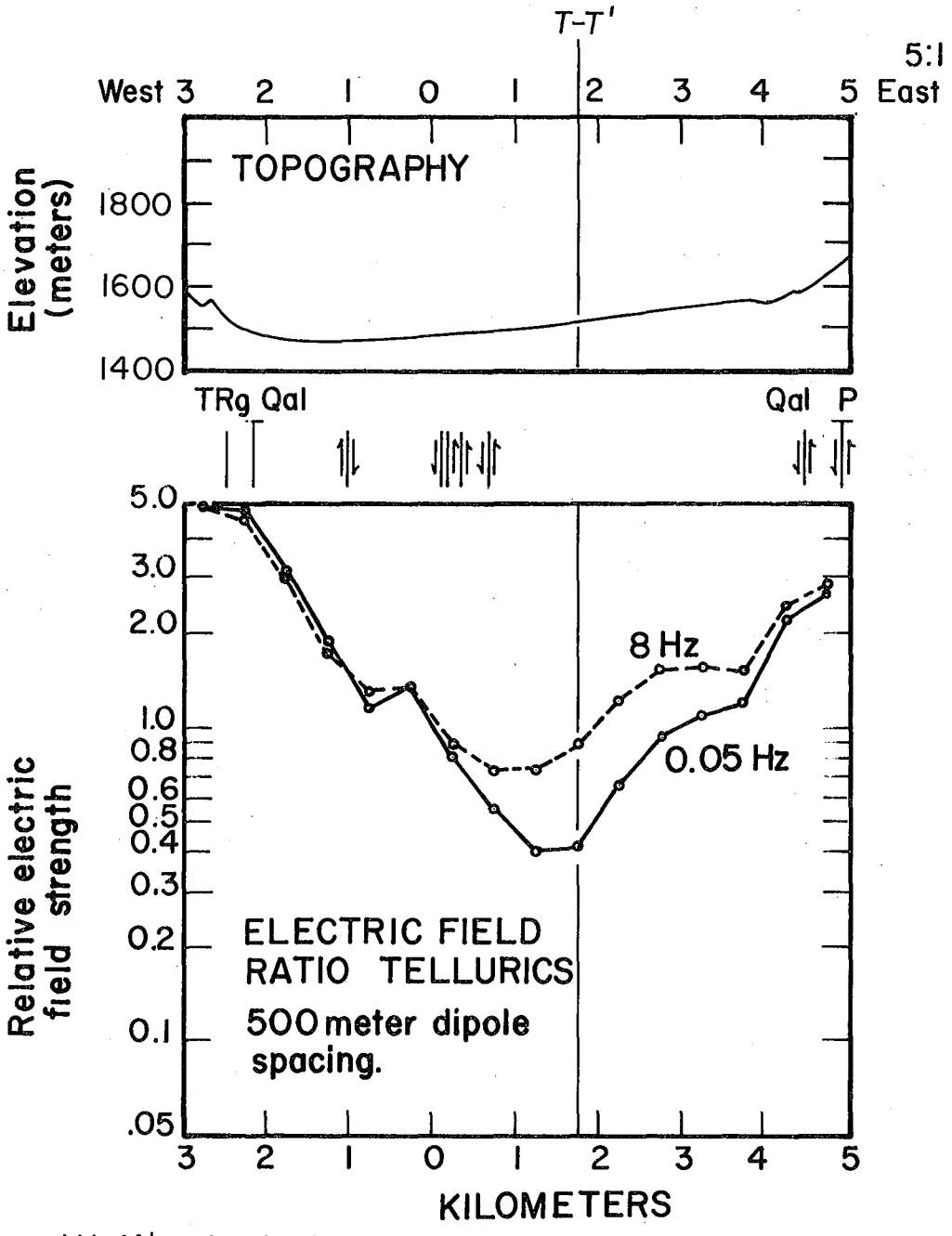

Figure III-A14. Geophysical data profile composite for Line P-P'.
XBL 763-617

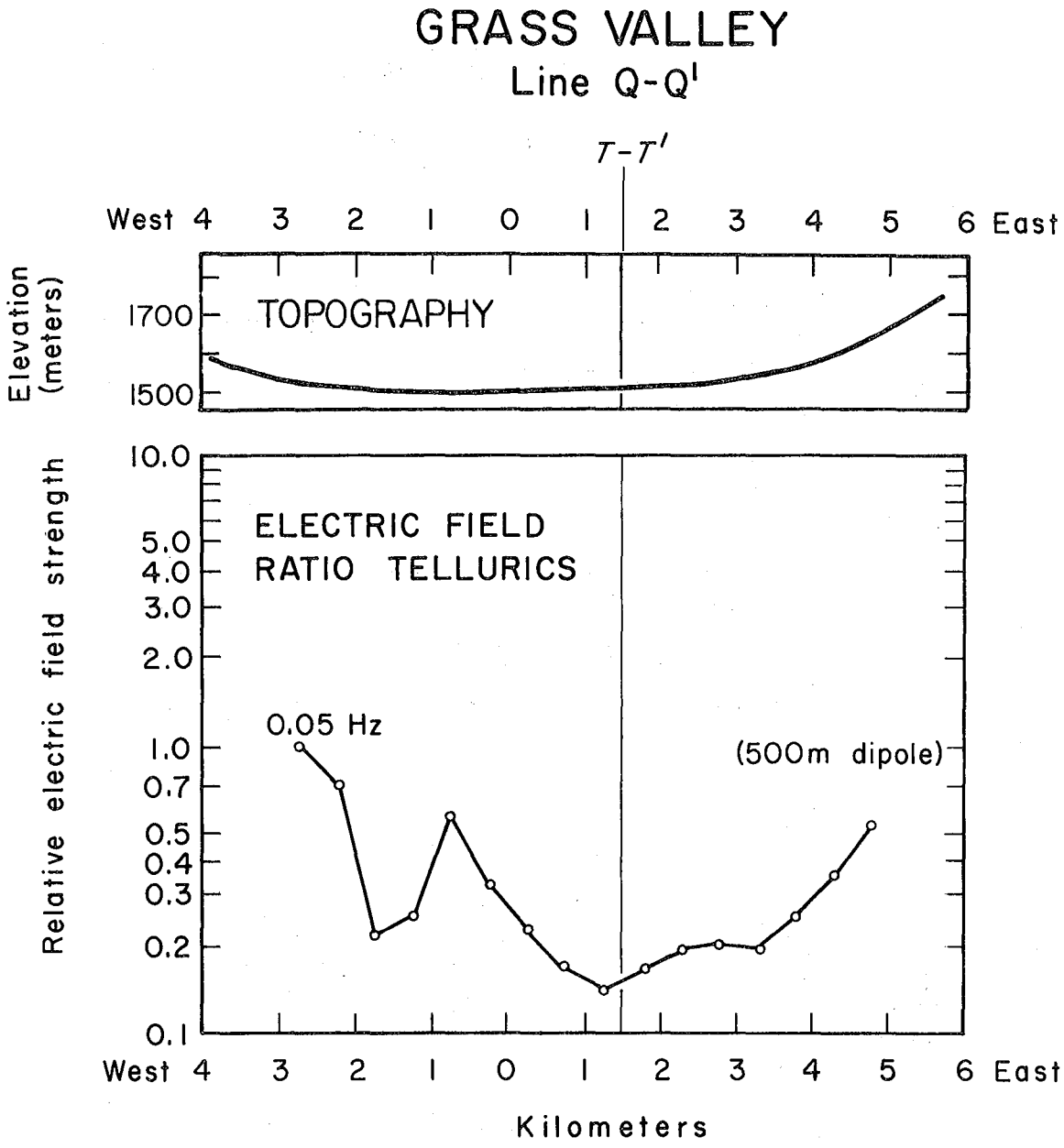

Figure III-A15. Geophysical data profile composite for Line Q-Q'.
XBL 763-636

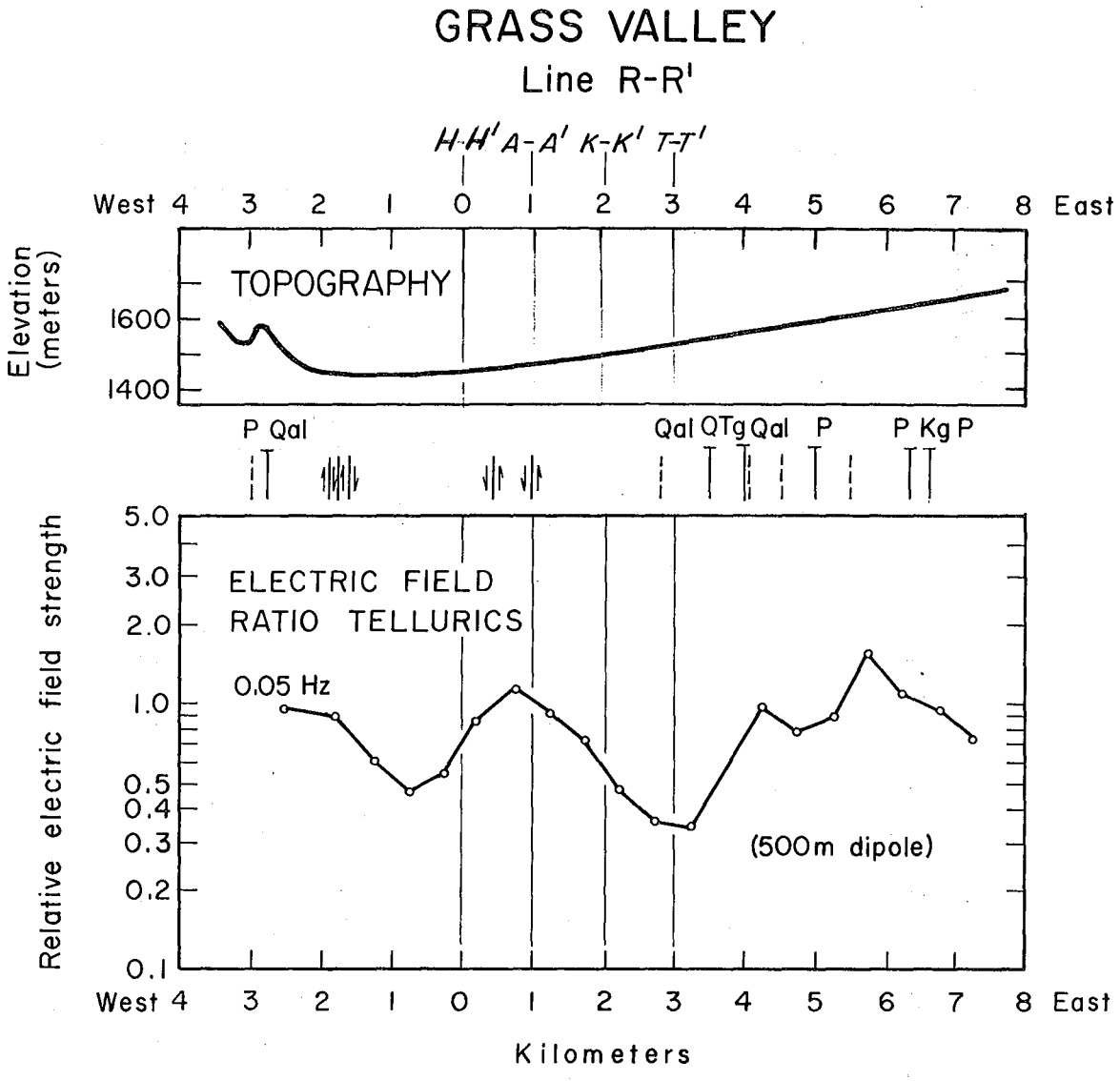

XBL 763-634

Figure III-A16. Geophysical data profile composite for Line R-R'.

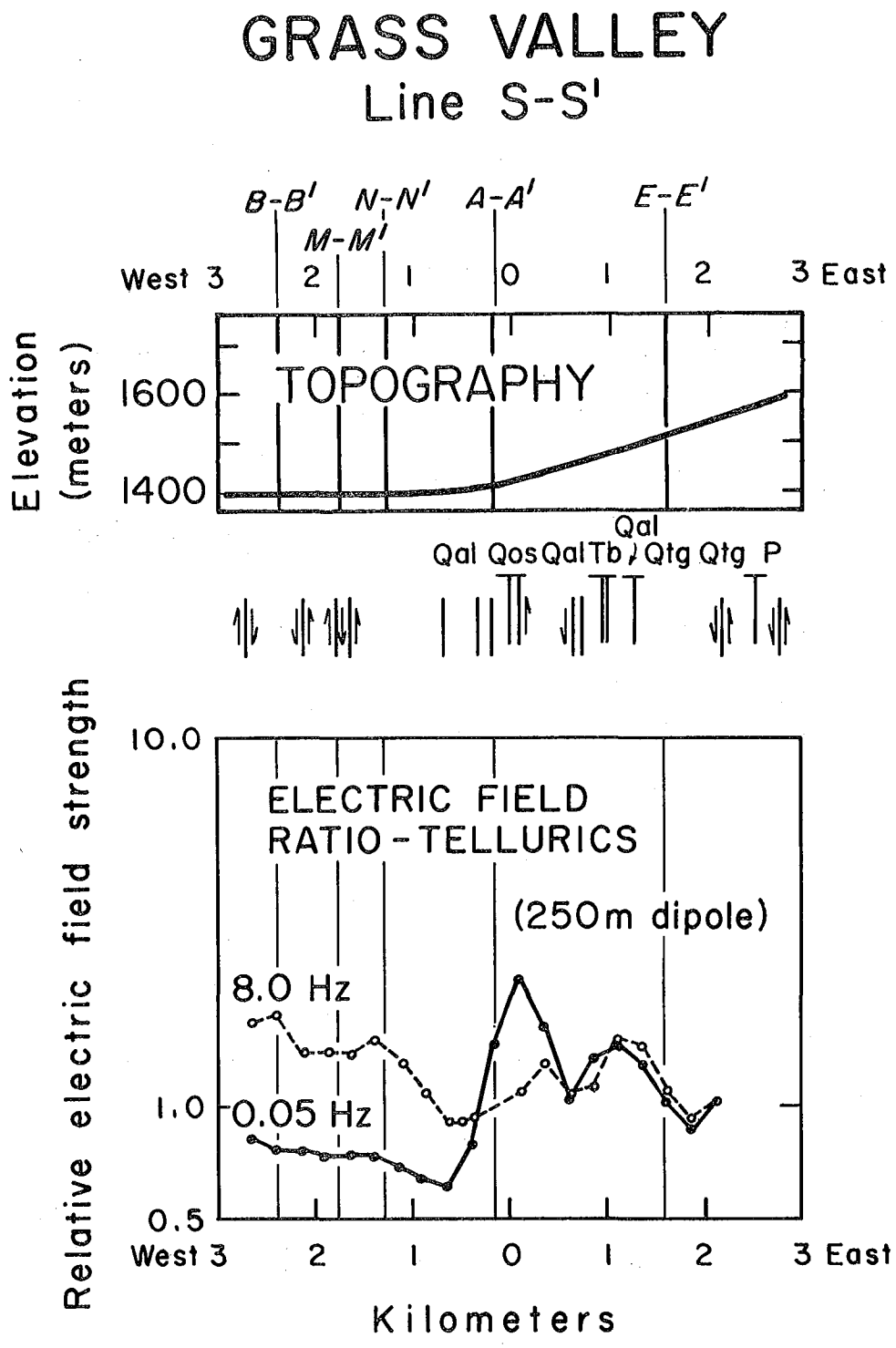

Figure III-A17. Geophysical data profile composite for Line S-S'.
XBL 763-635

If my hypothesis is not the truth itself it is least as naked: For I have not, with some of our learned moderns, disguised my nonsense in Greek, clothed it in algebra, or adorned it with fluxions. You have it in *puris naturalibus*. And as I now seem to have almost written a book instead of a letter, you will think it high time I should conclude; which I beg leave to do, with assuring you that I am, most sincerely, Dr. Sir, etc.,

B. Franklin

--from a letter to John Perkins,
February 4, 1753

This report was done with support from the United States Energy Research and Development Administration. Any conclusions or opinions expressed in this report represent solely those of the author(s) and not necessarily those of The Regents of the University of California, the Lawrence Berkeley Laboratory or the United States Energy Research and Development Administration.